UNIVERSITÀ DEGLI STUDI DI NAPOLI

"FEDERICO II"

PhD Thesis

"Analysis of differential gene expression in the aging brain: the case study of *Col4a1*, *Col25a1*, and *Id3* and their involvement in the adult neurogenesis of the short-lived teleost *Nothobranchius furzeri*"

Coordinator	**Author**	**Tutor**
Prof	Dr	Prof
Giuseppe Cringoli	Adele Leggieri	Luigi Avallone

“Love is always patient and kind. It is never jealous.

Love is never boastful or conceited.

It is never rude or selfish.

It does not take offense and is not resentful.

Love take no pleasure in other people’s sins, but delights in the truth.

It is always ready to excuse, to trust, to hope, and to endure

whatever comes"

(St Paul to the Corinthians, 1th letter, 13,1-13)

Contents

Acknowledgement

The last time I found myself, watching a white page and thinking about all those people who have been there for me was for my master thesis. At that time, I was hardly dreaming about doing a PhD, while now I am at its end. It has never been easy since the very first day, and it seemed to become harder during time, but I had many people by my side, helping and supporting me.

To my fiancé *Giovanni*, hardly to say in words how much I love him, how much I owe to all his encouragements, support, unconditional love, constant presence, and his desire in spending the rest of his life by my side. I would have been a different person without him.

I would thank my family. Thanks to my mother and my father, who raised me, helped me being who I am, and gave me the opportunity to study and follow my dreams. To my sister, who was always there supporting me, she wiped away my tears and helped me laugh even when life had been very tough. To my grandparents: I know how they are proud of me, and even if they could not be physically here with me, I can feel their constant presence. Thanks to the friends of a lifetime *Lucky*, *Theodore* and *Buster*, that made my days more sweet and delightful.

I am very grateful to my tutor, *Professor Luigi Avallone*, who gave me the opportunity to undertake this path and always had a great deal of confidence in me. I am also grateful to the Professors who "adopted" me in their working team, encouraging and supporting me during these three years: *Professor Luciana Castaldo*, who gave me infinite patience, and constant presence in the editing of this thesis; *Professor Paolo de Girolamo*, who has always trusted my job and skills, who permitted me profitable scientific discussions, which make my research more productive; *Professor Carla Lucini*, for her support and for sharing her knowledge and technical skills with me. I would express my gratitude to *Professor Livia D'Angelo*, who introduced me to the model organism *Nothobranchius furzeri*, teaching me her knowledge and exploring with me new ones; she has always been there for me, as mentor but, above all, as a friend; her encouragements and her confidence have always made me feel

sure of succeed during work and researches. I would like to thank also Professor *Marina Paolucci*, who has been the first person introducing me to the fascinating world of science and research and who first trusted in my skills.

I would like to thank also other member of the amazing team at Veterinary Medicine Department: *Antonio Calamo*, for sharing his graphic competences and for always answering at my numerous calls when I had troubles during imaging processing; *Michele Sammarco*, for being such a good mentor transmitting me his technical skills and making laboratory such a friendly place, together with *Sabrina Alì*. Thanks to the *Professor Lucianna Maruccio*, a dear friend of an infinite humanity and love. I am greatful to *Dr Elena De Felice*, with whom I confronted for her high technical skills, who has been always conforted me during the realization of this thesis, supporting me, and believing in me maybe even before really knowing me. I also express my gratitude to *Professor Caterina Squillacioti*, *Professor Lucia Francesca Menna*, and *Professor Alessandro Fioretti*, for sharing their competences, and laboratory machinery, together with their friendship and advises, giving me the opportunity to make my PhD experience more easy and productive.

I am also thankful to *Professor Alessandro Cellerino* and *Dr Mario Baumgart*, who gave me the opportunity of being a guest PhD student at FLI-Leibniz Institute on Aging of Jena and built with me the basis for the thesis project. I am also greateful to all members of Cellerino's group, particularly to *Sabine Matz* for her constant kindness and sweetness, *Dr Alessia Montesano*, and dr *Cinzia Caterino* for being a reference point and a good companion during my staying in Jena.

Thanks to the amazing friends met during these years, *Dr Antonio Santaniello*, *Dr Federica Gilardi*, *Dr Laura Pacifico*, *Dr Giovanni Sgroi*, *Dr Francesco Buono*, *Dr Luca Borriello*, *dr Francesca Daniele*, *dr Sergio Catalano*, *dr Giovanni Cataldi*, and *Giovanni Palermo*.

Acknowledgement

I am really grateful to my parents and brother in law, who have been my second family since almost ten years and have always had for me words of love and caring gestures.

Last, but not least, I would thank people who have constantly been by my side, everyday, in hard times more than better: my true friend *Eleonora Mazzarella,* who I met at the very beginning of this journey and since then has always been there in good times as in tough times, always remembering me that I will never be alone, because she will always be there for me; the constantly present *Simone Botticelli* and *Francesca Bosco,* we have been through a lot together, but we are still here strongest as ever and I am very lucky having two true friends like you; *Federica Ciullo,* my cousin in law that has always been patient and caring with me, mostly when I felt lost during my experience in Jena; my colleagues *Imma Prevenzano,* and *Sara Fioretti,* I am very happy to have met such amazing friends like them; *Luigi Adinolfi,* I can not forget how much you have done for me during my tough times in Naples; *Jessica Raffaella Madera,* a ten years old friend who never ask for something in turn of her true and deepest love.

Finally, thanks to all people that I forgot to mention, and have spent even only a second of their life helping mine being a little bit easier.

Abbreviations

A	anterior thalamic nucleus
aNCS	adult neural stem cell
bHLH	basic helix-loop-helix DNA-binding
Cans	ansulate commisure
Cant	anterior commisure
CC	cerebellar crest
CCe	corpus of cerebellum
Cmin	minor commissure
CNS	central nervous system
Col4a1	collagen type IV α 1 chain
Col25a1	collagen type XXV α 1 chain
CPN	central pretectal nucleus
Cpost	posterior commissure
CRISPR	clustered regularly interspaced short palindromic repeats
DAO	dorsal accessory optic nucleus
Dc1-4	central zone of dorsal telencephalon
DCX	doublecortin
Dd	dorsal zone of dorsal telencephalon
DEG	differentially expressed gene
DIL	inferior diffuse lobe of hypothalamus
Dl	lateral zone of dorsal telencephalon
Dld	dorso-lateral zone of dorsal telencephalon

Dll	latero-lateral zone of dorsal telencephalon
Dlv	ventro-lateral zone of dorsal telencephalon
Dm1-4	medial zone of dorsal telencephalon
dph	days post hatching
ecl	external cellular layer
EG	granular eminentiae
gc	central griseum
gl	glomerular layer
Ha	habenular nucleus
Hc	caudal hypothalamus
Hd	dorsal hypothalamus
HES	hairy/enhancer of split
Hl	lateral hypothalamus
I	intermediate thalamic nucleus
icl	internal cellular layer
Id	inhibitor of DNA binding
lfb	lateral forebrain bundle
llf	lateral longitudinal fascicle
LV	nucleus of lateral valvula
mfb	medial forebrain bundle
NE	neuroepithelial cell
NEP	neuroepithelial early progenitor cell
NG	glomerular nucleus

NRP	nucleus of posterior recess
NSC	neural stem cell
nIII	nerve III
NIII	nucleus of nerve III
(C)NS	(central) nervous system
OB	olfactory bulb
ON	optic nerve
on	over night
OT	optic tectum
PBS	phosphate buffer saline
PCNA	proliferating nuclear cell antigen
PGc	central preglomerular nucleus
PGm	medial preglomerular nucleus
PGZ	periventricular gray zone
PM	magnocellular preoptic nucleus
PPd	dorsal periventricular pretectal nucleus
PPp	parvocellular portion of preoptic nucleus
PPv	ventral periventricular pretectal nucleus
PVO	paraventricular organ
RER	rough endoplasmic reticulum
RMS	rostral migratory stream
RT	room temperature
sf	solitary fascicle

SGZ	subgranular zone
SOX	SRY-related HMG-box
SVZ	subventricular zone
TALENs	transcription activator-like effector nucleases
TH	tyrosine hydroxylase
Tl	longitudinal tori
TNp	posterior tuberal nucleus
TPp	periventricular nucleus of posterior tuberculum
TS1-4	layers of semicircular tori
ttb	tecto bulbar tract
Va	valvula of cerebellum
VAO	ventral accessory optic nucleus
Vc	central zone of ventral telencephalon
Vd	dorsal zone of ventral telencephalon
Vl	lateral zone of ventral telencephalon
VL	ventro-lateral thalamic nucleus
Vm	medial zone of ventral telencephalon
VM	ventro-medial thalamic nucleus
Vp	posterior zone of ventral telencephalon
Vs	supraccommissural zone of ventral telencephalon
Vv	vental zone of ventral telencephalon
wph	weeks post hatching

Figures

Figures

Tables

Abstract

Adult neurogenesis is a highly dynamic process, decreasing exponentially with aging in many vertebrate species. In mammalian brain, it is restricted to the subventricular and subgranular zones, while in teleost fish it occurs in approximately sixteen regions distributed along the entire rostro-caudal brain axis. Among teleost fish, *Nothobranchius furzeri* is a well-established model for aging studies, due to its very short lifespan together with anatomical and physiological aging features.

In vertebrates, *Col4a1* is mainly located in brain ventricular areas, is involved in axonal growth and guidance, and participates in nerve repair; *Col25a1* is specifically expressed in neurons and encodes for a protein named collagenous Alzheimer amyloid plaque component (CLAC), which binds to Alzheimer plaques reducing Aβ growth. *Id3* is another gene required for embryonic neurogenesis and angiogenesis, and it persists in adult brain, where it regulates adult neural stem cells maintenance and function.

Quantitative and qualitative analysis of *Col4a1*, *Col25a1* and *Id3* was assessed in *N. furzeri* young (5 weeks post hatching (wph)) and old (27 wph) brains, showing all the three genes are upregulated during aging and are expressed in recognizable neurogenic areas. Furthermore, double labeling of fluorescence *in situ* hybridization (FISH), for genes' mRNAs, and immunofluorescence (IF), for PCNA, confirms that *Col4a1*, *Col25a1* and *Id3* are expressed in numerous PCNA containing cells, confirming that their expression in nerogenic areas is related to cells proliferation and / or differentiation. The phenotype of *Col4a1*, *Col25a1* and *Id3* expressing cells was assessed by FISH/IF double labeling with neural markers S100, DCX, and HuC/D. Our data confirm that, as for other vertebrates, also in *N. furzeri Col4a1*, *Col25a1* and *Id3* are involved in adult neurogenesis. Furthermore, they colocalize mainly with DCX and HuC/D expressing cells, suggesting that they are involved in proliferation and differentiation of neural cells more than radial glial ones. These data lay the foundations to further studies on the pathways regulating *Col4a1*, *Col25a1* and *Id3*, to better understand their specific role in neural proliferation and differentiation pathways and identifying possible interactors.

Introduction

Collagen family comprises twenty-nine members, which mainly constitute extracellular matrices. However, few collagen molecules are expressed also in neuronal precursors, mature neurons, and glial cells (Sund et al., 2001; Hashimoto et al., 2002; Hubert et al., 2007; Seppanen et al., 2006). In the central nervous system (CNS), they are expressed in neurogenic areas where they regulate neural cells proliferation, differentiation and migration (Fox, 2008; Chernousov et al., 2006; Sertie et al., 2000). Members of the family are numbered from I to XXIX, even if collagen XXIX actually corresponds to a variant of collagen VI. They are all extracellular or transmembrane proteins, characterized by three α chains, which can assemble forming homo- or hetero-trimers (reviewed by Hubert et al., 2008). They are characterized by a triple helices structure, determined by a repetition of Gly-X-Y triplets in the primary sequence of each α chain, but sometimes triplets are interrupted by non-collagenous (NC) sequences. Homo- and hetero-trimers can assemble forming several superstructures that constitute seven different sub-families: fibrillary collagens (I, II, III, V, XI, XXIV, XXVII); fibril associated collagens with interrupted triple helices (FACITS) (IX, XII, XIV, XVI, XIX, XX, XXI, XXII and XXVI); collagens network forming (IV, VIII, X); collagen forming beaded filaments (VI); collagen forming anchoring fibrils (VII); collagens releasing anti-angiogenic NC fragment (endostatin) (XV, XVIII); transmembrane proteins (XIII, XVII, XXIII, XXV). For the collagen IV, six individual chains have been identified, α1 (IV) - α6 (IV), which assemble into three distinct protomers, α1.α1.α2 (IV), α3.α4.α5 (IV) and α5.α5.α6 (IV) (Boutaud et al., 2000; Hudson et al., 2003), but the major isoform is α1.α1.α2 (IV). In vertebrates, nervous system (NS), all isoforms are present in specific areas (Urabe et al., 2002). In details, chain α1 of collagen IV gene (*Col4a1*) is expressed in the pia mater and capillaries basement membranes (Hubert et al., 2008). More generally, *Col4* is involved in the development of the neuromuscular junction (Fox et al., 2007), while mutations of *Col4a1* are associated with intracerebral hemorrhages and porencephaly (Vahedi et al., 2007). Recently it was discovered that *Col4a1* is located in ventricular brain regions, which are

described as one of the main neurogenic niche, where it is involved in axonal growth and guidance, and participates in nerve repair. These regions also express another collagen gene, collagen XXV (*Col25*). The gene encoding for the α1 chain of Col25 (*Col25a1*), has been discovered as the main component of Aβ plaques characterizing Alzheimer disease. In fact, *Col25a1* encodes for a protein called collagenous Alzheimer amyloid plaque component (CLAC), which is supposed reducing Aβ growth. Furthermore, *Col25a1* has been discovered as a novel essential factor that regulates the initial phase of intramuscular motor innervation, which is required for subsequent target-dependent motoneuron survival and neuromuscular junction formation during embryonic development (Tanaka et al., 2014).

Inhibitor of DNA (Id) binding proteins are a family comprising four members implicated in the control of cell-cycle progression and cells differentiation through preventing transcription factors from binding DNA (Lyden et al., 1999). Since Id lacks a basic helix-loop-helix DNA-binding (bHLH) domain, they negatively regulate the DNA binding capacities of bHLH proteins, which promote instead DNA transcription. Mice that lack different Id genes die during embryonic development (Norton, 2000). In vertebrates, all Id genes are expressed in endothelia outside of the brain, whereas only *Id1* and *Id3* are expressed in brain embryonic endothelial cells. In mice, all Id members are expressed during neurogenesis, particularly *Id3* expression is observed in the roof and floor plate, and its signal become more intense along the ventricular zone in the third ventricle (Jen et al., 1996). The overall expression pattern of the Id genes during neurogenesis suggests that both *Id1* and *Id3* are expressed in undifferentiated neuroblasts cells (Jen et al., 1996).

Adult neurogenesis, also known as secondary neurogenesis, is a highly dynamic process that can be influenced by many factors and induced by many stimuli (Gould, 2007). It is an age-related process, decreasing exponentially with aging in many vertebrates' species (Kuhn et al., 1996; Pekcec et al., 2008; Knoth et al., 2010). In mammals, it occurs only into two neurogenic regions located in the subgranular zone (SGZ) of the dentate gyrus of the hippocampus and the subventricular zone (SVZ) of the lateral ventricles (Reynolds and Weiss, 1992; Eriksson et al., 1998; Gage,

2000). In contrast, teleost fish show a high rate of neurogenesis diffused in the entire brain (Zupanc 2001). These neural proliferating cells are mainly associated to the telencephalic region, mostly to the ventricular areas. However adult neurogenic niches are also present in preoptic and tectal areas, in the corpus of cerebellum (CCe) and in the medulla oblongata.

Among teleost fish, *N. furzeri* represents a very well-established aging model due to its very short lifespan (about 4-6 months) maintained also in captivity. It is well known as African killifish, since it inhabits annual pools subject to desiccation during Monsoon seasons (reviewed by Cellerino et al., 2015). For this reason, *N. furzeri* eggs are subjected to diapause, a phenomenon consists in the arrest of the development, which restarts when pools refill with water during wet seasons. Adult neurogenesis studies in *N. furzeri* were conducted from Terzibasi Tozzini and co-workers (2012), demonstrating that its neurogenic areas are substantially similar to that of zebrafish. However, mechanisms regulating secondary neurogenesis in *N. furzeri* still remain unclear. We therefore decided to investigate the presence of three genes belonging to the above-mentioned families and already known to be involved in secondary neurogenesis in other vertebrate species: *Col4a1*, *Col25a1*, and *Id3*.

Bibliography

Boutaud A, Borza DB, Bondar O, Gunwar S, Netzer KO, Singh N, Ninomiya Y, Sado Y, Noelken ME, Hudson BJ, 2000. Type IV collagen of the glomerular basement membrane: evidence that the chain specifity of network assembly is encoded by the noncollagenous NC1 domains. J Biol Chem, 275:30716-30724.

Cellerino A, Valenzano DR, Reichard M, 2015. From the bush to the bench: the annual Nothobranchius fishes as a new model system in biology. Biol Rev 91 (2): 511-533.

Chernousov M A, Rothblum K, Stahl RC, Evans A, Prentiss L, Carey DJ, 2006. Glypican-1 and alpha4 (V) collagen are required for Schwann cell myelination. J Neurosci 26, 508 – 517.

Eriksson PS, Perfilieva E, Björk-Eriksson T, Alborn AM, Nordborg C, Peterson DA, Gage FH, 1998. Nat Med 4, 1313-1317.

Fox MA, 2008. Novel roles for collagens in wiring the vertebrate nervous system. Curr Opin Cell Biol 20, 1 – 6.

Gage FH, 2000. Mammalian Neural Stem Cells. Sci 287 (5457): 1433-1438.

Gould E, 2007. How widespread is adult neurogenesis in mammals? Nat Rev Neuro 8, 481-488.

Hashimoto T, Wakabayashi T, Watanabe A, Kowa H, Hosoda R, Nakamura A, Kanazawa I, Arai T, Takio K, Mann DM, Iwatsubo T, 2002. CLAC, a novel Alzheimer amyloid plaque component derived from a transmembrane precursor, CLAC-P/collagen type XXV. Embo J 21, 1524-1534.

Hubert T, Grimal S, Ratzinger S, Mechaly I, Grassel S, Fichard-Carroll A, 2007. Collagen XVI is a neural component of the developing and regenerating dorsal root ganglia extracellular matrix. Matrix Biol 26, 206 – 210.

Hubert T, Grimal S, Carroll P, Fichard-Carroll A, 2008. Collagens in the developing and diseased nervous system. Cell Mol Life Sci 66, 1223-1238.

Hudson BG, Tryggvason K, Sundaramoorthy M, Neilson EG, 2003.

Alport's Syndrome, Goodpasture's Syndrome, and type IV collagen. N Engl J Med, 348, 2543-2556.

Jen Y, Manova K, Benezra R, 1996. Expression patterns of Id1, Id2, and Id3 are highly related but distinct from that of Id4 during mouse embryogenesis. Dev Dyn 207, 235-252.

Knoth R, Singec I, Ditter M, Pantazis G, Capetian P, Meyer RP, Horvat V, Volk B, Kemperman G, 2010. Murine Features of Neurogenesis in the Human Hippocampus across the Lifespan from 0 to 100 Years. PLoS One 5(1): e8809.

Norton JD, 2000. ID helix-loop-helix proteins in cell growth, differentiation and tumorigenesis. J of Cell Sci 113:3897-3905-.

Pekcec A, Fuest C, Mühlenhoff M, Gerardy- Schahn R, Potschka H, 2007. Targeting epileptogenesis- associated induction of neurogenesis by enzymatic depolysialylation of NCAM counteracts spatial learning dysfunction but fails to impact epilepsy development. J Neurochem 105, 389-400.

Reynolds BA, Weiss S, 1992. Generation of neurons and astrocytes from isolated cells of the adult mammalian central nervous system. Sci 255 (5052): 1707-1710.

Seppanen A, Autio-Harmainen H, Alafuzoff I, Sarkioja T, Veijola J, Hurskainen T, Bruckner-Tuderman L, Tasanen K, Majamaa K, 2006. Collagen XVII is expressed in human CNS neurons. Matrix Biol 25, 185 – 188.

Sertie AL. Sossi V, Camargo AA, Zatz M, Brahe C, Passos-Bueno MR, 2000. Collagen XVIII, containing an endogenous inhibitor of angiogenesis and tumor growth, plays a critical role in the maintenance of retinal structure and in neural tube closure (Knobloch syndrome). Hum Mol Genet 9, 2051 – 2058.

Sund M, Vaisanen T, Kaukinen S, Ilves M, Tu H, AutioHarmainen H, Rauvala H, Pihlajaniemi T, 2001. Distinct expression of type XIII collagen in neuronal structures and other tissues during mouse development. Matrix Biol 20, 215 – 231.

Terzibasi Tozzini E, Baumgart M, Battistoni G, Cellerino A, 2012. Adult neurogenesis in the short-lived teleost Nothobranchius furzeri: localization of neurogenic niches, molecular characterization and effects of aging. Aging Cell 11, 241-251.

Urabe N, Naito I, Saito K, Yonezawa T, Sado Y, Yoshioka H, Kusachi S, Tsuji T, Ohtsuka A, Taguchi T, Murakami T, Ninomiya Y, 2002. Basement membrane type IV collagen molecules in the choroid plexus, pia mater and capillaries in the mouse brain. Arch Histol Cytol, 65133-143.

Zupanc JKH, 2001. Adult neurogenesis and neuronal regeneration in the central nervous system of teleost fish. Brain Behav Evol 58, 250-275.

Chapter 1

Nothobranchius furzeri: an extremely short-lived vertebrate

1. *Nothobranchius furzeri*: an extremely short-lived vertebrate

The genus *Nothobranchius* comprises about 50 species, mostly small freshwater teleost that inhabit temporary African water streams subject to annual desiccations. For this reason, *Nothobranchius furzeri* is also known as turquoise killifish ("*kills*" in Dutch means "*stream*"), while the name *Nothobranchius* derives from the ancient Greek in which "*nothos*" means "*false*" and "*branchion*" means "*gill*". In fact, they are provided with false gills opening in the operculum. The word "*furzeri*" derives from the discoverer Richard Furzer, who collected eggs in South-Eastern Africa over 40 years ago.
N. furzeri originates from the Gona Re Zhou National Park in Zimbabwe (GRZ strain), while all recent population were collected far to the south, in Mozambique (MZM strain) (Reichard et al., 2009, 2014). Two colour morphs can be distinguished between males of the two strains. A yellow tail characterizes GRZ males, while red-tail chromatism is typical of the MZM strain. All species belonging to the genus express a stereotyped behavioral pattern in which the male drives the female toward the substrate in order to lay eggs in the muddy bottom.

1.1. Phylogeny

The teleost fish *N. furzeri* belongs to the order of *Cyprinodontiformes*, super-order *Acanthopterygii*, order *Cyprinodontiformes*, and comprises many other popular aquarium fish, such as other killifish and the so called live-bearing fish, comprising *Anablepidae*, *Goodeidae* and *Poecilidae* families. Molecular phylogenetic analyses have provided evidence that the order *Cyprinodontiformes* is a sister group and closest neighbours in a phylogenetic tree of *Beloniformes* [Fig 1]. *N. furzeri* phylogenetic position is very suitable for comparative genomics analysis and evolutionary studies, since its superorder *Acanthopterygii* comprehends also model genus for genomic and developmental studies, such as *Fundulus*, *Poecilia*, *Xiphophorus*, *Orizyas*, whose main representing species is *Orizyas latipes*,

the Japanese rice fish well known as Medaka (Setiamarga et al., 2008). *N. furzeri* is also very close to the species *Tetraodon nigroviridis*, and the stickleback *Gasterosteus aculeatus*.

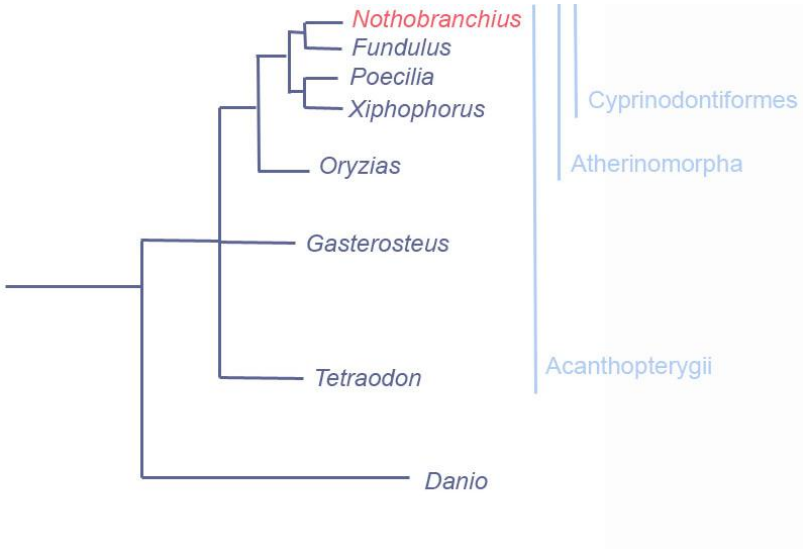

Fig 1 | N. furzeri phylogenetic position compared to the closest Acanthopterygii and the Ostariophysan Danio rerio. Source: NFIN - The Nothobranchius furzeri Information Network

1.2. Sexual dimorphism, male color polymorphisms and sex determination

Nothobranchius are relatively small fish with a median size of 5 cm (ranging from 3 to 15 cm) with females smaller than males [
Fig 2]. All Nothobranchius are characterized by a marked sexual dichromatism. Males are robust and are among the most colourful fresh-

water fish. Both sympatric and allopatric species occur in two or more colour forms. Females, on the other hand, are dull, their fins are translucent and body is pale brown, and it is very hard to distinguish between females of related species. N. furzeri females and females of other Nothobranchius species often possess iridescent scales. In some species, such as N. orthonotus, N. kadleci and N. melanospilus, female body may be pigmented with small dark dots. It is not clear yet whether this pigmentation arises as a by-product of male colouration (Sedlacek et al., 2014) or has any adaptive value. The bright male colouration is sexually selected and species-specific. In N. furzeri red and yellow morphs can be distinguished [
Fig 2] (Cellerino et al., 2016). A yellow caudal fin with a distal black band characterizes the yellow morph. The red morph occurs in two forms: one with a distal black band and the other with a homogeneously red tail. Red and yellow reflectance may provide an advantage in different visual environments: the wavelength of red colour is too short to be reflected by turbid water and it is rapidly absorbed, whereas yellow wavelength is more visible (Litjens et al., 1999). This may have consequences for sexual selection via mate choice, as males with specific colouration may be more visible to females in particular light environments as the muddy ponds in which they live (Cellerino et al., 2016). The yellow sub marginal band with black marginal band is almost unique to N. furzeri. However, the red morph is very common in the genus Nothobranchius, typically co-existing with blue (rather than yellow) male morphs within a species.

Sex determination in *N. furzeri* is strictly genetic. Indeed, they possess a sex determination system XY based, like humans: the male is the heterogametic sex, XY, while female is the homogametic one, XX (Valenzano et al., 2009). Normally male/female ratio is 50%. However, in wild populations females typically dominate (Reichard et al., 2009). Given the equal adult sex ratio in the laboratory, high male mortality is the most plausible explanation for a female-biased sex ratio in the wild (Cellerino et al., 2016). In the wild predation on males is significantly higher than in females. Their vibrant colour, together with increased male mobility, mate searching, and their larger size, may further elevate the risk of predation (Tobler et al., 2007; Tobler et al., 2008). This situation is reported for

many taxa with high degrees of sexual dimorphism (Promislow et al., 1992), including many fish (Rosenthal et al., 2001). In addition, males compete aggressively for access to females (Polacik et al., 2011) and male competition for mates may contribute significantly to male mortality.

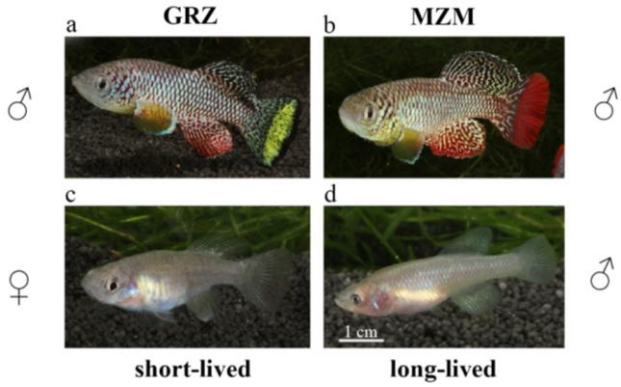

Fig 2 | N. furzeri, male and female. Yellow form, male (a); red form, male (b); adult female (c); and maturing male (d). Note opalescent hue on flanks and black pigmentation in the dorsal fin in d, temporary colours preceding the appearance of red, yellow and blue colours. Dorsal and anal fin are also relatively larger than in a female. Source: adapted from Polačik et al., 2016.

1.3. Distribution and habitat

Nothobranchius genus comprises four well-defined phylogenetic clades that are almost exclusively allopatric (Dorn et al., 2014). The basal northern clade inhabits particularly dry regions in northern Kenya and Somalia. The southern clade is distributed south of the Zambezi River, across a gradient from a humid coastal zone to dry habitats at higher altitudes. The inland clade is distributed in a high-altitude region between Lake Victoria in Uganda and Kafue basin in Zambia and separated from the coastal clade (coastal basins in southern Kenya, Tanzania, and northern Mozambique) by rift valleys (Dorn et al., 2014). Separation of the four

clades occurred by vicariance events (Cellerino et al., 2016). *Nothobranchius* pools are found in Savannah woodland, typically fed by rainwater or in remnant pools within the channels of temporary streams (Reichard et al., 2009). Several *Nothobranchius* species may inhabit the same pool (Reichard et al., 2009). *N. furzeri* populations are distributed along an altitudinal gradient that ranges between 16 and 422 m above sea level, but most populations inhabit areas between 16 and 200 m above sea level (Reichard et al., 2009). Only two populations are known from higher altitudes: MZCS-323 (222 m) and GRZ (422 m) (Cellerino et al., 2016) [

Fig 3]. *N. furzeri* often inhabited shallow isolated pools separated from active stream channels and alluvial plains (Reichard et al., 2009). Vegetation is often present in the form of Nymphaea sp., grass vegetation and, occasionally, submerging vegetation (Reichard et al., 2009). *N. furzeri* typically occurred in close proximity to open water or at the interface between vegetation and open water. Many pools, however, lack any vegetation (Reichard et al., 2014). Vertisol soils on alluvial deposits are typical of *N. Furzeri* pools. Vertisol in fact provide suitable soil substrate for survival of dormant eggs during the dry season more than laterite soils. The substrate is soft and muddy and the water very turbid [Fig 4]. Water may be less turbid and even transparent when vegetation is abundant. Water conductivity (describing total dissolved solids, i.e. water hardness related to its mineral content) in *N. furzeri* habitats, varies widely, from 50 to 625 µS/cm (Cellerino et al., 2016).

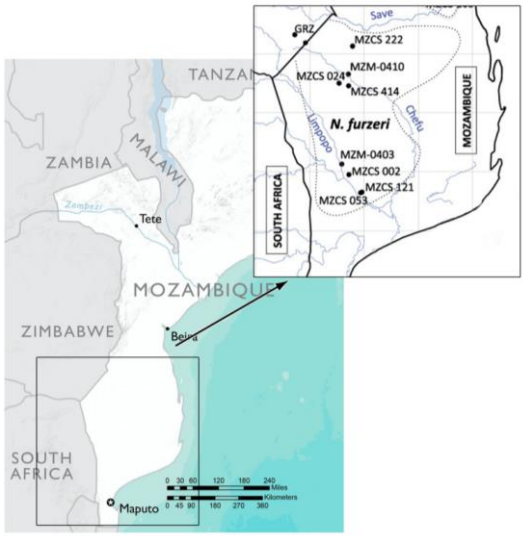

Fig 3 | Distribution of N. furzeri. Broken lines indicates the range of each species (the extent of the range in Zimbabwe is not known). MZM and MZCS strain inhabit Mozambique pools. MZM comprises two sub strains, 0403 - 0410, while MZCS comprises five sub strains, 222 - 414 - 002 - 121 - 053. GRZ strain is located in the Gona Re Zhou National Park in Zimbabwe.

Fig 4 | Small African N. furzeri pool. The capacity of such a small pool is of about 80 fishes.

1.4. Embryos development and life cycle

N. furzeri is an annual fish, with a median lifespan up to 12 months for the MZM strain (long-lived phenotype) and a median life-span of just three months for the GRZ strain (short-lived phenotype) (Terzibasi et al., 2007). Eggs are spawned in the substrate and fish die when the pool evaporates. Embryos development is characterized by an early phase of embryonic development (cleavage) consisting in a very slow segmentation compared to other *Cyprinodonts* (Cellerino et al., 2016). Moreover, teleost cleavage lack of both G1 and G2 phases, so that cell proceed directly from the S to M phase (Graham and Morgan, 1966). Accordingly, all non-annual killifish species exhibit an average cell cycle length during cleavage of 20 – 45 min (Cellerino et al., 2016). By contrast, *N. furzeri* has a cleavage time of 75 min in the absence of a G1 phase (Cellerino et al., 2016). Annual life cycle is an ancient character state that has been lost several times during evolutionary history of African and Neotropical killifish clades (Murphy & Collier, 1997; Hrbek & Larson, 1999). Due to the short term of the rainy season, annual fish spend the majority of their life cycle in the dormancy state of diapause [Fig 5] (Cellerino et al., 2016). This mechanism is adopted from some species to survive unfavourable environmental conditions (extreme temperature, food availability, adverse climate such as drought). This latter is the case of *N. furzeri* going in diapause. In fact, as already mentioned above, South African pools are subject to periodically desiccation due to the alternation of the rainy seasons typically of the monsoon climate. The average duration of *N. furzeri* habitats was only 75 days in one season (Terzibasi Tozzini et al., 2013). This means embryos are expected to spend at least 10 months in diapause and they can survive in this state more than a year in captivity (Cellerino et al., 2016). Under laboratory conditions, it is possible to distinguish three different stages of diapause called diapause I, II and III (Wourms 1972). At the end of blastogenesis two cell types are produced: cells committed to forming the enveloping layer, which migrate as a uniform sheet, and dispersed macroblastomeres that migrate under this sheet (Cellerino et al., 2016). At the end of epiboly, there is a phase of

morphogenetic stasis with no evidence of a multicellular organizing centre and the macroblastomeres are under cell cycle arrest and migrate apparently randomly (Dolfi et al., 2014). This phase has fixed duration but may be prolonged under unfavourable conditions and represents diapause I (Cellerino et al., 2016). At the end of the dispersed phase, macroblastomeres re-aggregate to form the embryonic axis (Cellerino et al., 2016). In *N. furzeri* (at 26°C), epiboly is completed in 48 h and the dispersed phase lasts about 5 days, so that the embryonic axis appears only after approximately 1 week (Cellerino et al., 2016). After re-aggregation, the neural keel is formed and then somitogenesis and morphogenesis of the NS proceed until the embryo enters diapause II, in which embryogenesis is complete but organogenesis has not begun (Cellerino et al., 2016). At this stage, the number of somites is fixed, the heart is tubular and contractile, and the major divisions of the encephalon are present and so are the optic cups with the lens (Cellerino et al., 2016). The duration of diapause II is highly variable, from 2 days to up to 3 years. Temperature plays a major role in its regulation; embryos incubated at 28°C skip diapause and can hatch 12 days after fertilization. After diapause II, the embryo proceeds to complete development. South American annual killifish have an obligatory diapause III at the end of development (Berois et al., 2014), where the embryo is completely formed but metabolism is inhibited, while *N. furzeri* does not show diapause III under standard incubation conditions (Cellerino et al., 2016).

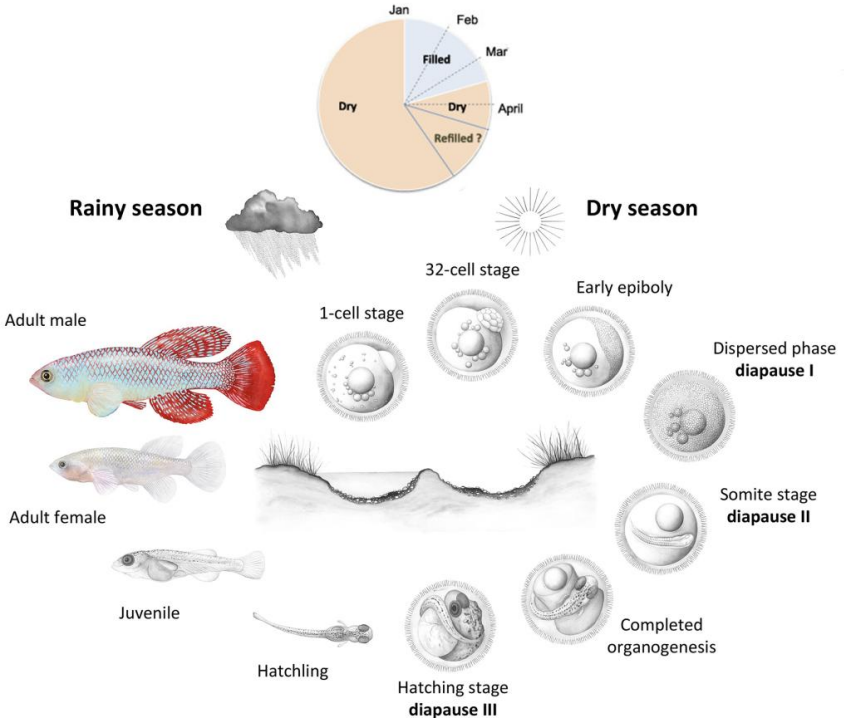

Fig 5 | N. furzeri annual life cycle. After flooding of the habitats (January - March), eggs hatch and the juveniles develop rapidly to reach sexual maturity. Eggs remain then diapause for about 10 months (April - December). Some embryos skip diapause and proceed through direct development and hatch if the habitat is wet. Source: adapted from Cellerino et al., 2015 and Platzer and Englert, 2016.

1.5. Diet

N. furzeri diet is mostly composed of aquatic invertebrates, both benthic and pelagic (Polacik and Reichard, 2010). In addition, terrestrial insects were occasionally found in the guts (Polacik & Reichard, 2010). Their diet appears opportunistic and largely depends on prey availability (Polacik and Reichard, 2010). Food selectivity indices indicated that *N. furzeri* and *N. rachovii* preferred to feed on small crustaceans (*Cladocera*, *Copepoda*, *Ostracoda* and Conchostraca) (Polacik & Reichard, 2010). Captive *N. furzeri*, as well as other species of the genus, readily consume live and frozen dipteran larvae such as larvae of the genus *Chironomus* and *Chaoborus* (Genade, 2005). Cannibalism has been observed in captivity in juvenile fish, especially in *N. orthonotus* younger than 14 days, with large individual differences in body sizes (Cellerino et al., 2016). There is no record of cannibalism in the wild (Polacik & Reichard, 2010), but it is expected in juvenile fish whenever size differences exceed approximately 30% or more (Cellerino et al., 2016).

The most common crustacean often used in laboratory to provide live food for killifish is the *Artemia salina* [Fig 6]. Artemia eggs, also known as cysts, can be stored for long periods and hatched on demand in salt water. In laboratory conditions, cysts can be hatched in water and marine salt (1 liter of water with 8–10 g of salt). The amount of the eggs depends on the number of fish to feed; 3 g of eggs produce an amount of nauplii sufficient to feed at least 1000 freshly hatched *N. furzeri.* The hatching will occur in 18-36 hours. To collect fresh hatched nauplii, aeration has to be removed from the cone, then, after several minutes, shells and baby brine shrimps separate: baby brine shrimps are attracted from lights sources, so it can be helpful to have a lamp on the cone to let them move towards the light source. Shells will float to the surface and can be easily removed with a Pasteur pipette. Then it is important, before feeding them to fish, to rinse baby brine shrimps in a fine mesh net or sieve using clean fresh water.

Fig 6 | Common crustacean used for N. furzeri diet known as Artemia salina. Artemia is a genus of aquatic crustacean also known as brine shrimp.

1.6. Housing

After collection, killifish eggs can be incubated at 26°C in petri dishes containing boiled damp peat. To promote synchronously hatching, eggs can be pre-incubated in Yamamoto's solution (17 mM NaCl, 2.7 mM KCl, 2.5 mM $CaCl_2$, and 0.02 mM $NaHCO_3$, pH 7.3) containing methylene blue 0.3%. Unfertilized eggs are characterized by a double-layered structure with a perivitelline space and remain clear [Fig 7 a], and should be removed by using a Pasteur pipette. Furthermore, if using methylene blue, they start decaying and acquire a bluish, rather opaque coloration [Fig 7 b]. Fertilized eggs will be translucent with no apparent structure inside [Fig 8 a], opaque with an advanced embryo [Fig 8 b, c], or white when dead [Fig 8 d] (Polacik et al., 20016). Ready-to-hatch embryos remain viable for only a limited time, as they are gradually consuming their energy reserves (Polacik et al., 20016), and the precise time interval depends on the incubation temperature (Polacik et al., 20016). The yolk sac begins diminishing ~60 d after the embryo reaches its pre-hatching stage (Polacik et al., 2016).

Eggs must be now moved with the peat (that maintains a slightly acidic environment, keeping waste nitrogenous substances in a safer, ammonium form) into a small aquarium (6 L for ~ 50 eggs). The peat layer on the bottom should be no deeper than 2 cm so that the freshly hatched fish can easily swim out and not get trapped in the peat (Polacik et al., 2016). Manipulation of fry, which are fragile, must be avoided, keeping them in their hatching aquarium with the peat for 3–4 dph; tank can be rearranged to a flat position ~24 h after hatching. Water temperature should be maintained at 27–28 °C with a small submersible aquarium heater and any aeration or filtration should be avoided. After 3-4 days, fry can be transferred into a larger aquarium without the peat (~4 L of water per fish). Water exchange can be provided by setting a recirculating system or by gradually exchanging of water adding mature system water to the tank with juveniles maintaining always the same water level (Polacik et al., 2016). When fish are sexually mature, at ~ 5 weeks post hatching (wph), they must be kept in a female biased ratio (1:3 ratio) to avoid lethal male–male interactions. In case, aggressive individual(s) should be removed from the aquarium.

Tanks have to be covered with lids and labeled with strain of fish contained, date of birth, number of fish and male/female ratio. Placing tanks with different strains adjacent to one another should be avoided. Colored labels are very helpful to indicate health status of fish and keep them monitored in order to their needs.

Young fish must be feed three times a day and adult fish, 5 days post hatching (dph)), two times per day, at regular intervals.

The tank must be provided with a spawning place, which could be a sieve in a bottle shaped glass jar (to prevent excessive spilling of the peat) filled with a 6 cm layer of wet autoclaved peat to protect eggs during long-term exposure to adult fish because *N. furzeri* tends to cannibalize their eggs. Before proceeding with eggs hatching, they should be bleached with a solution containing 0.1 mL of 5% sodium hypochlorite in 170 mL of system water: eggs are rinsed for 5 min in system water, placed in a second beaker of bleach solution for 5 min more, rinsed the with system water and placed into petri dishes.

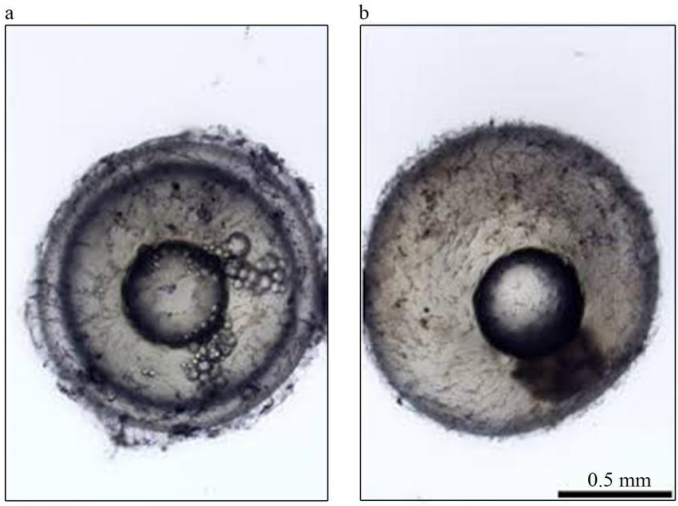

Fig 7 | Differences between fertilized (a) and unfertilized (b) N. furzeri eggs. Fertilized eggs with typical double-layered structure. Unfertilized eggs lacking perivitelline space. Source: adapted from Polačik et al., 2016.

Fig 8 | Gross staging of N. furzeri eggs incubated in peat. (a–d) Diapaused N. furzeri egg lacking structures that are readily visible to the naked eye (a); advanced, post diapause II embryo with black-pigmented eyes (b); egg with a fully developed, ready-to-hatch embryo with gold-pigmented eye iris (c); and dead, decaying egg (d).

1.7. Genetic structure

Each Savannah pool consists of genetically homogenous populations of *N. furzeri* and even adjacent pools containing genetically distinct populations (Polacik et al., 2016). The same strong structure was found for three other species: *N. orthonotus*, *N. kadleci* and *N. pienaari* (Bartakova et al., 2013). Genetic differentiation between populations increases with geographical distance. The same two lineages co-occur in at least one population in another part of their contact zone and nuclear genetic markers (microsatellites) indicate no reproductive barrier (Bartakova et al., 2013). In the future, the use of genome-wide markers should reveal greater details of the population structure within and among populations.
At Fritz Lipmann Institute laboratories (Leibniz Institute for Aging, Jena, Germany), *N. furzeri* genome has been sequenced and annotated on NFIN genome browser (NFINgb) at http://nfingb.leibniz-fli.de/. NFINgb provides access to sequencing data of different short- and long-lived *N. furzeri* strains: GRZ, MZM-0403, MZM-0410 and MZZW-0701 (Reichwald et al., 2015). It is also available a transcriptome browser, NFINtb (https://nfintb.leibniz-fli.de/nfintb/), in which are annotated 19,875 protein-coding genes plus comparisons data to Medaka, stickleback, tetraodon and zebrafish (Petzold et al., 2013).

1.3. Non-genetic and trans-genetic interventions

Species of the genus *Nothobranchius* are excellent model systems to test non-genetic interventions and their effects on ageing and survival (Cellerino et al., 2016). In particular, these fish offer a great opportunity to study the effects of water-soluble drugs and feeding on vertebrate survival and ageing on a large scale (Cellerino et al., 2016). Non-genetic manipulations, including changes in temperature, diet and drug administration on vertebrate survival and ageing-related phenotypes have recently been tested using several species of the genus *Nothobranchius*, (Cellerino et al., 2016). *N. furzeri* and *N. rachovii* ageing rate and overall survival in captivity can be modified by water temperature (Valenzano et al., 2006 b; Hsu & Chiu, 2009), with lower temperature increasing

lifespan, slowing down the appearance of ageing biomarkers, reducing adult body size and delaying the age-dependent decline in spontaneous activity (Cellerino et al, 2016). Dietary restriction by feeding every other day in inbred and wild-derived *N. furzeri* strains was effective in prolonging the survival of inbred strains and slowing down ageing but had a mixed effect in wild-derived strains, increasing early mortality while prolonging maximum lifespan (Terzibasi et al., 2009), similarly to results reported in mice (Weindruch, 1996). Different research groups have shown that in both *N. furzeri* and *N. guentheri*, the natural polyphenol resveratrol can slow down ageing and prolong lifespan (Valenzano et al., 2006 a; Yu & Li, 2012; Genade & Lang, 2013). Additionally, supplementation of melatonin into aged *N. korthausae* reduced age-dependent disruption of circadian rhythms (Lucas-Sanchez et al., 2013).

Due to its very short life cycle *Nothobranchius* fish are particularly suited for transgenic experiments. Transgenic *N. furzeri* lines are now available, with fish ubiquitously expressing green fluorescent protein (GFP) under several promoters (Valenzano et al., 2011; Hartmann & Englert, 2012; Allard, Kamei and Duan, 2013). Current work is aimed at further developing the transgenesis toolkit in this species and applying the recently developed transcription activator-like effector nucleases (TALENs) and systems (Zu et al., 2013; Sung et al., 2014) to introduce loss-of function mutations and perform site-specific genome editing (Cellerino et al., 2016). Since *Nothobranchius* is the shortest-lived vertebrate, transgenic mutants of its genus could be used to identify novel genes and genomic regions that modulate vertebrate survival and ageing. *Nothobranchius* transgenic studies could strongly promote its development as new powerful genetic models in several science fields, from developmental biology to ageing research.

1.8. N. furzeri in neurobiological and aging research

Vertebrates represent a model organism widely employed in laboratory research. In fact they are very suitable for biomedical and veterinary studies directed in identifieng and understanding mechanisms

characterizing human diseases. Among vertebrates, fish constitute the largest group and as early as 1978 the use of fish in research showed great potential (Woodhead, 1978) for the relatively low cost of maintaining large numbers of individuals for lifetime studies, well-developed genetics, in addition to the fact that they possess organs and system similar to ones of other vertebrates. The most common model so far employed in research is zebrafish and it is the best-characterised animal at genetic level (Gerhard et al., 2003). However, zebrafish does not provide a suitable model for aging studies (Yu et al., 2006) mainly because of the long lifespan in laboratory conditions (~ 5 years, Gerhard et al., 2003).

Many *Cyprinodontiformes* like *Anablepidae*, *Goodeidae* and *Poecilidae* families are often used in biomedical research and for ecology, evolutionary and genomic studies. In the recent years *N. furzeri* has been proposed as new non-mammalian model system in many fields, especially in aging research (Terzibasi et al., 2007). The African turquoise killifish possess in fact the shortest life span (4-6 months) among vertebrates that can be cultured in laboratory and it reproduces very fast (14-20 days between the spawn and the hatch) in captivity too [Fig 9]. More generally, teleost fish are very similar to mammals in many aspects. They have a telomeric human-like structure, an amazing regenerative capacity, human-like organs and systems (blood, spleen, bones), evident aging related characters (mitochondrial functional decline, neurodegeneration). Moreover, unlike other fish, *N. furzeri* possess an XY chromosomes sex determination system. Another interesting aspect is that their eggs can be stored dry at room temperature (RT) for months, even years, offering inexpensive methods of embryo storage (Cellerino et al., 2016). Fish organs are characterized by a continuous turnover and cellular proliferation and differentiation that change with aging. Even their skin undergoes continuously to age-dependent cellular turnover, changes in caudal fin colouration, and variation in gene expression.

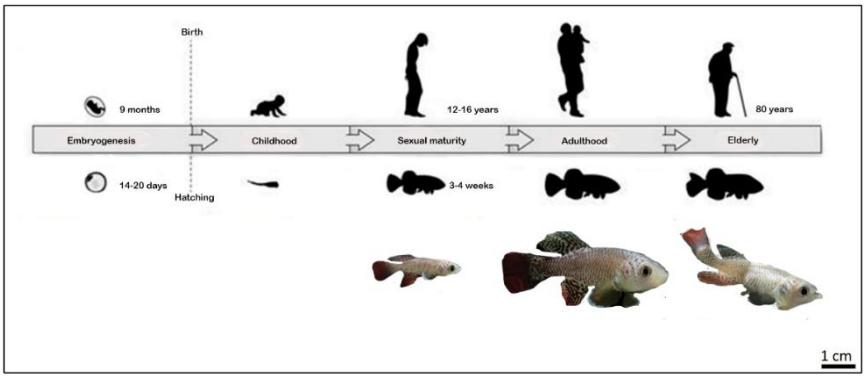

Fig 9 | N. furzeri complete life cycle. From fertilization to hatching (usually between 14 and 20 days), animals are referred to as 'embryos'. Freshly hatched fish are referred to as 'fry' for the first few days and shortly after they are referred to as 'juvenile fish' (until the animals reach sexual maturity). At the age of 20-30 days post hatching (dph), the animals reach sexual maturity and are considered adults. The life cycle (from 'egg to egg') of the turquoise killifish is 5-7 weeks. Source: adapted from Harel et al., 2016.

1.9. Fish brain structure

Fish brain is relatively small if compared to body size, except for some fish like mormyrid and sharks, which have a brain/body weight proportion like that of birds and marsupials (Helfman et al., 1997). The braincase may constrain brain size only in some of the smallest representatives of modern, perciform teleost. In most fish, however, the brain is considerably smaller than the space available and, in some cases, may occupy only about 6% of the brain cavity in an elasmobranch (Kruska, 1988). The excess space is commonly filled with lymphatic, fatty tissue (Kotrschal et al., 1998). Fish brain shows structures like mammals, and also their brain organization is overall similar, consisting of the three major regions of the forebrain, midbrain and hindbrain [Fig 10]. The telencephalon consists of paired cerebral hemispheres with olfactory bulbs attached to the rostral

hemispheres in most fish. The mesencephalon is capped by a pair of optic lobes (optic tectum), and the cerebellum arises from its rostral roof. Rostral, the spinal cord merges with the brain stem and tegmentum of mesencephalon and diencephalon (Kotrschal et al., 1998).

Forebrain performs functions associated with hormones and homeostasis. The pineal body lies just above the diencephalon. This structure detects light, maintains circadian rhythms, and controls color changes (Helfman et al., 1997). Forebrain olfactoy bulbs dimension depends of the development of smell sense (Kotrschal et al., 1998). Fish with larger olfactory bulbs are for example hagfish, catfish and sharks. Olfactory bulbs receive signals from one of two channels of the nose, the nostril, through the olfactory nerves (Helfman et al., 1997).

Midbrain dorsal region comprises the two optic lobes, which are very large in species that hunt by sight, such as rainbow trout and cichlids (Helfman et al., 1997).

Hindbrain division is particularly involved in swimming and balance (Helfman et al., 1997). It is divided in a rostro-dorsal area comprising the cerebellum, a rostro-ventral area comprising the pons and a caudal area comprising the medulla oblongata. Cerebellum is a single-lobed structure (Helfmann et al., 1997). Hagfish and lampreys have relatively small cerebellum, while the mormyrid cerebellum is massive and apparently involved in their electrical sense (Helfmann et al., 1997).

With few pathways descending from the brain, the motor system resides largely within the spinal cord except for several prominent brainstem reflexes (e.g. the Mauthner neuron system for escape (Kotrschal et al., 1998). Somatosensory information reaches the brain primarily via specialized cranial nerves, notably trigeminus (V), facialis (VII), vagus (X) and three lateral line nerves, two anterior and one posterior, rather than through ascending fiber systems of the spinal cord (Kotrschal et al., 1998).

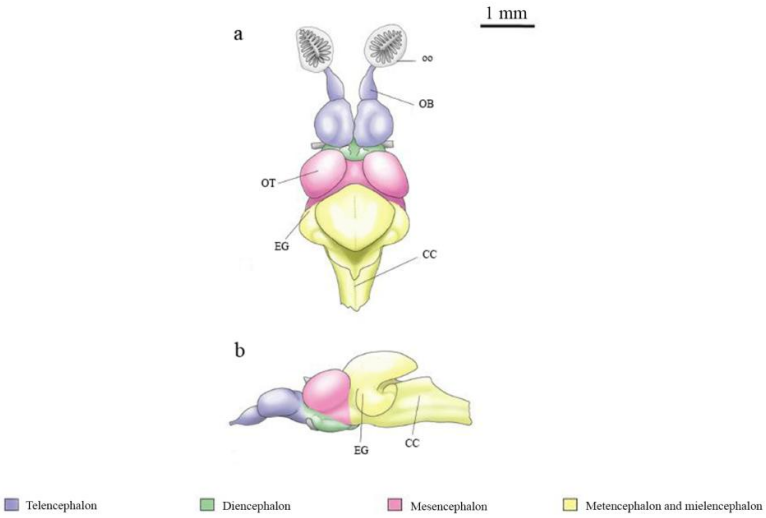

Fig 10 | Fish brain in dorsal (a) and lateral views (b). Abbreviations: CC, crista cerebellaris; EG, eminentia granularae; OB, olfactory bulbs; oo, olfactory organ; OT, optic tectum. Lateral view does not include olfactory organs.

1.10. Fish brain versus mammalian brain

Both fish and mammalian brains are broadly structured similarly, but, generally, fish brain is quite small relative to their body mass (~ 1/15 the brain mass of a similarly size bird or mammal. They share similar areas and structures, the ability to direct visual attention at targets to achieve a goal, ignoring distracting stimuli that prevent to reach the goal (Gabay et al., 2013), the response to fear and pain. To make a comparison between teleost and mammals brain, it is remarkable to notice two different way of embryonic development: evagination and eversion [Fig 11]. The evagination process occurs in mammals, while the eversion process is typical of teleost fish. Consequently, there is a shift in the position of some telencephalic areas: teleost dorsal telencephalic areas correspond to the

mammalian pallial formation; ventral telencephalic areas to the subpallium; dorso-lateral telencephalon to the medial pallium or hippocampus; the everted part of dorso-medial telencephalon corresponds to the dorsal pallium (isocortex homologue); the posterior zone of dorsal telencephalic area would be the lateral pallium (the olfactory cortex homologue); the midline portion of the medial zone of dorsal telencephalic area would correspond to the homologue of the pallial amygdala. The pallial masses ventral to dorso-lateral would not be everted (Wullimann and Mueller, 2004) [

Fig 12, *Tab 1*]. However, exists also a partial eversion theory of teleostean telencephalon, contrasting the complete eversion theory (Nieuwenhuys, 2009). According to this latter theory, the dorso-lateral telencephalon is homologous to the medial pallial formation, the ventro-dorsal and ventro-central to the striatal formation, and the ventro-ventral and ventro-lateral to the septal formation. Generally, fish forebrain is bigger and much more primitive than mammalian one; it is mostly associated with olfaction, which is the reason why olfactory bulbs are larger and acute than those of mammals. On the other hand, mammals have a highly developed cerebral cortex. In fish, cerebellum, is involved in both swimming and balance maintenance and represents the biggest structure in fish brain, while in mammals it takes up only about 15% of volume.

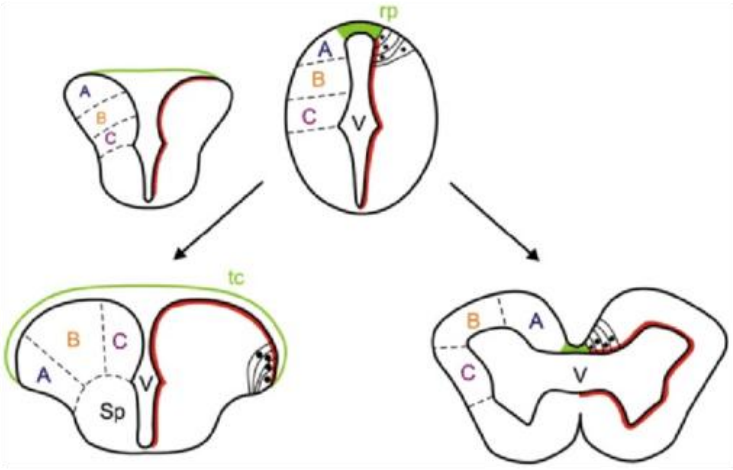

Fig 11 | Model for eversion (left) in teleost fish in contrast with evagination of telencephalic vesicles that occurs in other vertebrates (right). In teleost fish, it is thought that the dorsal region of the telencephalic neural tube (pallium) folds over the ventral region (subpallium), stretching the dorsal roof-plate region of the neural tube (green) to form the tela choroidea. This would also relocate some ventricular cells to the dorsal telencephalic surface (red line) and cause medial to lateral rearrangements of pallial regions (compare the location of regions A, B, and C between everted and evaginated telencephalon). Abbreviations: rp, roof plate; Sp, subpallium; tc, tela choroidea; V, ventricle. Source: Folgueira et al., 2012.

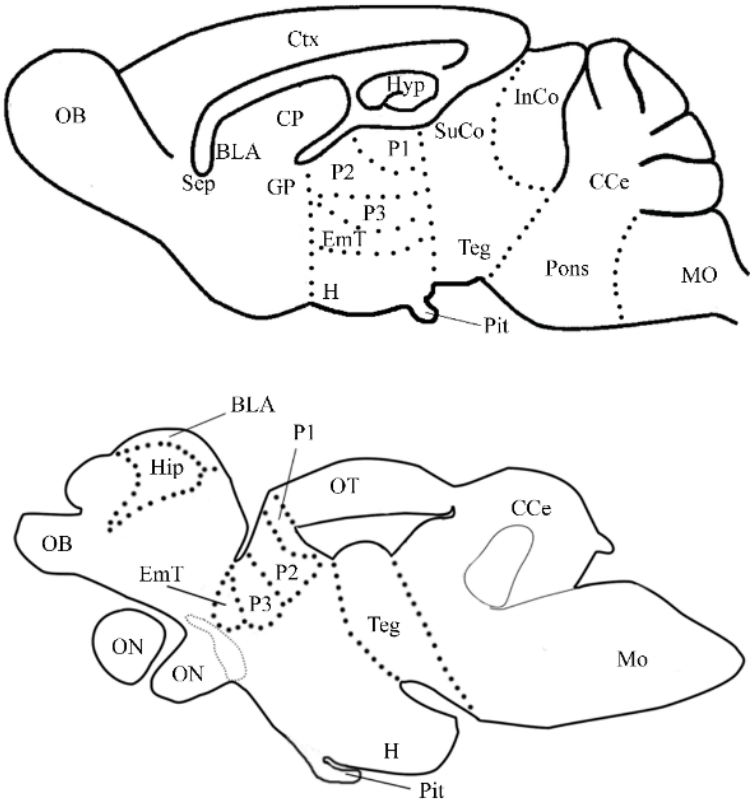

Fig 12 | Schematic representation of mammal (mouse) brain versus teleost (N. furzeri) brain. The massive difference is caused by the two different telencephalic development: eversion (teleost) and evagination (mammal). For this reason, mouse brain telencephalon shows two bilateral symmetric hemispheres surrounding by centrally located ventricles. In contrast, teleost telencephalon consists by two massive symmetric lobes covered by a dorsally located T-shaped ventricle. Teleost show a medial pallial region, homologous to the mammalian hippocampus (Hip), a dorsal pallial region, which corresponds to mammalian isocortex (Ctx), a ventral one corresponding to the mammalian amygdala (BLA), and a lateral pallial division corresponding to the piriform cortex (pirCtx). Abbreviations follow Muller et al., 2011.

Forebrain divisions	
Nothobranchius furzeri	**Mus musculus**
Dc1-2-3-4	Ctx
Dld-Dlv	Hyp
Dm1-2-3-4	BLA
Dp	pirCtx
Vd	Str
Vv	Sep

Tab 1 | Schematic correspondence between N. furzeri and M. musculus forebrain divisions.

1.11. N. furzeri brain structure

The basic morphology of *N. furzeri* brain has been described in the *N. Furzeri* brain atlas published in 2013 from D'Angelo. Anatomical structure and abbreviations will follow atlas nomenclature. Its brain structure resembles that of close teleost (Setiamarga et al., 2008) i.e. *Oryzias latipes* (Ishikawa et al., 1999), *Xiphophorus helleri* (Anken & Rahmann, 1994), *Fundulus heteroclitus* (Peter et al., 1975), with no significant morphological differences between males and females. The gross morphology of *N. furzeri* CNS is characterized by: two small and elongate olfactory bulbs (OB), placed anterior-ventrally to the small telencephalic hemispheres; the diencephalon with the large paired inferior lobes of hypothalamus, bulgs out on the ventral surface of the brain; two pronounced lobes of the optic tectum, dorsal to diencephalon most rostrally, and the midbrain tegmentum most caudally; a prominent body of cerebellum; large medulla oblongata [
Fig 13].

Forebrain is placed in the most rostral region of the CNS and includes the two sessile paired structures of the OB, interconnected via the medial olfactory tract and organised in concentric layers, and the two telencephalic hemispheres, distinguished in dorsal and ventral areas. OB most external layer is made of olfactory nerve fibers running towards the telencephalic hemispheres. Below this layer, there is the glomerular layer (GL), followed by the external cellular layer (ECL), containing the somata of secondary olfactory neurons projecting to the telencephalon. The deeper region is the internal cellular layer (ICL), a layer of small densely packed cells. The dorsal telencephalon is the homologous of the mammalian pallium and represents the everted region of the telencephalon. The ventral telencephalon is homologous of the mammalian subpallium. The dorsal area can be divided in medial (Dm), central (Dc), dorsal (Dd), lateral (Dl) and posterior (Dp) divisions. The lateral part of dorsal division is large and highly elaborated and includes dorsal part (Dld), ventral part (Dlv) and lateral part (Dll). In the ventral telencephalon of *N. furzeri*, four main sub-regions were observed, dorsal (Vd), ventral (Vv), supracommissural (Vs), and post-commissural (Vp). The subpallium is also characterized by medial (mfb) and lateral (lfb) fiber tracts. The diencephalon is located between the telencephalon and the mesencephalon and does not present precise boundaries with the telencephalon. The rostral region consists of the preoptic area (PP), partially covered by the caudal portions of the dorsal telencephalic divisions, while the caudal margin represents the pretectal area. The diencephalon is further subdivided into epithalamus, thalamus, hypothalamus, tuberal region, pretectum, and optic tracts. The PP surrounds the preoptic periventricular recess and is located between anterior commissure (Cant) and the optic chiasm. It forms a functional continuum with the most caudal tuberal hypothalamus. In this area, there are two important nuclei: the magnocellular preoptic nucleus (PM), dorsally in the periventricular zone, and the suprachiasmatic nucleus (SC) located in the superior part of the periventricular zone. The epithalamus represents the rostro-dorsal part of diencephalon and comprises the habenular nuclei (Ha) and the epiphysis. All these structures are involved in the synchronization of movement and in circadian rhythm cycle. The thalamus comprises the anterior (A), intermediate (I), posterior (DP) and

central posterior (CP) nuclei. Here are kept all the major sensory stimuli (except olfaction). The hypothalamus emerges ventrally to the caudal pole of the PP, and consists of (Hd) dorsal, ventral (Hv), lateral (Hl), and caudal (Hc) hypothalamic subdivisions, and the paired diffuse inferior lobes of hypothalamus (DIL), connected via the pituitary stalk, containing hypothalamic and preoptic neuroendocrine fibres, to the hypophysis. The pretectal region, is placed directly anteriorly to the rostral margin of the OT and includes both diencephalic and mesencephalic structures. Functionally, the pretectum may be characterised as a primarily visual region, receiving both retinal and tectal visual inputs. It comprises the central pretectal (CPN), the dorsal (DAO) and ventral (VAO) nuclei.

N. furzeri midbrain can be divided into two main regions: the OT, in the dorsal area, and the midbrain tegmentum, in ventromedial part. OT is involved in sensory functions and integration of messages from the optic tract with sensory information, with the combination and translation in coordination outputs. OT consists of two large lobes organized in layers. From the inner-out direction, we can distinguish the PGZ, the deep white zone (DWZ), the central zone (CZ) and the superficial white and gray zone (SWGZ). Rostrally, along the medial tectal margin, the paired longitudinal tori (Tl) are recognized, which are involved in perception of visual message from OT. The midbrain tegmentum, including the semicircular tori (TS1-4), lies at the caudal pole of the diencephalon and is placed above the inferior lobe of hypothalamus. In the dorsal zone, facing the ventricle, a structure, morphologically membranous appears well evident. This structure, not described in other teleost brain, is characterized by glial cells (D'Angelo et al., 2012). It thickens progressively along the ventral lines of mesencephalic ventricle, and, at the rhomboencephalic level, is replaced by the central griseum (gc). The more medial zone of the tegmentum is rostrally bounded by the nucleus of medial longitudinal fascicle (Nmlf), placed on the top of the medial longitudinal fascicle (mlf). The lateral region houses the lateral longitudinal fascicle (llf) and the respective nucleus (Nllf), placed dorsally, together with a number of fiber tracts. In the central and ventral areas of tegmentum, the mesencephalic reticular formation (RFmid), without well-defined margins, is identified, and caudally it continues with the rhomboencephalic reticular formation.

Hindbrain represents the most caudal part of the encephalon. It consists of dorso-cranial and ventro-caudal regions and comprises cerebellum, pons and medulla oblongata. The cerebellum, mainly responsible for coordinated movements, occupies the dorso-cranial region of rhomboencephalon and is characterized by the typical teleostean cerebellar subdivisions: the valvula (Va), the corpus of cerebellum (CCe), the granular eminentiae (EG) and cerebellar cristae (CC). The Va occupies most of the mesencephalic ventricle. More caudally, the CCe replaces the Va and shows a similar layer organization of Va, consisting of a molecular layer (ml) and a granular layer (gl) and the Purkinje cells layer. The two paired protuberances EG are apparently continuous with the gl of the CCe, and caudally, are placed at the lateral surface of the brain. The medulla oblongata is organized in four zones: dorsal, inter medio-dorsal, inter medio-ventral and ventral (Meek & Nieuwenhuys, 1998). The dorsal zone encompasses sensory component of trigeminal nucleus (NVs) and the nuclei belonging to the lateral area.

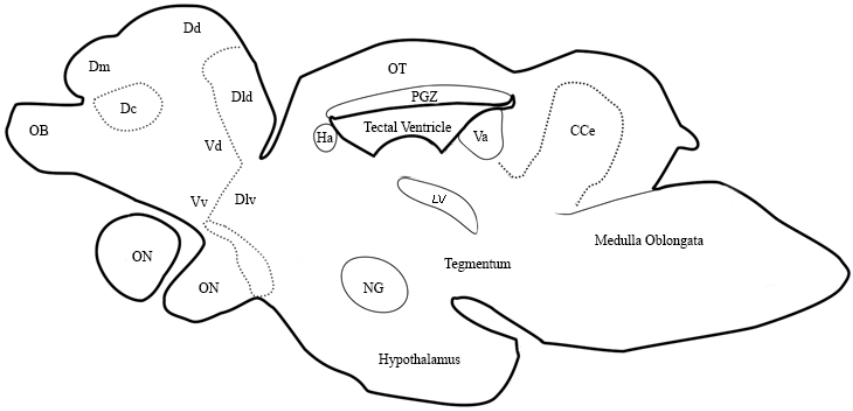

Fig 13 | Sagittal overview of N. furzeri brain. Abbreviations: Dc, central division of dorsal telencephalon; Dd, dorsal division of dorsal telencephalon; Dld, dorso-lateral division of dorsal telencephalon; Dlv, dorso-lateral division of ventral telencephalon; Dm, medial division of dorsal telencephalon; Ha, habenular nucleus; OB, olfactory bulb; ON, optic nerve; OT, optic tectum; NG, glomerular nucleus; CCe, corpus cerebellum; PGZ, periventricular gray zone; Va, valvula cerebellum; Vd, dorsal division of ventral telencephalon; Vv, ventral division of ventral telencephalon.

Allard, J. B., Kamei, H. and Duan, C. (2013) Inducible transgenic expression in the short-lived fish Nothobranchius furzeri. Journal of Fish Biology, 82, 1733-1738.

Anken RH, Rahmann H, 1996. Brian atlas of the adult swordtail fish *Xiphophorus helleri* and of certain developmental stages. Stuttgart: Gustav Fisher.

Bartakova, V., Reichard, M., Janko, K., Polacik, M., Blazek, R., Reichwald, K., Cellerino, A. and Bryja, J. (2013) Strong population genetic structuring in an annual fish, Nothobranchius furzeri, suggests multiple savannah refugia in southern Mozambique. Bmc Evolutionary Biology, 13.

Cellerino, A., Valenzano, D. R. and Reichard, M. (2016) From the bush to the bench: the annual Nothobranchius fishes as a new model system in biology. Biological Reviews, 91, 511-533.

D'Angelo, L. (2013) Brain Atlas of an Emerging Teleostean Model: Nothobranchius furzeri. Anatomical Record-Advances in Integrative Anatomy and Evolutionary Biology, 296, 681-691.

D'Angelo, L., de Girolamo, P., Cellerino, A., Tozzini, E. T., Varricchio, E., Castaldo, L. and Lucini, C. (2012) Immunolocalization of S100-Like Protein in the Brain of an Emerging Model Organism: Nothobranchius Furzeri. Microscopy Research and Technique, 75, 441-447.

Dorn, A., Musilova, Z., Platzer, M., Reichwald, K. and Cellerino, A. (2014) The strange case of East African annual fishes: aridification correlates with diversification for a savannah aquatic group? Bmc Evolutionary Biology, 14.

Folgueira, M., Bayley, P., Navratilova, P., Becker, T. S., Wilson, S. W. and Clarke, J. D. W. (2015) Morphogenesis underlying the development of the everted teleost telencephalon (vol 7, 32, 2012). Neural Development, 10.

Gabay, S., Leibovich, T., Ben-Simon, A., Henik, A. and Segev, R. (2013) Inhibition of return in the archer fish. Nature Communications, 4.

Genade, T. and Lang, D. M. (2013) Resveratrol extends lifespan and preserves glia but not neurons of the Nothobranchius guentheri optic tectum. Experimental Gerontology, 48, 202-212.

Gerhard, G. S. (2003) Comparative aspects of zebrafish (Danio rerio) as a model for aging research. Experimental Gerontology, 38, 1333-

1341.
Graham CF, Morgan RW, 1966. Changes in the cell cycle during early amphibian development. Dev Bio 14, 3: 439-460.
Hartmann, N. and Englert, C. (2012) A microinjection protocol for the generation of transgenic killifish (Species: Nothobranchius furzeri). Developmental Dynamics, 241, 1133-1141.
Helfman GS, Collette BB, Facey DE, 1997. The diversity of fishes. *Review* Animal Conservation, 1,2: 151.
Hrbek, T. and Larson, A. (1999) The evolution of diapause in the killifish family Rivulidae (Atherinomorpha, Cyprinodontiformes): A molecular phylogenetic and biogeographic perspective. Evolution, 53, 1200-1216.
Hsu, C. Y. and Chiu, Y. C. (2009) Ambient temperature influences aging in an annual fish (Nothobranchius rachovii). Aging Cell, 8, 726-737.
Ishikawa, Y., Yoshimoto, M., Yamamoto, N. and Ito, H. (1999) Different brain morphologies from different genotypes in a single teleost species, the medaka (Oryzias latipes). Brain Behavior and Evolution, 53, 2-9.
Kotrschal, K., Van Staaden, M. J. and Huber, R. (1998) Fish brains: evolution and environmental relationships. Reviews in Fish Biology and Fisheries, 8, 373-408.
Kruska, D. C. T. (1988) THE BRAIN OF THE BASKING SHARK (CETORHINUS-MAXIMUS). Brain Behavior and Evolution, 32, 353-363.
Litjens, R. A. J., Quickenden, T. I. and Freeman, C. G. (1999) Visible and near-ultraviolet absorption spectrum of liquid water. Applied Optics, 38, 1216-1223.
Lucas-Sanchez, A., Almaida-Pagan, P. F., Mendiola, P. and de Costa, J. (2014) Nothobranchius as a model for aging studies. A review. Aging and Disease, 5, 281-291.
Meer H, Nieuwenhuys R, 1998. The central nervous system of vertebrates, vol. 2, Springer-Verlag, Berlin. pp 759-937.
Mueller, T., Dong, Z. Q., Berberoglu, M. A. and Guo, S. (2011) The dorsal pallium in zebrafish, Danio rerio (Cyprinidae, Teleostei). Brain Research, 1381, 95-105.
Murphy, W. J. and Collier, G. E. (1997) A molecular phylogeny for

aplocheiloid fishes (Atherinomorpha, Cyprinodontiformes): The role of vicariance and the origins of annualism. Molecular Biology and Evolution, 14, 790-799.

Nieuwenhuys, R. (2009) The Forebrain of Actinopterygians Revisited. Brain Behavior and Evolution, 73, 229-252.

Petzold, A., Reichwald, K., Groth, M., Taudien, S., Hartmann, N., Priebe, S., Shagin, D., Englert, C. and Platzer, M. (2013) The transcript catalogue of the short-lived fish Nothobranchius furzeri provides insights into age-dependent changes of mRNA levels. Bmc Genomics, 14.

Peter RE, Macey MJ, Gill VE, 1975. A stereotaxic atlas and technique for forebrain nuclei of the killifish, *Fundulus heteroclitus*. J Comp Neurol. 159: 103-127.

Polacik, M., Blazek, R. and Reichard, M. (2016) Laboratory breeding of the short-lived annual killifish Nothobranchius furzeri. Nature Protocols, 11, 1396-1413.

Polacik, M., Donner, M. T. and Reichard, M. (2011) Age structure of annual Nothobranchius fishes in Mozambique: is there a hatching synchrony? Journal of Fish Biology, 78, 796-809.

Promislow, D. E. L., Montgomerie, R. and Martin, T. E. (1992) MORTALITY COSTS OF SEXUAL DIMORPHISM IN BIRDS. Proceedings of the Royal Society B-Biological Sciences, 250, 143-150.

Reichard, M., Polacik, M., Blazek, R. and Vrtilek, M. (2014) Female bias in the adult sex ratio of African annual fishes: interspecific differences, seasonal trends and environmental predictors. Evolutionary Ecology, 28, 1105-1120.

Reichard, M., Polacik, M. and Sedlacek, O. (2009) Distribution, colour polymorphism and habitat use of the African killifish Nothobranchius furzeri, the vertebrate with the shortest life span. Journal of Fish Biology, 74, 198-212.

Reichwald, K., Petzold, A., Koch, P., Downie, B. R., Hartmann, N., Pietsch, S., Baumgart, M., Chalopin, D., Felder, M., Bens, M., Sahm, A., Szafranski, K., Taudien, S., Groth, M., Arisi, I., Weise, A., Bhatt, S. S., Sharma, V., Kraus, J. M., Schmid, F., Priebe, S., Liehr, T., Gorlach, M., Than, M. E., Hiller, M., Kestler, H. A., Volff, J. N., Schartl, M., Cellerino, A., Englert, C. and Platzer, M.

(2015) Insights into Sex Chromosome Evolution and Aging from the Genome of a Short-Lived Fish. Cell, 163, 1527-1538.

Rosenthal, G. G., Martinez, T. Y. F., de Leon, F. J. G. and Ryan, M. J. (2001) Shared preferences by predators and females for male ornaments in swordtails. American Naturalist, 158, 146-154.

Sedlacek, O., Baciakova, B. and Kratochvil, L. (2014) Evolution of body colouration in killifishes (Cyprinodontiformes: Aplocheilidae, Nothobranchiidae, Rivulidae): Is male ornamentation. constrained by intersexual genetic correlation? Zoologischer Anzeiger, 253, 207-215.

Setiamarga, D. H. E., Miya, M., Yamanoue, Y., Mabuchi, K., Satoh, T. P., Inoue, J. G. and Nishida, M. (2008) Interrelationships of Atherinomorpha (medakas, flyingfishes, killifishes, silversides, and their relatives): The first evidence based on whole mitogenome sequences. Molecular Phylogenetics and Evolution, 49, 598-605.

Sung, Y. H., Kim, J. M., Kim, H. T., Lee, J., Jeon, J., Jin, Y., Choi, J. H., Ban, Y. H., Ha, S. J., Kim, C. H., Lee, H. W. and Kim, J. S. (2014) Highly efficient gene knockout in mice and zebrafish with RNA-guided endonucleases. Genome Research, 24, 125-131.

Terzibasi, E., Lefrancois, C., Domenici, P., Hartmann, N., Graf, M. and Cellerino, A. (2009) Effects of dietary restriction on mortality and age-related phenotypes in the short-lived fish Nothobranchius furzeri. Aging Cell, 8, 88-99.

Terzibasi, E., Valenzano, D. R. and Cellerino, A. (2007) The short-lived fish Nothobranchius furzeri as a new model system for aging studies. Experimental Gerontology, 42, 81-89.

Tobler, M., Schlupp, I. and Plath, M. (2007) Predation of a cave fish (Poecilia mexicana, Poeciliidae) by a giant water-bug (Belostoma, Belostomatidae) in a Mexican sulphur cave. Ecological Entomology, 32, 492-495.

Tobler, M., Schlupp, I. and Plath, M. (2008) Does divergence in female mate choice affect male size distributions in two cave fish populations? Biology Letters, 4, 452-454.

Tozzini, E. T., Dorn, A., Ng'oma, E., Polacik, M., Blazek, R., Reichwald, K., Petzold, A., Watters, B., Reichard, M. and Cellerino, A. (2013) Parallel evolution of senescence in annual fishes in response to extrinsic mortality. Bmc Evolutionary Biology, 13.

Valenzano, D. R., Kirschner, J., Kamber, R. A., Zhang, E., Weber, D., Cellerino, A., Englert, C., Platzer, M., Reichwald, K. and Brunet, A. (2009) Mapping Loci Associated With Tail Color and Sex Determination in the Short-Lived Fish Nothobranchius furzeri. Genetics, 183, 1385-1395.

Valenzano, D. R., Sharp, S. and Brunet, A. (2011) Transposon-Mediated Transgenesis in the Short-Lived African Killifish Nothobranchius furzeri, a Vertebrate Model for Aging. G3-Genes Genomes Genetics, 1, 531-538.

Valenzano, D. R., Terzibasi, E., Cattaneo, A., Domenici, L. and Cellerino, A. (2006a) Temperature affects longevity and age-related locomotor and cognitive decay in the short-lived fish Nothobranchius furzeri. Aging Cell, 5, 275-278.

Valenzano, D. R., Terzibasi, E., Genade, T., Cattaneo, A., Domenici, L. and Cellerino, A. (2006b) Resveratrol prolongs lifespan and retards the onset of age-related markers in a short-lived vertebrate. Current Biology, 16, 296-300.

Weindruch, R. (1996) Caloric restriction and aging. Scientific American, 274, 46-52.

Woodhead AD, 1978. Fish in studies of aging. Exp Geront, 13: 125-140.

Wullimann, M. F. and Mueller, T. (2004) Teleostean and mammalian forebrains contrasted: Evidence from genes to behavior (vol 475, pg 143, 2004). Journal of Comparative Neurology, 478, 427-428.

Yu, B. P. and Chung, H. Y. (2006) Adaptive mechanisms to oxidative stress during aging. Mechanisms of Ageing and Development, 127, 436-443.

Yu, X. and Li, G. R. (2012) Effects of resveratrol on longevity, cognitive ability and aging-related histological markers in the annual fish Nothobranchius guentheri. Experimental Gerontology, 47, 940-949.

Zu, Y., Tong, X. J., Wang, Z. X., Liu, D., Pan, R. C., Li, Z., Hu, Y. Y., Luo, Z., Huang, P., Wu, Q., Zhu, Z. Y., Zhang, B. and Lin, S. (2013) TALEN-mediated precise genome modification by homologous recombination in zebrafish. Nature Methods, 10, 329-331.

Chapter 2

Neurogenesis in vertebrates' brain: focus on teleost fish

2. Neurogenesis in vertebrates' brain: focus on teleost fish

The term "neurogenesis" refers to the differentiation of neural stem cells (NCSs) in neural precursors with distinct fates. In vertebrates, it occurs not only during embryonic development (primary neruogenesis) but also during adulthood (secondary neurogenesis) (Alvarez-Buylla and Kirn, 1997; Doetsch and Scharff, 2001; Zupanc, 2001).
Embryonic or primary neurogenesis occurs during development of the CNS begins with the induction of the neuroectoderm, which forms the neural plate and then folds to give rise to the neural tube. These structures host a heterogeneous population of neuroepithelial early progenitor cells (NEPs) dividing symmetrically during the embryonic development to extend NSCs population. NEPs undergo to asymmetric division, giving birth to intermediate neuronal progenitors, which subsequently differentiate in various types of neurons: radial glial restricted progenitors cells, which can differentiate in astrocytes and oligodendrocytes, and neuronal restricted progenitors cells, which can differentiate in adult neurons.
Adult neurogenesis, also known as secondary neurogenesis, is a process observed in many species and consists in the functional capacity of generating neurons from neural cells precursors. The first anatomical evidence of adult neurogenesis dates to 1965 when it was detected the presence of newly generating neurons from dentate granule cells in rat postnatal hippocampus (Altman and Das, 1965).

2.1. Adult neurogenesis in vertebrates

Adult neurogenesis is influenced and can be induced by different stimuli and factors, like injuries (Gould, 2007), pathologies and drugs. It is strictly linked to aging (Lee et al., 2000), decreasing exponentially with aging in rodents (Kuhn et al., 1996), dogs (Pekcec et al., 2008) and humans (Knoth et al., 2010). In mammals, under normal conditions, adult neurogenesis is spatially restricted into the two brain regions of the SGZ and SVZ [Fig 14]

(Reynolds and Weiss, 1992; Reichards et al., 1992; Eriksson et al., 1998; Gage, 2000). SGZ and SVZ contain microenvironments that anatomically house stem cells and functionally control their development in vivo (Ming and Song, 2011). These regions are called niches (Schofield, 1978) and their major components are endothelial cells, ependymal cells, astrocytes, microglia, mature neurons and progeny of neural precursors (Ming and Song, 2011). The whole process of hippocampal neurogenesis is physically localized to the dentate gyrus. In addition, the SGZ is enriched with different nerve terminals and subjected to dynamic circuit activity-dependent regulation through different neurotransmitters. In the SGZ of rodents, new granule neurons are produced during adulthood (Altman and Das, 1965; Cameron et al., 1993; Kaplan and Bell, 1984; Seri et al., 2001). In contrast, the SVZ does not reside within a dense neuronal network and is physically segregated from OB where integration of new neurons occurs (Ming and Song, 2011). In rodents and songbirds, adult neurogenesis in the SVZ lead to the production of new cells, destined to distinct telencephalic regions (Altman, 1969; Luskin, 1993; Lois and Alvarez- Buylla, 1994). In rodents and some primates, the neuroblasts tangentially migrate from the SVZ to the OB in long chains that are often enveloped by a tunnel of astrocytes (Lois et al., 1996). This stream of neuroblasts tangentially and rostrally migrating is often referred to as the rostral migratory stream (RMS) [Fig 14]. When cells reach OB, neuroblasts migrate radially away from the RMS. Vascular cells play an important role in regulating proliferation of adult neural stem cells (aNSCs) precursors. In the adult SGZ, dense cluster of dividing cells was found to be anatomically close to the vasculature, especially capillaries (Palmer et al., 2000). In the adult SVZ, vasculature comprises an extensive network of planar interconnected blood vessels (Shen et al., 2008; Tavazoie et al., 2008). The vasculature also provides the substrate for new neurons migration after injury in the adult striatum (Kojima et al., 2010). They may serve as an interface to modulate influences of endothelial and circulation-derived factors as well as the availability of cytokines and growth factors in the basal lamina (Ming and Song, 2011). Via feedback, new-born progeny can regulate the behaviour of neural precursors. In both adult SVZ and SGZ, quiescent radial glia-like cells are rapidly activated to support continuous

neurogenesis (Doetsch et al., 1999; Seri et al., 2001). In the adult SVZ, neuroblasts, through neurotransmitters releasing, stimulate the activation of aNSCs and induce a decrease in proliferation (Liu et al., 2005). Net brain growth occurs during adulthood also in reptiles, amphibians and fish (Kaslin et al., 2008). The forebrain of lizards shows an age- and bodyweight-dependent increase in neuronal numbers (Grandel et al., 2006).

Adult neurogenesis is regulated by different mechanism, both intrinsic and extrinsic. Between the extracellular players there are several morphogens which act as niche signals to regulate maintenance, activation and fate choice of aNSCs (i.e. Shh and BMPs). Growth factors, neurotrophins, cytokines and hormones are also major regulation of adult neurogenesis (Zhao et al., review, 2008). Among neurotransmitters, γ-aminobutyric acid, glutamate and acetylcholine, directly regulate migration, maturation, integration, and survival of newborn neurons (Ming and Song, 2011). Among the intracellular players there are cell cycle regulators, transcription factors and epigenetic regulators (Zhao et al., 2008). There are also many players associated with neurological disorders. The deletion of the doublecortin (DCX) gene for example, causes severe morphologic defects (Koizumi et al., 2006). DCX gene in fact codifies for a microtubule associated protein and is specifically expressed from neuroblasts and neural precursors of both embryonic and adult brain. In the adult SGZ, physical exercise increases cell proliferation (van Praag et al., 1999), while an enriched environment promotes new neuron survival (Kempermann et al., 1997). Stroke induces cell proliferation and migration of newborn neurons to infarct sites, the clear majority of which fail to survive over the long term, presumably due to a lack of functional connections and trophic support (Arvidsson et al., 2002). In both insulin-deficient rats and insulin-resistant mice, diabetes impairs cell proliferation in the adult SGZ through a glucocorticoid-mediated mechanism (Stranahan et al., 2008). Inflammation is a negative regulator of adult neurogenesis when induced by injuries, degenerative neurological diseases, and irradiation (reviewed by Carpentier and Palmer, 2009).

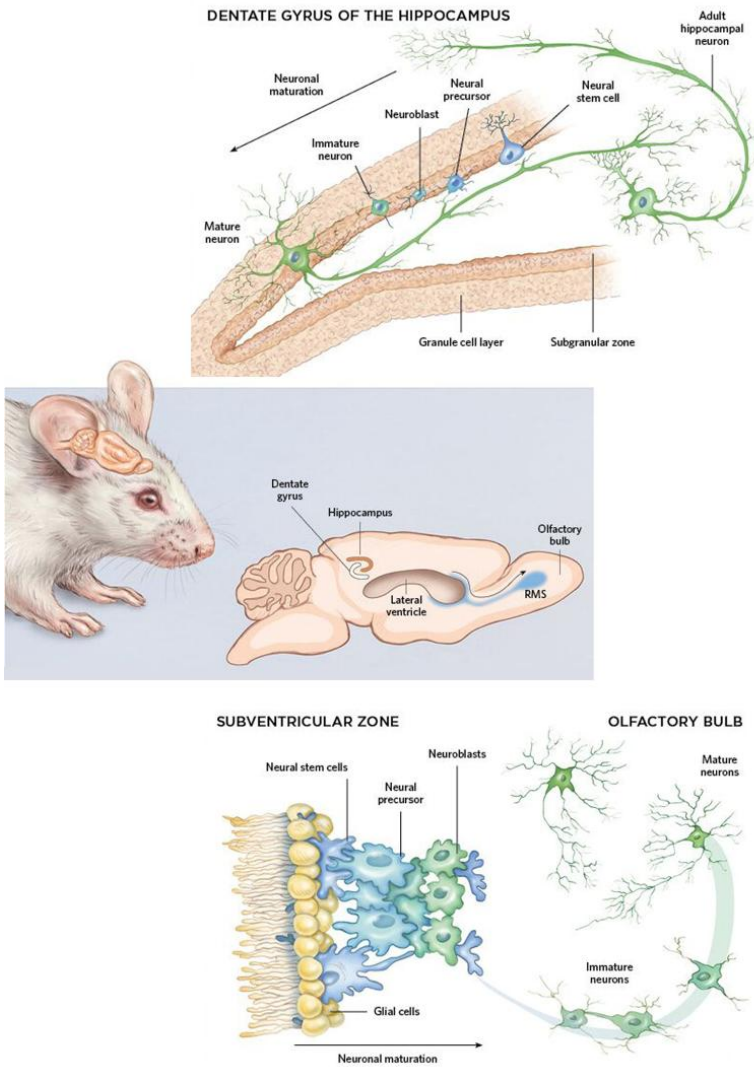

Fig 14 | Example of adult neurogenesis in rodents. In the rodent SGZ, neural stem cells differentiate into neuroblasts before maturing and integrating with hippocampal circuits involved in learning and memory. In SVZ, neural stem cells differentiate into neuroblasts, which make their way to the olfactory bulb, where they complete their development. Source: adapted from The Scientist – Exploring life, inspiring innovation, Oct 1, 2015, Jef Akst.

2.2. Adult neurogenesis in teleost fish

It has long been known that brains of adult teleost fish show widespread cell proliferation in all subdivisions along its rostro-caudal axis (Zupanc and Horschke, 1995, Zupanc et al., 2005, Ekström et al., 2001). The generation of new cells may in fact account for the lifelong brain growth observed in different fish species (Brandstätter and Kotrschal, 1990), together with the ability of regenerate neurons after injuries (Zupanc et al., 2011). This feature is common in all the species so far studied: guppy (*Poecilia reticulata*) (Kranz & Richter, 1970), brown ghost knife fish (*Apteronotus leptorhynchus*) (Zupanc & Horschke, 1995), gilt-head sea bream (*Sparus aurata*) (Zikopoulos et al., 2000), three-spined stickleback (*Gasterosteus aculeatus*) (Ekström et al., 2001), zebrafish (Zupanc et al., 2005; Grandel et al., 2006), and the annual killifish *Austrolebias* sp. (Fernández et al., 2011). In teleost fish brain, more than 10 distinct adult proliferative zones have been identified: OB, telencephalon, thalamus, epithalamus, PP, hypothalamus, tectum, cerebellum, rhomboencephalon, and spinal cord (Kaslin et al., 2008). In the adult zebrafish, 16 distinct constitutively proliferating domains were identified along the whole rostro-caudal brain axis [Fig 15] (Grandel et al., 2006). Most of the cells generated in these regions, seem to migrate slowly and later differentiate into neurons (Zupanc et al., 2005; Grandel et al. 2006). In the telencephalon, some of the produced neurons differentiate into glutamic acid decarboxylase, tyrosine hydroxylase and parvalbuminic neurons (Grandel et al., 2006), while in the diencephalon both serotonin and tyrosine hydroxylase-containing neurons, of which some are long projecting, are generated (Grandel et al., 2006). Teleost neurogenic niches, particularly ones belonging to the telencephalon and diencephalon, are located at or near the surfaces of ventricles, while cerebellar proliferation zones are distant from any ventricle (Zupanc et al., 2011).

In the OB, scattered proliferating cells are distributed throughout the bulbs, where cycling cells are dispersed in the anterior part, and clustered ones are accumulated along the dorsal surface, near the attachment region to the dorsal telencephalic area (Grandel et al., 2006).

In the telencephalon, distinct proliferation zones can be discerned both in the dorsal and the ventral areas: anterior to Cant, a prominent ventral proliferation zone is located along the ventricular surface; close to the OB, it spans the ventricular territory adjacent to the Vv and Vd; rostrally, it is especially massive along the Vv; further posteriorly, this proliferation domain leaves the ventricular zone adjacent to Vv and remains restricted to the ventricular zone adjacent to Vd where it becomes less prominent towards the Cant.

In the mesencephalon it is possible to recognize two proliferation zones: OT and Tl. The tectal proliferation zone runs around the margin of the OT. It starts anterior-dorsally at the level of the posterior commissure, surrounds the tectal commissure further caudally and continues around the posterior tectal tip. Tl is located below the tectal commissure, in the tectal ventricle. Proliferating cells are founded along the ventricular surface of the torus, distinctly separated from the dorsomedial tectal proliferation domain depending level (Grandel et al., 2006).

A characteristic feature of the adult teleost brain is that the largest relative numbers of new cells are generated in the cerebellum. Quantitative analysis has shown that approximately 75% of adult-born cells in the brain originate from the various subdivisions of the cerebellum (Zupanc & Horschke, 1995; Hinsch & Zupanc, 2007). Young cells may either reside near the respective proliferation zone or migrate to specific target areas. Approximately half of the newly generated cells persist for the rest of the life, and many of them differentiate into neurons (Zupanc et al., 2011). In CCe and Va, newborn neurons are generated in the ml and then they migrate over several hundred micrometers into the associated gl (Zupanc et al., 1996, 2005). Surrounding the rhomboencephalic ventricle below the caudal part of CCe, a ventricular proliferation domain emerges. Proliferating cells can be followed from there across the gl of the caudal lobe towards its surface. At the caudal tip of the cerebellum, the caudal lobe forms a cap of gl cells covered by proliferating cells.

Based on the labeling of S-phase cells with the thymidine analog 5-bromo-2'-deoxyuridine, quantitative analysis of the rate of cell proliferation in the whole brain has been performed in two species: *A. leptorhynchus*, a weakly electric fish of the order *Gymnotiformes*, and the *Cypriniformes*

zebrafish. In the brain of *A. leptorhynchus*, 100 000 cells, on average, are generated within any 2 hours period (Zupanc & Horschke, 1995). In zebrafish brain, approximately 6000 cells are produced within any 30 minutes period (Hinsch & Zupanc, 2007). From a comparative point of view, the most interesting neurogenic regions are OB, Dl, Dp. In fact, part of the Dl of teleost is thought to be homologous to the mammalian hippocampus (Nieuwenhuys & Meek, 1990; Northcutt, 1995; Butler, 2000; Vargas et al., 2000; Rodríguez et al., 2002; Portavella et al., 2004). The existence of proliferation zones in these regions suggests that adult neurogenesis in the mammalian OB and the hippocampus is a conserved trait of vertebrates (Zupanc, 2006).

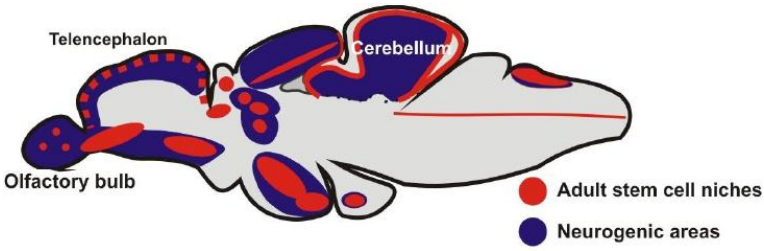

Fig 15 | Neurogenic regions of the zebrafish brain. Stem cell niches are more abundant than in mammals and distributed along the whole rostro-caudal brain axis. Source: adapted from Kizil, 2011.

2.3. Adult neurogenesis in the short-lived teleost Nothobranchius furzeri

As a teleost, *N. furzeri* shows the same neurogenic niches described so far. In the telencephalon, neurogenic areas can be distinguished in the telencephalic subventricular region, homologous of mammalian SVZ. aNSCs are also scattered in both dorsal and ventral telencephalic surfaces (Tozzini et al., 2012). High proliferating activity is observed in the PP

segment of the ventricular system, along the midline surface and the caudal margin of cerebellum, and lining the fourth ventricle (Tozzini et al., 2012).
According to the double labeling with 5-ethynyl-2'-deoxyuridine and proliferating cell nuclear antigen (PCNA), nine different neurogenic regions were identified in *N. furzeri* adult brain: I, telencephalic proliferative niche corresponding to the thin line of highly packed proliferating cells which connect the two telencephalic hemispheres, and extend from the dorsal to the ventral surface; II, niche corresponding to the most rostral region of ventral telencephalon; III, niche corresponding to the most caudal region of telencephalon; IV, PP proliferative niche of the ventricular system; V, dorso-medial proliferative niche of optic area; VI, caudal and ventral proliferative niches of optic area; VII, dorsal midline niches of the cerebellum; VIII, dorso-caudal proliferative niche of the cerebellum; IX, caudal margins of the cerebellum and of the IV ventricle (Tozzini et al, 2012) [Fig 15].
Regions I, II and III correspond to telencephalic neurogenic niches [Fig 16 a, b, c]. Region I starts from the rostral telencephalic area, extends to the third ventricle in caudal direction. Region II corresponds to the dorso-lateral zone of ventral telencephalon. Region III is located near the dorso-lateral and posterior zones of dorsal telencephalon. Region IV corresponds to the ventricular system in the PP [Fig 16 a, d, e]. Here neurogenic niches were observed widespread along the ventricle, in the hypothalamus and caudally to the medulla oblongata and spinal cord. Region V corresponds to the medial margin of OT, at the border with Tl. Region VI extends from the dorsal posterior to the ventral margin of the OT, including the SGZ of the OT. Cerebellar neurogenic niches are comprised in region VII and VIII [Fig 16 a, e]. Its medial region contains numerous highly active cells, increasing dorsally and decreasing ventrally in rostro-caudal direction. In fact, in the most caudal region of CCe, only the posterior area is visible. A rod of dividing cells in the Va connects dorsal and ventral neurogenic niches (Tozzini et al., 2012).

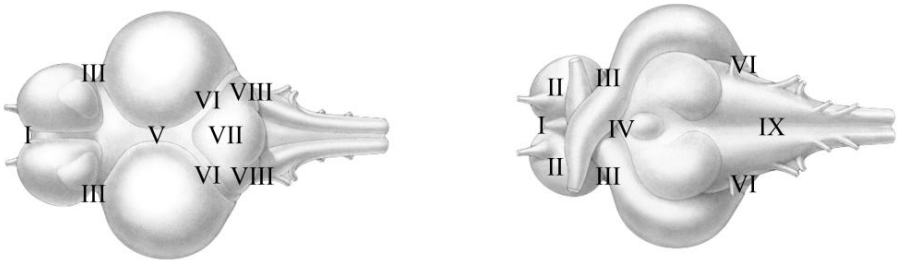

Fig 16 | Adult neurogenic niches distribution in the short-lived teleost N. furzeri, dorsal (a) and ventral (b) view. I = telencephalic proliferative niche extending from the dorsal to the ventral thin line which connects the two telencephalic hemispheres. II, III = telencephalic proliferative niches corresponding repectively to the ventral zone and to the most caudal lateral margin of telencephalic hemispheres. IV = preoptic proliferative niche. V = rostro-dorsal part of the proliferative niche in the optic tectum. VI = caudal part of the proliferative niche in the optic tectum. VII = medial proliferative niche of the cerebellum. VIII = caudal proliferative niche of the cerebellum. IX = caudal proliferative niche along the roof of the IV ventricle. Source: adapted from Tozzini et al., 2012.

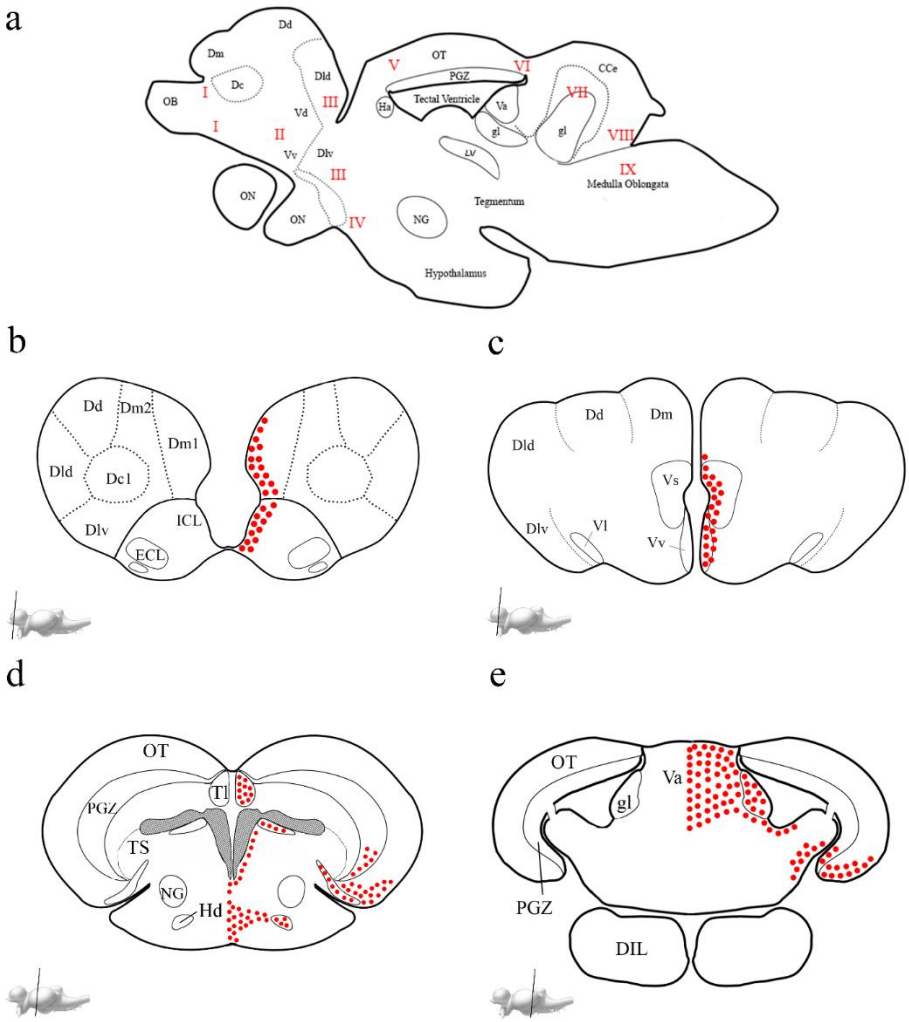

Fig 17 | Schematic depiction (red dots) of N. furzeri adult major neurogenic niches. (a) Parasagittal view of whole brain and transversal section of rostral (b) and caudal (c) telencephalon, optic tectum (d) and cerebellum (e). Source: adapted from D'Angelo, 2013 and D'Angelo et al., 2018. Abbreviations: I = telencephalic proliferative niche corresponding to the subpallial region. II, III = telencephalic proliferative niches corresponding to the pallial region. IV = preoptic proliferative niche. V = rostro-dorsal part of the proliferative niche in the optic tectum. VI = caudal part of the proliferative niche in the optic tectum. VII = medial proliferative niche of the cerebellum. VIII =

caudal proliferative niche of the cerebellum. IX = caudal proliferative niche along the roof of the IV ventricle; Dc, central division of dorsal telencephalon; Dd, dorsal division of dorsal telencephalon; Dld, dorso-lateral division of dorsal telencephalon; Dlv, dorso-lateral division of ventral telencephalon; Dm, medial division of dorsal telencephalon; ECL, external cellular layer; gl, glomerular layer of cerebellum; Ha, habenular nucleus; Hd, dorsal hypothalamus; ICL, internal cellular layer; OB, olfactory bulb; ON, optic nerve; OT, optic tectum; NG, glomerular nucleus; CCe, corpus cerebellum; PGZ, periventricular gray zone; Tl, longitudinal tori; TS, layers of semicircular tori; Va, valvula cerebellum; Vd, dorsal division of ventral telencephalon; Vl, lateral division of ventral telencephalon; Vv, ventral division of ventral telencephalon; Vs, supracommissural zone of ventral telencephalon.

2.4. Adult neurogenesis in the aging brain

Aging leads to a significant decline in neuronal production. Mammalian brain is perhaps the organ with the lowest regenerative potential but the one in which the signs of aging are more manifested (Artegiani and Calegari, 2012). In mammals, an age-related decline has been observed in cell proliferation of both adult SGZ and SVZ. In rat and mice SGZ the reduction in production of new neurons is about 80% or more and occurs relatively early in the aging process. In fact, the greatest decline in adult neurogenesis in SGZ occurs by middle age whereas in later senescence, there is just a modest additional decline (Bondolfi et al., 2004). In SVZ as in the hippocampus, the greatest reduction in cell genesis occurs between young adulthood and middle age (Luo et al., 2006). Furthermore, during aging, neurogenesis in the SVZ becomes restricted to the Dl area of the lateral ventricle. In OB, the aging-related reduction in the appearance of newborn neurons is greater than the decline in proliferation within the SVZ.

Age related neurogenic decline reflects into the decreasing of progenitor cells, cell survival, neuronal commitment and differentiation. With aging, proliferation rate of progenitor cells become slower and/or less frequent division of a constant population of progenitors, and/or changes in cell cycle kinetics. Quantitative analysis of cell division in both SGZ and SVZ of young adult and old rats, have shown a reduction of 50-90% rate

(McDonald and Wojtowicz, 2005). Aging can also alter the balance of cell death among undifferentiated, differentiating, and mature cells in a manner that is not apparent with currently available methods (Riddle and Lichtenwalner, 2007). In young adult rats, 50% of newborn (BrdU-labeled) cells in the dentate gyrus of hippocampus die within 28 days after labeling (Riddle and Lichtenwalner, 2007). In addition, the development of new neurons is compromised in older animals.
The list of factors influencing adult neurogenesis is large, diverse, and ever growing (for review see Hagg, 2005). Stress hormones, like corticosteroids, are negative regulators of adult neurogenesis effecting on proliferation rate (Mirescu and Gould, 2006). The growth hormone/insulin-like growth factor-1 axis is another mediator of aging-related changes characterizing adult neurogenesis. In fact it appears to regulate angiogenesis (Sonntag et al., 1997). Furthermore, neurogenesis decreases with hypophysectomy, which decreases levels of growth hormone and other pituitary hormones (Aberg et al., 2000). As growth hormone/insulin-like growth factor-1 acts fibroblast growth factor 2.

2.5. Neural cells: from progenitors to mature neurons

Stem cells are defined by the self-renewal capacity and the potential to generate all cell types (Taverna et al., 2014). In the CNS, stem cells give rise to neurons and various glial cell types. In the developing mammalian forebrain, only neuroepithelial cells (NE) and their direct progeny, the apical radial glial cells, self-renew for several rounds of cell division (Taverna et al., 2014). NE cells are the first neural cells forming during embryonic development: they symmetrically divide forming the neural plate and tube during embryonic development. During neurogenesis, NE cells differentiate into radial glial cells. Some of the apical radial glia may persist beyond development and, depending on their location, may function in adult neurogenesis. However, few of these apical radial glial cells generate cells other than neurons and are multipotent (Malatesta et al. 2000, Pinto & Gotz 2007), with the remaining generating neurons only. This is the case even when apical radial glial cells are taken out of their

environment and either cultured in conditions favouring multipotency or transplanted into an environment favouring specific lineages (Taverna et al., 2014). Thus, both NE and apical radial glia are a mixture of cells with a variable extent of fate restriction. Radial glial cells asymmetrically divide producing one radial glia cell and one intermediate progenitor cell, which differentiate into post-mitotic immature neurons and migrate to their final destination in the nervous system and integrate into the neuronal network. Oligodendrocyte and Schwann cells are responsible for the production of myelin respectively in the in peripheral nervous system (PNS) and CNS. A particular type of star shaped glial cells is the astrocyte. Astrocytes serve a wide variety of functions in the CNS, which are vital for brain development, physiology and pathology. The terminally differentiated cells of CNS are mature neurons. These cells are no longer able to divide, and their function is to receive process and transfer information in CNS and PNS.

2.6. Main neural cells markers

2.6.1. Proliferating cell nuclear antigen (PCNA)

PCNA is a protein expressed during DNA synthesis, which helps to anchor the DNA polymerase δ to the DNA filament during its replication. Depending on the replication phase, it is expressed from different district. During the G1/G2 phases it is equally distributed over the whole nucleus; during the early S phase it assumes a granular distribution and it is absent from nucleoli; in late S phase it is expressed in the nucleoli; finally, in the M phase it displaces from the condensed chromosomes.
PCNA distribution pattern in teleost fish has been already described in Par 2.3, when describing the main neurogenic niches. Briefly, proliferating adult areas are well distributed in the whole encephalon: rostrally in the OB and in its contact area with the telencephalon, in the ventral telencephalic area, preoptic regions, thalamic area, OT, Tl, tectal ventricle, Va, CCe, ml, and gl [
Fig *18*].

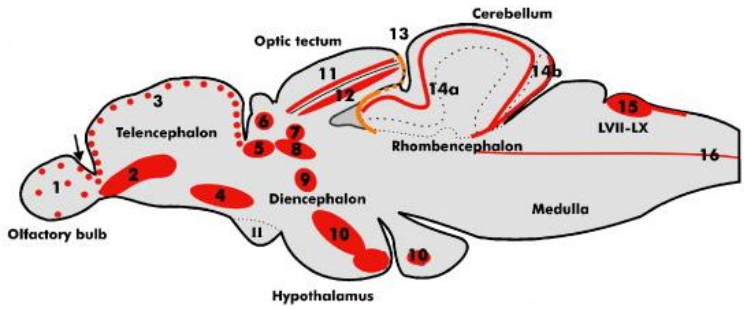

Fig 18 | Depiction of PCNA positive cells (red dots) in zebrafish brain. (1) scattered proliferating cells in the OB; (2, 3) telencephalic proliferation zones; (4) preoptic proliferation zone; (5, 8), thalamic proliferating areas; (6) habenular proliferating region; (7) pretectal proliferating area; (9), posterior tubercular proliferating zone; (10), hypothalamic proliferating zone; (11) tectal and (12) torus longitudinalis proliferation zones; (13) posterior mesencephalic lamina connects the tectum to the cerebellum; (14a) molecular layer proliferation zone extending through the valvula and copus cerebelli; (14b) proliferation zone of the cerebellar caudal lobe extending from the ventricular lumen through the granular layer to its surface; (15) proliferation zones in the medulla oblongata in the facial (LVII) and vagal (LX) lobes extending caudally into the nucleus of Cajal; (16) rhombencephalic ventricular proliferation zone extends into the spinal cord. (Grandel et al., 2006).

2.6.2. S100

S100 proteins belong to the superfamily of S100/calmodulin/troponin C, characterized by a low-molecular weight, and two calcium-binding sites having helix-loop-helix conformations. Anti-S100 identifies cells derived from the neural crest like Schwann cells, melanocytes and glial cells. S100 proteins play an important role in the regulation of the neuronal differentiation, glial proliferation, plasticity, development, axonal growth, and in neurogenic processes (D'Angelo et al., 2012).

2.6.3. Doublecortex (DCX)

DCX is a protein associated with microtubule in neuronal precursor cells and immature neurons in embryonic and adult cortical substructure. In mammals, DCX is expressed by neuroblasts and newly generated neurons (Brown et al., 2003). A DCX orthologue is present neither in the assembled zebrafish genome nor in the collections of zebrafish expressed sequence tags. *N. furzeri* possesses a DCX transcript, which was called NfuDCX and shows 86.5 % similarity with the aminoacidic sequence of mouse (Tozzini et al., 2012). Furthermore, a DCX gene is also present in the genomes of the *Actynopterigyan* fish *Gastrosteleus aculeatus*, *Tetradon nigroviridis*, and *Takifugu rubripes*.

2.6.4. HuC/D

The Elav/HuC/D proteins belong to a family of RNA-binding proteins required for neural differentiation and maintenance. They are expressed in neurons from early development at about the time that they leave the mitotic cycle, and still persist in mature neurons. HuC is also known as ELAV (embryonic lethal abnormal visual system) like protein 3, while HuD is also known as ELAV-like protein 4. HuC and HuD contain three binding domains enabling to bind the RNA, are expressed only in neurons and they bind to AU-rich-elements containing mRNAs.

2.6.5. Tyrosine Hydroxylase (TH)

Tyrosine Hydroxylase is an enzyme expressed throughout the CNS, which converts the L-tyrosine to L-3, 4- dihydroxyphenylalanine, the precursor for dopamine, which, in turn, is the precursor for norepinephrine and epinephrine. Hence, it is used as marker for mature dopaminergic neurons. Furthermore, it is also used as marker of neurogenic rate because of the age-related decreasing production of dopaminergic neurons (Grandel et al., 2006).

Aberg, M. A. I., Aberg, N. D., Hedbacker, H., Oscarsson, J. and Eriksson, P. S. (2000) Peripheral infusion of IGF-I selectively induces neurogenesis in the adult rat hippocampus. Journal of Neuroscience, 20, 2896-2903.

AlvarezBuylla, A. and Kirn, J. R. (1997) Birth, migration, incorporation, and death of vocal control neurons in adult songbirds. Journal of Neurobiology, 33, 585-601.

Altman J, Das GD, 1965. Autoradiographic and histological evidence of postnatal hippocampal neurogenesis in rats. Journal of Comparative Neurology, 124: 3.

Artegiani, B. and Calegari, F. (2012) Age-related cognitive decline: Can neural stem cells help us? Aging-Us, 4, 176-186.

Arvidsson, A., Collin, T., Kirik, D., Kokaia, Z. and Lindvall, O. (2002) Neuronal replacement from endogenous precursors in the adult brain after stroke. Nature Medicine, 8, 963-970.

Bondolfi, L., Ermini, F., Long, J. M., Ingram, D. K. and Jucker, M. (2004) Impact of age and caloric restriction on neurogenesis in the dentate gyrus of C57BL/6 mice. Neurobiology of Aging, 25, 333-340.

Brown, J. P., Couillard-Despres, S., Cooper-Kuhn, C. M., Winkler, J., Aigner, L. and Kuhn, H. G. (2003) Transient expression of doublecortin during adult neurogenesis. Journal of Comparative Neurology, 467, 1-10.

Cameron, H. A., Woolley, C. S., McEwen, B. S. and Gould, E. (1993) DIFFERENTIATION OF NEWLY BORN NEURONS AND GLIA IN THE DENTATE GYRUS OF THE ADULT-RAT. Neuroscience, 56, 337-344.

Carpentier, P. A. and Palmer, T. D. (2009) Immune Influence on Adult Neural Stem Cell Regulation and Function. Neuron, 64, 79-92.

D'Angelo, L. (2013) Brain Atlas of an Emerging Teleostean Model: Nothobranchius furzeri. Anatomical Record-Advances in Integrative Anatomy and Evolutionary Biology, 296, 681-691.

D'Angelo, L., de Girolamo, P., Cellerino, A., Tozzini, E. T., Varricchio, E., Castaldo, L. and Lucini, C. (2012) Immunolocalization of S100-Like Protein in the Brain of an Emerging Model Organism: Nothobranchius Furzeri. Microscopy Research and Technique, 75, 441-447.

Doetsch, F., Caille, I., Lim, D. A., Garcia-Verdugo, J. M. and Alvarez-

Buylla, A. (1999) Subventricular zone astrocytes are neural stem cells in the adult mammalian brain. Cell, 97, 703-716.

Doetsch, F. and Scharff, C. (2001) Challenges for brain repair: Insights from adult neurogenesis in birds and mammals. Brain Behavior and Evolution, 58, 306-322.

Ekstrom, P., Johnsson, C. M. and Ohlin, L. M. (2001) Ventricular proliferation zones in the brain of an adult teleost fish and their relation to neuromeres and migration (secondary matrix) zones. Journal of Comparative Neurology, 436, 92-110.

Eriksson, P. S., Perfilieva, E., Bjork-Eriksson, T., Alborn, A. M., Nordborg, C., Peterson, D. A. and Gage, F. H. (1998) Neurogenesis in the adult human hippocampus. Nature Medicine, 4, 1313-1317.

Fernandez, A. S., Rosillo, J. C., Casanova, G. and Olivera-Bravo, S. (2011) PROLIFERATION ZONES IN THE BRAIN OF ADULT FISH AUSTROLEBIAS (CYPRINODONTIFORM: RIVULIDAE): A COMPARATIVE STUDY. Neuroscience, 189, 12-24.

Gage, F. H. (2000) Mammalian neural stem cells. Science, 287, 1433-1438.

Gould, E. (2007) Opinion - How widespread is adult neurogenesis in mammals? Nature Reviews Neuroscience, 8, 481-488.

Grandel, H., Kaslin, J., Ganz, J., Wenzel, I. and Brand, M. (2006) Neural stem cells and neurogenesis in the adult zebrafish brain: Origin, proliferation dynamics, migration and cell fate. Developmental Biology, 295, 263-277.

Hagg, T. (2005) Molecular regulation of adult CNS neurogenesis: an integrated view. Trends in Neurosciences, 28, 589-595.

Hinsch, K. and Zupanc, G. K. H. (2007) Generation and long-term persistence of new neurons in the adult zebrafish brain: A quantitative analysis. Neuroscience, 146, 679-696.

Kaplan MS, Bell DH, 1984. Mitotic neuroblasts in the 9-day-old and 11-month-old rodent hippocampus. Journ of Neuros, 4 (6), 1429-1441.

Kaslin, J., Ganz, J. and Brand, M. (2008) Proliferation, neurogenesis and regeneration in the non-mammalian vertebrate brain. Philosophical Transactions of the Royal Society B-Biological Sciences, 363, 101-122.

Kempermann, G., Kuhn, H. G. and Gage, F. H. (1997) More hippocampal

neurons in adult mice living in an enriched environment. Nature, 386, 493-495.

Knoth, R., Singec, I., Ditter, M., Pantazis, G., Capetian, P., Meyer, R. P., Horvat, V., Volk, B. and Kempermann, G. (2010) Murine Features of Neurogenesis in the Human Hippocampus across the Lifespan from 0 to 100 Years. Plos One, 5.

Koizumi, H., Higginbotham, H., Poon, T., Tanaka, T., Brinkman, B. C. and Gleeson, J. G. (2006) Doublecortin maintains bipolar shape and nuclear translocation during migration in the adult forebrain. Nature Neuroscience, 9, 779-786.

Kojima, T., Hirota, Y., Ema, M., Takahashi, S., Miyoshi, I., Okano, H. and Sawamoto, K. (2010) Subventricular Zone-Derived Neural Progenitor Cells Migrate Along a Blood Vessel Scaffold Toward the Post-stroke Striatum. Stem Cells, 28, 545-554.

Kuhn, H. G., DickinsonAnson, H. and Gage, F. H. (1996) Neurogenesis in the dentate gyrus of the adult rat: Age-related decrease of neuronal progenitor proliferation. Journal of Neuroscience, 16, 2027-2033.

Lee, C. K., Weindruch, R. and Prolla, T. A. (2000) Gene-expression profile of the ageing brain in mice. Nature Genetics, 25, 294-297.

Liu, X. X., Wang, Q., Haydar, T. F. and Bordey, A. (2005) Nonsynaptic GABA signaling in postnatal subventricular zone controls proliferation of GFAP-expressing progenitors. Nature Neuroscience, 8, 1179-1187.

Lois, C. and Alvarezbuylla, A. (1994) LONG-DISTANCE NEURONAL MIGRATION IN THE ADULT MAMMALIAN BRAIN. Science, 264, 1145-1148.

Lois, C., GarciaVerdugo, J. M. and AlvarezBuylla, A. (1996) Chain migration of neuronal precursors. Science, 271, 978-981.

Luo, J., Daniels, S. B., Lennington, J. B., Notti, R. Q. and Conover, J. C. (2006) The aging neurogenic subventricular zone. Aging Cell, 5, 139-152.

Luskin, M. B. (1993) RESTRICTED PROLIFERATION AND MIGRATION OF POSTNATALLY GENERATED NEURONS DERIVED FROM THE FOREBRAIN SUBVENTRICULAR ZONE. Neuron, 11, 173-189.

Malatesta, P., Hartfuss, E. and Gotz, M. (2000) Isolation of radial glial cells by fluorescent-activated cell sorting reveals a neuronal

lineage. Development, 127, 5253-5263.
McDonald, H. Y. and Wojtowicz, J. M. (2005) Dynamics of neurogenesis in the dentate gyrus of adult rats. Neuroscience Letters, 385, 70-75.
Ming, G. L. and Song, H. J. (2011) Adult Neurogenesis in the Mammalian Brain: Significant Answers and Significant Questions. Neuron, 70, 687-702.
Mirescu, C. and Gould, E. (2006) Stress and adult neurogenesis. Hippocampus, 16, 233-238.
Northcutt, R. G. (1995) THE FOREBRAIN OF GNATHOSTOMES - IN SEARCH OF A MORPHOTYPE. Brain Behavior and Evolution, 46, 275-318.
Nieuwenhuys R, Meek J. 1990. The telencephalon of actinoptery-gian fishes. In: Jones EG, Peter A, editors. Cerebral cortex. New York: Plenum Press. 31–73.
Palmer, T. D., Willhoite, A. R. and Gage, F. H. (2000) Vascular niche for adult hippocampal neurogenesis. Journal of Comparative Neurology, 425, 479-494.
Pekcec, A., Baumgartner, W., Bankstahl, J. P., Stein, V. M. and Potschka, H. (2008) Effect of aging on neurogenesis in the canine brain. Aging Cell, 7, 368-374.
Pinto, L. and Gotz, M. (2007) Radial glial cell heterogeneity - The source of diverse progeny in the CNS. Progress in Neurobiology, 83, 2-23.
Portavella, M., Torres, B. and Salas, C. (2004) Avoidance response in goldfish: Emotional and temporal involvement of medial and lateral telencephalic pallium. Journal of Neuroscience, 24, 2335-2342.
Reynolds, B. A. and Weiss, S. (1992) GENERATION OF NEURONS AND ASTROCYTES FROM ISOLATED CELLS OF THE ADULT MAMMALIAN CENTRAL-NERVOUS-SYSTEM. Science, 255, 1707-1710.
Richards, L. J., Kilpatrick, T. J. and Bartlett, P. F. (1992) DENOVO GENERATION OF NEURONAL CELLS FROM THE ADULT-MOUSE BRAIN. Proceedings of the National Academy of Sciences of the United States of America, 89, 8591-8595.
Riddle DR, Lichtenwalner RJ, 2007. Neurogenesis in the adult and aging brain.
Rodriguez, F., Lopez, J. C., Vargas, J. P., Gomez, Y., Broglio, C. and

Salas, C. (2002) Conservation of spatial memory function in the pallial forebrain of reptiles and ray-finned fishes. Journal of Neuroscience, 22, 2894-2903.

Schofield R, 1978. The relationship between the spleen colony-forming cell and the hemopoietic stem cell. A hypothesis. Blood Cells, 4, 4-7.

Seri, B., Garcia-Verdugo, J. M., McEwen, B. S. and Alvarez-Buylla, A. (2001) Astrocytes give rise to new neurons in the adult mammalian hippocampus. Journal of Neuroscience, 21, 7153-7160.

Shen, Q., Wang, Y., Kokovay, E., Lin, G., Chuang, S. M., Goderie, S. K., Roysam, B. and Temple, S. (2008) Adult SVZ stem cells lie in a vascular niche: A quantitative analysis of niche cell-cell interactions. Cell Stem Cell, 3, 289-300.

Sonntag, W. E., Lynch, C. D., Cooney, P. T. and Hutchins, P. M. (1997) Decreases in cerebral microvasculature with age are associated with the decline in growth hormone and insulin-like growth factor 1. Endocrinology, 138, 3515-3520.

Stranahan, A. M., Norman, E. D., Lee, K., Cutler, R. G., Telljohann, R. S., Egan, J. M. and Mattson, M. P. (2008) Diet-Induced Insulin Resistance Impairs Hippocampal Synaptic Plasticity and Cognition in Middle-Aged Rats. Hippocampus, 18, 1085-1088.

Tavazoie, M., Van der Veken, L., Silva-Vargas, V., Louissaint, M., Colonna, L., Zaidi, B., Garcia-Verdugo, J. M. and Doetsch, F. (2008) A specialized vascular niche for adult neural stem cells. Cell Stem Cell, 3, 279-288.

Taverna, E., Gotz, M. and Huttner, A. B. (2014) The Cell Biology of Neurogenesis: Toward an Understanding of the Development and Evolution of the Neocortex. Annual Review of Cell and Developmental Biology, Vol 30, 30, 465-502.

Tozzini, E. T., Baumgart, M., Battistoni, G. and Cellerino, A. (2012) Adult neurogenesis in the short-lived teleost Nothobranchius furzeri: localization of neurogenic niches, molecular characterization and effects of aging. Aging Cell, 11, 241-251.

van Praag, H., Kempermann, G. and Gage, F. H. (1999) Running increases cell proliferation and neurogenesis in the adult mouse dentate gyrus. Nature Neuroscience, 2, 266-270.

Zhao, C. M., Deng, W. and Gage, F. H. (2008) Mechanisms and functional

implications of adult neurogenesis. Cell, 132, 645-660.
Zupanc, G. K. H. (2001) Adult neurogenesis and neuronal regeneration in the central nervous system of teleost fish. Brain Behavior and Evolution, 58, 250-275.
Zupanc, G. K. H., Hinsch, K. and Gage, F. H. (2005) Proliferation, migration, neuronal differentiation, and long-term survival of new cells in the adult zebrafish brain. Journal of Comparative Neurology, 488, 290-319.
Zupanc, G. K. H. and Horschke, I. (1995) PROLIFERATION ZONES IN THE BRAIN OF ADULT GYMNOTIFORM FISH - A QUANTITATIVE MAPPING STUDY. Journal of Comparative Neurology, 353, 213-233.
Zupanc, G. K. H. and Sirbulescu, R. F. (2011) Adult neurogenesis and neuronal regeneration in the central nervous system of teleost fish. European Journal of Neuroscience, 34, 917-929.

Chapter 3

Aim of the study

3. Aim of the study

Studies on genome-wide transcript regulation have shown common features in vertebrates' brain. Both rodents and humans are characterized, during aging, by a down-regulation of synaptic and axonal protein coding genes, an increased activity of the polycomb repressive complex, and reduced adult neurogenesis (Loerch et al., 2008; Horvath et al., 2012; Kempermann, 2011). Analyses on the entire postnatal life, have demonstrated that these processes, characterizing aging brain, are either the continuation, or the inversion, of events started during embryonic development (Somel et al., 2010; Colantuoni et al., 2011). Unfortunately, no sufficient data are available on gene regulation during aging in fish. In 2014, Baumgart and co-workers have quantified *N. furzeri* genome wide transcript regulation by means of RNA-Seq analysis. Comparison between human and *N. furzeri* data revealed conserved regulation of many complexes and organs. Up-regulation is conserved for ribosome, lysosome, and complement activation, while down-regulation is conserved for synapse, mitochondrion, proteasome, and spliceosome.

Taking these studies in balance and bearing in mind genes already described in literature to be involved in both primary and secondary neurogenesis, in this research in-depth studies on three differentially expressed genes (DEGs) have been took: collagen type IV α 1 chain (*Col4a1*), collagen type XXV α 1 chain (*Col25a1*), and the inhibitor of DNA binding 3 (*Id3*). Moreover, *Id3* in *N. furzeri* has been also annotated as positive selected gene during aging. Specifically, in this survey is proposed the evaluation of the three DEGs quantitative expression in young and old specimens, their morphological identification in both young and old animals, and their involvement in adult neurogenesis by the characterization of cells type expressing Col4a1, Col25a1, and Id3 mRNAs.

3.1. Differentially expressed and positive selected genes in N. furzeri

DEGs in *N. furzeri* were identified by means of three independent statistical tests (Baumgart et al., 2014). The availability of high-quality genomic references facilitates the identification of genes under positive selection. In fact, the search of signature for positive selection in protein-coding sequences has become a standard analysis to apply when new genomes or transcriptomes become available (Sahm et al., 2016). In 2015, Reichwald et al., have further analysed genomic clustering of aging-related genes, identifying genes under positive selection, and revealing significant similarities of gene expression profiles between diapause and aging, particularly for genes controlling cell cycle and translation. Furthermore, they analysed also whether there were similar gene expression changes in diapause and aging, focusing on genes showing a monotonic increase or decrease of transcript levels in aging. They have shown a significantly high number of genes which are either down- or up-regulated in both aging and diapause. In contrast to previous hypothesis (Tozzini et al., 2012), it was demonstrated that translational elongation and ribonucleoprotein complex biogenesis are the two major processes enriched in upregulated genes during diapause and aging (Reichwald et al., 2015).

3.2. Collagen molecules

Collagen is the most abundant protein in animals' connective tissue. It is synthetized as pre-pro-collagen from different cells type depending on the tissue (fibroblasts in connective tissue, osteoblasts in bones, etc.). Collagen main structure consists of amino acids wound together forming a triple helix structure. Protein translation takes place in ribosomes, close to the lumen of the rough endoplasmic reticulum (RER), in which are produced two types of pre-pro-collagen chain, α-1 and α-2, characterized by both N- and C -terminals. Then, when lysines and prolines are hydroxylated and hydroxylisines are glycosylated, the pre-pro-chains become pro-collagen.

Pro-collagen shows the typical triple helix structure: between α-chains C-terminals peptides, disulphide bridges are formed that take α-chains in a favourable position that lead to the formation of the triple helix structure. Pro-collagen is then transferred into the Golgi, where it is completed the glycosylation and the molecules are transported in the extra-cellular space into vesicles. Here, pro-collagen's N and C-terminals are removed by peptidases and the neo formed molecule is called tropo-collagen, which maintains the triple helix structure. Tropo-collagen molecules aggregate to each other in parallel and offset way, called fibrils. Fibrils can arrange in wavy or parallel bundles forming collagen fibers, and fibers can aggregate to form fibers bundles [Fig 19] (Champe, Harvey, Ferrier, Biochemistry). There are many types of collagen, but only 28 types have been described in literature so far. However over 90% of the collagen in the human body is type I. Collagen types can be divided into several groups according to the structure forming: fibrillary (type I, II, III, V, XI), short chain (type VIII, X), basement membrane (type IV), multiplexin (multiple triple helix domains with interruptions) (type XV, XVIII), MACIT (Membrane Associated Collagens with Interrupted Triple Helices) (type XIII, XVII), other (type VI, VII, IX, XII, XIV, XVI, XIX-XXVIII).

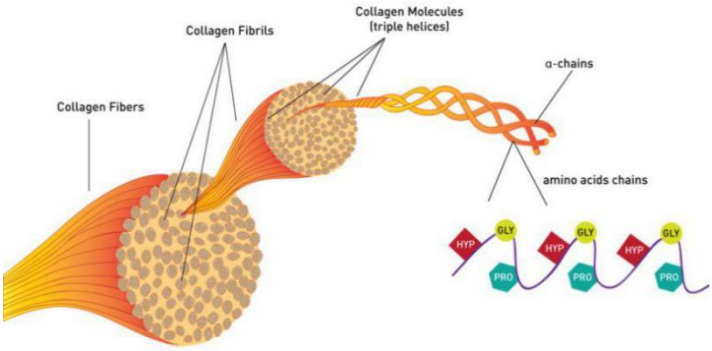

Fig 19 | Collagen structure. Pre-pro-collagen chains are characterized by both N and C -terminals. After post tradutional modfications, pre-pro- become pro-collagen (triple helix structure). N- and C-terminals are removed forming tropo-collagen, which aggregate to each other in parallel and offset fibrils. Fibrils can arrange in wavy or parallel bundles forming collagen fibers, and fibers can aggregate to form fibers bundles.

3.2.1. Collagen type IV alpha 1 chain (Col4a1)

Collagen type IV is one of the most common type of collagen. It forms the basal lamina, the epithelium-secreted layer of the basement membrane, which second component is the reticular connective tissue. It is a laminar structure of extracellular matrix (ECM) with a thickness between 70 and 300 nm and it is always comprised between connective and epithelial tissue. In fact, its primary function is to anchor the epithelium to the loose connective tissue (dermis) underneath. Notable examples of basement membranes are the glomerular kidney's one and the alveolar basement membrane, which is where oxygen and CO_2 diffusion happens. Basement membranes can also be found enveloping capillary endothelia, muscle fibers, adipocytes, but also in peripheral nerves, externally to the Schwann cells. It acts as mechanical barrier and is essential for angiogenesis, in fact its proteins have been found to accelerate differentiation of endothelial cells, but it is involved also in processes such as blood filtration and muscle homeostasis maintenance (Kubota et al., 1988; Pozzi et al., 2017).
For all these reasons it is clear how type IV collagen interacts with many cells, growth factors and other basement membrane components such as laminin, nidogenin and perlecan (Karsdal et al., 2017). Six different α chains of type IV collagen are expressed in vertebrates, named α1- α6, encoded by the genes *Col4a1-Col4a6* (Karsdal et al., 2017). Collagenous domain of type IV collagen differs from the other ones as it contains 21–26 characteristic interruptions of the proline-rich Gly-Xaa-Yaa triple repeat (Khoshnoodi et al., 2008). These frequent interruptions result in a less rigid structure and provide type IV collagen with extensive flexibility that enables the formation of a network and may allow for specific proteolytic cleavages of the triple helix or serve as sites of cell binding and interchain crosslinking (Vandenberg et al., 1991). Three α chains self-assemble into a heterotrimeric protomer by the association of their globular C-terminal non-collagenous (NC) 1 domains and the subsequent supercoiling of the triple helical domains in a zipper-like manner. The association of the NC1 domain is stabilized by domain-swapping interactions (Sundaramoorthy et al., 2002), and the presence of recognition sequences ensures the formation

of only three different protomer isoforms: α1α1α2 (IV), α3α4α5 (IV), and α5α5α6 (IV) (Boutaud et al., 2000). After secretion to the ECM, protomers self-assemble into complex lattice-shaped networks. The NC1 domain of two protomers associate end-to-end, forming an NC1 hexamer, and the 7S domains of four protomers form a 7S tetramer (Timpl et al., 1981). The N-terminal collagenous 7S domain is rich in cysteine and lysine residues that stabilize the 7S tetramer by forming disulphide bonds and lysine–hydroxylysine crosslinks. Furthermore, the 7S tetramer is heavily glycosylated, making it resistant to collagenase activity (Risteli et al., 1980). The type IV collagen networks consist of α1α1α2 (IV), α3α4α5 (IV), or a combination of α1α1α2 (IV) and α5α5α6 (IV) connected through their NC1 domains (Borza et al., 2001). The predominant network α1α1α2 (IV) is found in basement membranes of all tissues, but it is replaced by the other networks in restricted tissue throughout embryonic development. The network α3α4α5 (IV) has a major degree of crosslinking and resistance than α1α1α2 (IV) one. It has been identified in the glomerular basement membrane of the kidney and in the alveolar basement membrane of the lung as well as in basement membranes of testis, inner ear cochlea, and eye. α5α5α6 (IV) network is expressed in the basement membrane of the bronchial epithelium, smooth muscle cells, skin, and Bowman capsule and tubular basement membrane of the kidney (Karsdal et al., 2017).

Inherited mutations in the genes encoding different type IV collagen α chains have been implicated in several severe diseases mainly showing cerebrovascular and renal manifestations. Mutations in the genes encoding for α1 (IV) and α2 (IV) chains are mainly expressed as vascular defects resulting in intracerebral haemorrhages and intracranial aneurysms (Gould et al., 2006). Mutations in *Col4a1* gene lead to patients with familial porencephaly, intracerebral haemorrhage, haemorrhagic stroke, small-vessel disease, intracranial aneurysms, HANAC syndrome and retinal artery tortuosity, causing a systemic phenotype due to the widespread distribution of the α1 (IV) chain and involving renal, vascular, and ocular manifestations (Plaisier et al., 2007). Patients retain a fetal distribution of the α1α1α2 (IV) network instead of switching to α3α4α5 (IV) during development, leaving especially the glomerular basement membrane

susceptible to proteolytic degradation (Kalluri et al., 1997). Type IV collagen is the target of two autoimmune diseases affecting the kidney: Goodpasture syndrome and Alport post transplantation disease. Both diseases are characterized by autoantibodies attacking the glomerular basement membrane and causing rapidly progressive glomerulonephritis (Chen et al., 2012).

3.2.2. Collagen type XXV alpha 1 chain (Col25a1)

Collagen type XXV alpha 1 chain (Col25a1), also known as Alzheimer's amyloid plaque component precursor, is a collagenous type II transmembrane protein purified from senile plaques of Alzheimer's diseased (AD) brains (Tong et al., 2010). It is specifically expressed in brain. In fact, Real Time Polymerase Chain Reaction (RT-PCR) experiments confirmed the brain specific expression of *Col25a1* both in human and murine tissues (Hashimoto et al., 2002). *In situ* hybridization experiments have shown that in murine brain *Col25a1* is a specifically collagen of neurons of cerebral neocortices, hippocampus and other subcortical neuronal nuclei (Hashimoto et al., 2002). Lower expression was detected in heart, testis and eye (Hashimoto et al., 2002).
In AD brains it co-localizes with αβ in senile plaques (Hashimoto et al., 2002), but its contribution to the pathogenesis of AD and in vivo function are unknown (Tong et al., 2010). *Col25a1* encodes for a protein precursor called collagenous Alzheimer amyloid plaque component precursor (CLAC-P). CLAC-P domain structure and aminoacidic sequences are partially homologous to those of *Col13a1*. CLAC is the fragment deriving from the proteolytic cleavage by furin convertase, and the N-terminus is pyroglutamate modified (Hashimoto et al., 2002). CLAC shows a unique, membrane-bound collagen-like structure harbouring three Gly–X–Y collagen-like (COL) repeat motifs (COL1 – COL3) in the putative extracellular domain that are flanked by four NC domains (NC1–NC4) as well as one putative transmembrane domain at the N-terminus (Hashimoto et al., 2002). This COL1-COL3/NC1-NC4 structure may define a novel

class of neuronal collagens. However, there were detected at least four alternatively spliced isoforms that confer variability at the extracellular COL repeats, in addition to another splice variant that codes for an alternative NC4 domain (Hashimoto et al., 2002). CLAC is deposited preferentially in the primitive or neuritic types of senile plaques in cerebral cortices that are highly characteristic of AD brains but not in the diffuse plaques of non-demented aged individuals, diffuse deposits in subcortical structures and cerebellum in AD nor in cerebral amyloid angiopathy (Hashimoto et al., 2002). This relative specificity of CLAC deposition in AD brain parenchyma, strongly argues for its significance in the neuro degenerative process of AD (Hashimoto et al., 2002).

3.3. Inhibitor of DNA binding 3 (Id3)

During neurogenesis, neural precursor cells start to proliferate before to differentiate (Tzeng, 2003). Both proliferation and differentiation processes are regulated by different transcription factors. Between these regulators, the helix-loop-helix (HLH) proteins have a major role (Tzeng, 2003). HLH proteins may have (bHLH) or not (HLH) their HLH structure adjacent to a basic DNA binding region (Norton et al., 1998; Norton, 2000). Members of HLH family are negative regulators of bHLH and are referred to as dominant negative HLH (dnHLH) transcription factors (Tzeng, 2003). Inhibitor of DNA (Id) members belong to dnHLH transcription factors family and they functionally inhibit gene transcriptional activities binding bHLH proteins preventing their dimerization, which is necessary to explicate their activity (Norton et al., 1998; Norton, 2000). Id family includes four members: *Id1* (Benezra, 1990), *Id2* (Sun et al., 1991), *Id3* (Christy et al., 1991; Ellmeier et al., 1992; Deed et al., 1993) and *Id4* (Riechmann et al., 1994). Studies conducted in mice (Duncan et al., 1992; Evans and O'Brien, 1993; Ellmeier and Weith, 1995; Duncan et al., 1997; Jen et al., 1997), rats (Tzeng, 1998) and human tissues (Ellmeier et al., 1992), have shown that *Id1* and *Id3* are mostly expressed in proliferating neuroepithelial cells and

in undifferentiated regions of the central nervous system (CNS) in early development, while their expression levels decrease during the late stages of development (Evans and O'Brien, 1993; Ellmeier and Weith, 1995; Jen et al., 1997).

In the nervous system *Id3* is expressed specifically by neural precursor cells, immature oligodendroglia, S100-a1/GFAP1 astroglia, astroglial progenitor cell line, PC-12 cells line, both Schwann cell precursors and mature cells (Tzeng, 2003). In all these cellular types it functions as promotor of neural proliferation and inhibitor of neural differentiation (Tzeng, 2003). Moreover, after CNS injuries, *Id3* transcription transiently increases, suggesting that it may be involved in astroglial reactivation (Tzeng, 1999, 2001; Aronica, 2001). Several factors regulate *Id* transcription in neural cells (Nagata, 1994; Einarson and Chao, 1995; Persengiev and Kilpatrick, 1997; Tzeng, 1997). *Id3* expression, as well as *Id2*'s, are induced by the bone morphogenetic proteins (BMPs), but the physiological role for such regulation remains unknown (Miyazono and Miyazawa, 2002). $Id1^{-/-}Id3^{-/-}$ mutant mice have shown small brain size, maybe due to a decrease in proliferation of neuroblasts or an increase in apoptosis (Lyden et al., 1999). Furthermore, the overlapping expression of *Id1* and *Id3* in the neuroepithelium, and the lack of a neural phenotype in *Id1* or *Id3* single knockout mice indicates that either *Id1* or *Id3* are required for normal neurogenesis (Lyden et al., 1999). $Id1^{-/-}Id3^{-/-}$ mouse embryos show enlarged, dilated blood vessels and an anastomotic network, while laminin and fibronectin are expressed normally in the basement membrane (Lyden et al., 1999). This suggests that *Id1* and *Id3* are necessary for a normal CNS vasculature development (Lyden et al., 1999). In fact, only *Id1* and *Id3* are expressed in the endothelium within the brain (Lyden et al., 1999).

Aronica, E., Vandeputte, D. A. A., van Vliet, E. A., da Silva, F. H. L., Troost, D. and Gorter, J. A. (2001) Expression of Id proteins increases in astrocytes in the hippocampus of epileptic rats. Neuroreport, 12, 2461-2465.

Benezra, R. (1993) ID AS A GENERAL NEGATIVE REGULATOR OF THE HELIX-LOOP-HELIX FAMILY OF DNA-BINDING PROTEINS. Pharmacology of Cell Differentiation, 1016, 171-180.

Borza, D. B., Bondar, O., Ninomiya, Y., Sado, Y., Naito, I., Todd, P. and Hudson, B. G. (2001) The NCI domain of collagen IV encodes a novel network composed of the alpha 1, alpha 2, alpha 5, and alpha 6 chains in smooth muscle basement membranes. Journal of Biological Chemistry, 276, 28532-28540.

Boutaud, A., Borza, D. B., Bondar, O., Gunwar, S., Netzer, K. O., Singh, N., Ninomiya, Y., Sado, Y., Noelken, M. E. and Hudson, B. G. (2000) Type IV collagen of the glomerular basement membrane - Evidence that the chain specificity of network assembly is encoded by the noncollagenous NC1 domains. Journal of Biological Chemistry, 275, 30716-30724.

Champe PC, Harvey RA, Ferrier DR. Biochemistry. (4th ed.), Wolters Kluwer Health/Lippincott Williams & Wilkins, Philadelphia (2008).

Chen, Y. M. and Miner, J. H. (2012) Glomerular basement membrane and related glomerular disease. Translational Research, 160, 291-297.

Christy, B. A., Sanders, L. K., Lau, L. F., Copeland, N. G., Jenkins, N. A. and Nathans, D. (1991) AN ID-RELATED HELIX LOOP HELIX PROTEIN ENCODED BY A GROWTH FACTOR-INDUCIBLE GENE. Proceedings of the National Academy of Sciences of the United States of America, 88, 1815-1819.

Deed, R. W., Bianchi, S. M., Atherton, G. T., Johnston, D., Santibanezkoref, M., Murphy, J. J. and Norton, J. D. (1993) AN IMMEDIATE EARLY HUMAN GENE ENCODES AN ID-LIKE HELIX LOOP HELIX PROTEIN AND IS REGULATED BY PROTEIN-KINASE-C ACTIVATION IN DIVERSE CELL-TYPES. Oncogene, 8, 599-607.

Duncan, M., Diciccobloom, E. M., Xiang, X., Benezra, R. and Chada, K.

(1992) THE GENE FOR THE HELIX LOOP HELIX PROTEIN, ID, IS SPECIFICALLY EXPRESSED IN NEURAL PRECURSORS. Developmental Biology, 154, 1-10.

Duncan, M. K., Bordas, L., DiciccoBloom, E. and Chada, K. K. (1997) Expression of the helix-loop-helix genes Id-1 and NSCL-1 during cerebellar development. Developmental Dynamics, 208, 107-114.

Einarson, M. B. and Chao, M. V. (1995) REGULATION OF ID1 AND ITS ASSOCIATION WITH BASIC HELIX-LOOP-HELIX PROTEINS DURING NERVE GROWTH FACTOR-INDUCED DIFFERENTIATION OF PC12 CELLS. Molecular and Cellular Biology, 15, 4175-4183.

Ellmeier, W., Aguzzi, A., Kleiner, E., Kurzbauer, R. and Weith, A. (1992) MUTUALLY EXCLUSIVE EXPRESSION OF A HELIX LOOP HELIX GENE AND N-MYC IN HUMAN NEUROBLASTOMAS AND IN NORMAL DEVELOPMENT. Embo Journal, 11, 2563-2571.

Ellmeier, W. and Weith, A. (1995) EXPRESSION OF THE HELIX-LOOP-HELIX GENE ID3 DURING MURINE EMBRYONIC-DEVELOPMENT. Developmental Dynamics, 203, 163-173.

Evans, S. M. and Obrien, T. X. (1993) EXPRESSION OF THE HELIX-LOOP-HELIX FACTOR ID DURING MOUSE EMBRYONIC-DEVELOPMENT. Developmental Biology, 159, 485-499.

Gould, D. B., Phalan, F. C., van Mil, S. E., Sundberg, J. P., Vahedi, K., Massin, P., Bousser, M. G., Heutink, P., Miner, J. H., Tournier-Lasserve, E. and John, S. W. M. (2006) Role of COL4A1 in small-vessel disease and hemorrhagic stroke. New England Journal of Medicine, 354, 1489-1496.

Hashimoto, T., Wakabayashi, T., Watanabe, A., Kowa, H., Hosoda, R., Nakamura, A., Kanazawa, I., Arai, T., Takio, K., Mann, D. M. A. and Iwatsubo, T. (2002) CLAC: a novel Alzheimer amyloid plaque component derived from a transmembrane precursor, CLAC-P/collagen type XXV. Embo Journal, 21, 1524-1534.

Jen, Y., Manova, K. and Benezra, R. (1997) Each member of the Id gene family exhibits a unique expression pattern in mouse gastrulation and neurogenesis. Developmental Dynamics, 208, 92-106.

Kalluri, R., Shield, C. F., Todd, P., Hudson, B. G. and Neilson, E. G. (1997) Isoform switching of type IV collagen is developmentally

arrested in X-linked alport syndrome leading to increased susceptibility of renal basement membranes to endoproteolysis. Journal of Clinical Investigation, 99, 2470-2478.

Karsdal MA, Leeming DJ, Henriksen K, Bay-Jensen A. Biochemistry of collagens, laminins and elastin. Structure, function and biomarkers, 978-0-12-809847-9, Elsevier Academic Press (2017).

Khoshnoodi, J., Pedchenko, V. and Hudson, B. G. (2008) Mammalian collagen IV. Microscopy Research and Technique, 71, 357-370.

Kubota, Y., Kleinman, H. K., Martin, G. R. and Lawley, T. J. (1988) ROLE OF LAMININ AND BASEMENT-MEMBRANE IN THE MORPHOLOGICAL-DIFFERENTIATION OF HUMAN-ENDOTHELIAL CELLS INTO CAPILLARY-LIKE STRUCTURES. Journal of Cell Biology, 107, 1589-1598.

Lyden, D., Young, A. Z., Zagzag, D., Yan, W., Gerald, W., O'Reilly, R., Bader, B. L., Hynes, R. O., Zhuang, Y., Manova, K. and Benezra, R. (1999) Id1 and Id3 are required for neurogenesis, angiogenesis and vascularization of tumour xenografts. Nature, 401, 670-677.

Miyazono, K. & Miyazawa, K. Id: a target of BMP signaling. Sci. STKE 2002, PE40 (2002).

Nagata, Y. and Todokoro, K. (1994) ACTIVATION OF HELIX-LOOP-HELIX PROTEINS ID1, ID2 AND ID3 DURING NEURAL DIFFERENTIATION. Biochemical and Biophysical Research Communications, 199, 1355-1362.

Norton, J. D. (2000) ID helix-loop-helix proteins in cell growth, differentiation and tumorigenesis. Journal of Cell Science, 113, 3897-3905.

Norton, J. D., Deed, R. W., Craggs, G. and Sablitzky, F. (1998) Id helix-loop-helix proteins in cell growth and differentiation. Trends in Cell Biology, 8, 58-65.

Persengiev, S. P. and Kilpatrick, D. L. (1997) The DNA methyltransferase inhibitor 5-azacytidine specifically alters the expression of helix-loop-helix proteins Id1, Id2 and Id3 during neuronal differentiation. Neuroreport, 8, 2091-2095.

Plaisier, E., Gribouval, O., Alamowitch, S., Mougenot, B., Prost, C., Verpont, M. C., Marro, B., Desmettre, T., Cohen, S. Y., Roullet, E., Dracon, M., Fardeau, M., Van Agtmael, T., Kerjaschki, D., Antignac, C. and Ronco, P. (2007) COL4A1 mutations and

hereditary angiopathy, nephropathy, aneurysms, and muscle cramps. New England Journal of Medicine, 357, 2687-2695.
Pozzi, A., Yurchenco, P. D. and Lozzo, R. V. (2017) The nature and biology of basement membranes. Matrix Biology, 57-58, 1-11.
Riechmann, V., Vancruchten, I. and Sablitzky, F. (1994) THE EXPRESSION PATTERN OF ID4, A NOVEL DOMINANT-NEGATIVE HELIX-LOOP-HELIX PROTEIN, IS DISTINCT FROM ID1, ID2 AND ID3. Nucleic Acids Research, 22, 749-755.
Risteli J, Bachinger HP, Engel J, Furthmayr V, Timpl R, (1980). 7- S collagen: characterization of an unusual basement membrane structure. Eur. J. Biochem. 108, 239-250.
Sun, X. H., Copeland, N. G., Jenkins, N. A. and Baltimore, D. (1991) ID PROTEINS ID1 AND ID2 SELECTIVELY INHIBIT DNA-BINDING BY ONE CLASS OF HELIX-LOOP-HELIX PROTEINS. Molecular and Cellular Biology, 11, 5603-5611.
Sundaramoorthy, M., Meiyappan, M., Todd, P. and Hudson, B. G. (2002) Crystal structure of NC1 domains - Structural basis for type IV collagen assembly in basement membranes. Journal of Biological Chemistry, 277, 31142-31153.
Timpl, R., Wiedemann, H., van Delden, V., Furthmayr, H. and Kuhn, K. (1981). A network model for the organization of type IV collagen molecules in basement membranes. Eur. J. Biochem. 120, 203-211.
Tong, Y., Xu, Y., Scearce-Levie, K., Ptacek, L. J. and Fu, Y. H. (2010) COL25A1 triggers and promotes Alzheimer's disease-like pathology in vivo. Neurogenetics, 11, 41-52.
Tzeng, S. F. (2003) Inhibitors of DNA binding in neural cell proliferation and differentiation. Neurochemical Research, 28, 45-52.
Tzeng, S. F., Bresnahan, J. C., Beattie, M. S. and de Vellis, J. (2001) Upregulation of the HLH Id gene family in neural progenitors and glial cells of the rat spinal cord following contusion injury. Journal of Neuroscience Research, 66, 1161-1172.
Tzeng, S. F. and deVellis, J. (1997) Expression and functional role of the Id HLH family in cultured astrocytes. Molecular Brain Research, 46, 136-142.
Tzeng, S. F., Kahn, M., Liva, S. and de Vellis, J. (1999) Tumor necrosis factor-alpha regulation of the Id gene family in astrocytes and microglia during CNS inflammatory injury. Glia, 26, 139-152.

Vandenberg, P., Kern, A., Ries, A., Luckenbilledds, L., Mann, K. and Kuhn, K. (1991) CHARACTERIZATION OF A TYPE-IV COLLAGEN MAJOR CELL BINDING-SITE WITH AFFINITY TO THE ALPHA-1-BETA-1 AND THE ALPHA-2-BETA-1 INTEGRINS. Journal of Cell Biology, 113, 1475-1483.

Chapter 4

Materials and Methods

4. Materials and Methods

4.1. Protocols

The protocols for animal care and use were approved by the appropriate Committee at the University of Naples Federico II (2015/0023947) approved. All animal experimental procedures were carried out in accordance with The European Parliament and The Council of The European Union Directive of 22nd of September 2010 (2010/63/UE) and Italian law (D. lgs. 26/2014).

4.2. Animals and tissue preparation

All experiments were performed on group-housed *N. furzeri*, wild-type MZM-04/10 strain (Terzibasi et al., 2008), males, maintained in the following conditions: 12 adult fish were housed in 40L tanks at 25 °C, with an "air supplied" water filtration and low water flow; food was supplied twice a day, and consisted of commercially available brine-shrimps eggs (*Artemia salina*) and frozen and live bloodworm larvae (Chironomus sp.); fish were maintained on 12-hour light/dark cycles; adult subjects were allowed to spawn on a river sand substrate, which was weekly sieved and returned to the bottom of the tanks. Animals were anesthetized at around 10 a.m., to avoid alteration of circadian rhythm, by immersion in tricaine methanesulfonate (MS-222, Sigma-Aldrich, 300 mg/L of in aqueous solution). For RNA extraction fish were decapitated, brains were rapidly dissected, kept in sterile tubes (Eppendorf) with 500 µL of RNA later (Qiagen), and stored at 4°C until the RNA extraction. For FISH experiments, fish were decapitated; heads were rapidly excised and fixed in 4% paraformaldehyde (PFA) in PBS treated with diethylpyrocarbonate (DEPC), for 24 hours at 4°C. Successively, for cryostatic embedding, brains were incubated in 30% sucrose solution overnight (on), 4°C; 20% sucrose solution on, 4°C; finally, they were

embedded in cryomounting and frozen at -80°C. Serial transversal sections of 14µ thickness were cut with a Leica cryostat (Deerfield, IL).

4.3. RNA isolation and cDNA synthesis

Tissues were taken out of RNAlater and cleaned with sterile papers. *N. furzeri* total RNA was isolated from different animals at two different time points (young, 5 weeks post hatching (wph), and old, 27 wph) with QIAzol (Qiagen), following manufacturers' protocol with modifications (Baumgart et al., 2012). Total RNA was then quantized with Eppendorf BioPhotometer and retrotranscribed to cDNA in a 20 µL volume, using the QuantiTect® Reverse Transcription Kit (Qiagen) and following the supplier's protocol. 500 ng of RNA and 2 µL of gDNA Wipeout Buffer were incubated at 42°C for 2 min. Then the sample was immediately putted on ice and 6 µL of Master Mix (4 µL Quantiscript RT Buffer x, 1 µL of RT Primer Mix, 1 µL of Quantiscript Reverse Transcriptase) were added. The so obtained mix was subsequently incubated at 42°C for 15 min and at 95°C for 3 min. newly synthetized cDNA was then diluted to a final volume of 200 µL with ultra-pure sterile nuclease free water to an approximate final cDNA concentration of 40 ng/µL.

4.4. Identification of Col4a1, Col25a1 and Id3

According to the sequence information (Nofu_GRZ_cDNA_3_0012842), one set of primers was designed to amplify *N. Furzeri Col4a1, Col25a1,* and *Id3* cDNAs:

Col4a1 (forward 5'-GGATTCCCTGGAGAAAAAGG-3′- reverse 5′-ACAGCTTCCTGCCGTACCTA-3′);

Col25a1 (forward 5'- TGCTTCAAACCCCTCCCTCTT-3′ and reverse 5′-TGTATCAGAGGCTGCGAGA-3′);

Id3 (forward 5'-CAAGTCTTGCATTACCTCGCA-3′ and reverse 5′-AGTTCGGCACCATCCAAAAC-3′).

PCR reaction was carried out with Phusion® High-Fidelity PCR Master Mix (NEW ENGLAND BioLabs®Inc. following manufacturer's instruction. Reaction mixture was made of a final volume of 25µl, including 1.25 µL of each 10 µM primer, 0.75 µL of DMSO, 12.5 µL of 2x Phusion Master Mix, 1µl of cDNA template obtained from the retro-transcription PCR, and nuclease free water to 25 µL. Primers were designed to amplify a fragment of 465 base pairs (bp), 390 bp and 372 bp respectively for *N. furzeri Col4a1*, *Col25a1* and *Id3*. Cycling conditions were as follows: 94°C for 3 min, followed by 35 cycles at 94 °C for 30 s, 54° C for 30 s and 72 °C for 1 min and a final extension at 72°C for 7 min. PCR products were run on 2% agarose gel at 120 V for 50 min. DNA was precipitated with ethanol (addition of 100% ethanol 3:1, incubation at -80°C for 15 min, centrifugation at 20'000 rcf at 4°C for 30 min, elimination of supernatant, addition of 1 mL of 70% ethanol, centrifugation at 10'000 rcf at 4°C for 10 min, elimination of supernatant, well drying under chemical hood, addition of 12 µL of free nuclease water) and quantified. 300 ng of DNAs were sequenced at the Leibniz Institute on Aging - Fritz Lipmann Institute laboratories (Jena, Germany). Sequences thus obtained were compared and matched with the information available on NFINtb Nothobranchius furzeri transcriptome browser (http://nfintb.leibniz-fli.de/nfintb/).

4.5. Quantitative Real Time PCR (qPCR)

Quantitative Real Time-PCR was assessed to evaluate brain expression of *N. furzeri* Col4a1, Col25a1 and Id3 mRNAs in young and old animals. Primers were designed with Primer3 tool (Untergasser et al., 2007). According to the sequence information, one set of primers was designed to quantize each cDNA:

Col4a1 left 5'-CTGGAATCCCTGGAGAGCC-3' and right 5'-CCTGGAGGCCTTGTGTACC-3';

Col25a1 left 5'-AACCTGAAACGCATGCAGTT-3' and right 5'-TCACGGCAGGACACTCAG-3';

Id3 5'-AGATCCTGCAGCACGTCAT-3' and right 5'-GTGTTTCCCTGCACCATGAG-3').

Reactions were performed in 20 µL volume containing 1 µL of diluted cDNA, 10 µL of BrightGreen 2x qPCR MasterMix, 0.6 µL of each 10 µLM primer, free nuclease water up to 20 µL and using BrightGreen 2X qPCR MasterMix kit (abm®) following the manufacturer's instructions. Reactions were performed in triplicates and negative control (water) was always included as well as TATA box binding protein (TBP) for the normalization (left 5'-CGGTTGGAGGGTTTAGTCCT-3' and right 5'-GCAAGACGATTCTGGGTTTG-3'). Experiment was run on 7300 Real-Time PCR System (Applied Biosystems). Expression levels were analysed by the ΔΔCt method and normalized to the reference gene TATA-binding protein (TBP).

4.6. Riboprobes *(mRNA) synthesis*

mRNA riboprobes to identify *N. furzeri Col4a1*, *Col25a1* and *Id3* were synthesized by in vitro transcription (IVT) using in vitro transcription kit (INVITROGEN, cat. AM1320), and DIG RNA Labeling Mix, 10x concentrated solution containing 10 mM ATP, 10 mM CTP, 10 mM GTP, 6.5 mM UTP, 3.5 mM DIG-11-UTP, pH 7.5 (Roche, cat. 11 277 073 910). 1 µg of DNA template was retrotranscribed to RNA in 50 µL volume reaction, including 5 µL of 10x DIG RNA labelling mix, 5 µL of 10x transcription buffer, 4 µL of T7 RNA polymerase. Polymerase T7 promoter sequence (5'-GGTAATACGACTCACTATAGG-3') was associated upstream to *N. furzeri Col4a1*, *Col25a1* and *Id3* PCR reverse primers. Components were briefly centrifuged and incubated at 37°C for 2 h. Then 2 µL of EDTA 0.2 M pH 8.8 were added to stop the reaction. Reaction products were analyzed by gel electrophoresis and quantified.

4.7. Probe validation with Dot Blot technique

To validate and determine probes concentration, Dot Blot technique was employed. Probe's fresh dilution buffer was prepared mixing DEPC H_2O, saline sodium citrate buffer (SSC) 20x and formaldehyde 37% (5:3:2). Probes were then diluted in the dilution buffer as indicated in

Tab 2, in a final volume of 20 µL. Negative control was included for each probe. 1 µL of each probe dilution plus negative controls were then pipetted on a nitrocellulose membrane forming little separated spots. The membrane was then fixed in the Stratalinker® UV Crosslinker for 30'', gently washed in PBS/DEPC and incubated for 30' in the fluorescence in situ blocking solution (FISH-BS) (PBS 1x, 10% of sheep serum heat inactivated, 0.5% of Roche Blocking Reagent, 0.1% of Tween-20, DEPC H_2O to final volume). A second incubation in FISH-BS 1:2000 in Anti-Digoxigenin-AP, Fab fragments from sheep (Roche) was performed. Then the membrane was washed twice for 15' in PBS/DEPC and incubated with BM purple AP substrate (Roche), until the detection of the mRNA's spots.

Dilution number	Final concentration
1	2 ng / µL
2	500 pg / µL
3	100 pg / µL
4	50 pg / µL
5	25 pg / µL
6	10 pg / µL
7	5 pg / µL
8	2.5 pg / µL
9	1 pg / µL
10	0.1 pg / µL

Tab 2 | Serial dilution of mRNA probes in dilution buffer (DEPC H2O, SSC 20x and formaldehyde 37%, 5:3:2) for Dot Blot validation.

4.8. Fluorescence in situ hybridization (FISH)

FISH experiments have been conducted both on cryostatic and paraffin sections and by means of sterile solutions and materials. Diethylpyrocarbonate (DEPC) was added to phosphate-buffered saline (PBS) and water 1mL/L to inactivate RNase enzymes; solutions were shaken vigorously and autoclaved.

Cryostatic sections were dried for 2 h at room temperature (RT), while paraffin sections were dewaxed in xylene and hydrated in series of descending ethanol. Sections were well washed in 1xDEPC/PBS and treated with 10 µg/µL Proteinase K (Sigma–Aldrich) 1:200 in DEPC/PBS for 10 min. Proteinase K action was then inactivated by two washes in 2mg/mL glycine, 5 min each. Sections were post fixed in 4% PFA for 20 min and well washed in 1x DEPC/PBS at RT. Thereafter, the pre-hybridization was carried out in a hybridization solution (HB) containing 50% formamide, 25% 20x SSC, 50 µg/ml Heparin, 10 µg/ml yeast RNA, 0.1% Tween 20, 0.92% citric acid at 55 °C for 1 h. Before prehybridization step, paraffin sections were briefly immersed in series of ascendant ethanol (40% ethanol 3 min, 70% ethanol 3 min, 100% ethanol twice for 5 min each). Probes were denaturated for 10 min at 80 °C and sections were then incubated, in HB containing an mRNA probes concentration of 500 pg/µL, on at 52°C. Riboprobes concentration was evaluated with the dot blot technique. Post-hybridization washes were carried out at 52°C as follows: 2 x 20 min in SSC1x, 2 x 10 min in SSC0.5x, and then in 1x DEPC/PBS at RT. Sections were blocked in FISH-BS for 1h at RT. After, sections were incubated in a 1:2000 dilution of anti-digoxigenin Fab fragments conjugated with alkaline phosphatase (Roche) in FISH blocking solution (BS) for 2h at RT, containing 10% normal sheep serum heat inactivated, and 0.5% blocking reagent (Roche, Germany). Sections were well washed in 1x DEPC/PBS. Chromogenic reaction was carried out by using Fast Red tablets (Sigma-Aldrich) in Tris buffer and incubating the slides at RT, in the dark. Signal was observed every 20 min until the signal detection (1-10 h, depending on the probe used). After the signal was developed, sections were washed in 1x DEPC/PBS at RT and mounted with Fluoreshield Mounting Medium with DAPI (abcam) as counterstaining for the nuclei. Images were observed and analysed with a Zeiss AxioScope AX 1.0 microscope (Carl Zeiss, Jena, Germany) with AxioCam MC5 and AxioVision software and Leica – DM6B (Leica, Wetzlar, Germany) and LasX software. Digital raw images were optimized for image resolution, contrast, evenness of illumination, and background using Adobe Photoshop CC 2018 (Adobe Systems, San Jose, CA). Anatomical structures were identified according to the adult *N. furzeri* brain atlas (D'Angelo, 2013).

4.9. FISH and immunofluorescence (IF) double labeling

FISH reaction was carried out as mentioned in the paragraph 4.8. After the detection of the chromogenic reaction, sections were well washed in DEPC/PBS and incubated at RT for 1 h with IF-BS (normal goat serum, 1:5 in PBS containing 0.1% Triton X-100, Sigma) and subsequently with different neural markers (see Tab 3), on at 4°C. DEPC/PBS washes preceded the incubation with secondary antibodies: goat anti-rabbit IgG (H+L) Alexa fluor™ Plus 488 (Invitrogen by Thermo Fisher Scientific, ref A32731), goat anti-mouse IgG (H+L) Alexa fluor™ Plus 488 (Invitrogen by Thermo Fisher Scientific, ref A32723) 1:1000 in PBS/DEPC, and Alexa Fluor 488 – conjugated Streptavidin, 1:500 (Jackson Immunoresearch, ref 016 – 540 – 084). Images were observed and analysed with Leica – DM6B (Leica, Wetzlar, Germany) and LasX software. Digital raw images were optimized for image resolution, contrast, evenness of illumination, and background using Adobe Photoshop CC 2018 (Adobe Systems, San Jose, CA). Anatomical structures were identified according to the adult *N. furzeri* brain atlas (D'Angelo, 2013).

Antibody	Source	Host	Expression	Dilution
anti-PCNA	Santa Cruz Biotechnology (PC10): sc-56	Mouse Monoclonal	G1/G2 phases (equally distributed over the whole nucleus. Early S phase (granular distribution, absent from nucleoli). Late S phase (nucleoli). M phase (displaced from the condensed chromosomes.	1:75
anti-S100	Agilent Dako Z0311	Rabbit Polyclonal	Strong reactivity for S100ß (astrocytes' cytoplasm and nuclei, few astrocytes and neurons) and weakly for S100α1 (predominantly in neuronal cells, endothelium, neuropil, granular and	1:200

			molecular layers of cerebellum) and S100α6 (neurons of restricted brain areas such as amygdala and entorhinal cortex, and in some astrocytes).	
anti-DCX	Abcam (18723)	Rabbit polyclonal	Microtubule expressed by neuronal precursor cells and immature neurons in embryonic and adult cortical substructure.	1:100
anti-HuC/HuD	Invitrogen by Thermo Fisher Scientific (A21272)	Mouse IgG2b, biotin-XX conjugate	Neurons from early development at about the time that they leaves the mitotic cycle.	1:50
anti-TH	Abcam (ab75875)	Rabbit Polyclonal	Early neurons, differentiated post-mitotic neuronal cells, dopaminergic neurons	1:50

Tab 3 | Lists of primary antisera.

Bibliography

Baumgart, M., Groth, M., Priebe, S., Appelt, J., Guthke, R., Platzer, M. and Cellerino, A. (2012) Age-dependent regulation of tumor-related microRNAs in the brain of the annual fish Nothobranchius furzeri. Mechanisms of Ageing and Development, 133, 226-233.

D'Angelo, L. (2013) Brain Atlas of an Emerging Teleostean Model: Nothobranchius furzeri. Anatomical Record-Advances in Integrative Anatomy and Evolutionary Biology, 296, 681-691.

Terzibasi, E., Valenzano, D. R., Benedetti, M., Roncaglia, P., Cattaneo, A., Domenici, L. and Cellerino, A. (2008) Large Differences in Aging Phenotype between Strains of the Short-Lived Annual Fish Nothobranchius furzeri. Plos One, 3.

Untergasser, A., Nijveen, H., Rao, X., Bisseling, T., Geurts, R. and Leunissen, J. A. M. (2007) Primer3Plus, an enhanced web interface to Primer3. Nucleic Acids Research, 35, W71-W74.

Chapter 5

Results

5. Results

5.1. Identification and evolutionary history

5.1.1. Col4a1

A putative *Col4a1* coding sequence was retrieved from the *N. furzeri* transcriptome browser (Petzold et al., 2013): the sequence is deposited under the GenBank accession number GAIB01100805.1. *N. furzeri Col4a1* was aligned with the predicted *Col4a1* sequences available in GeneBank. Phylogenetic tree was inferred from the aligned Col4a1 mRNA sequences using Maximum likelihood method and with the Molecular Evolutionary Genetics Analysis (Mega) software [Fig 20]. The tree was constructed on the following sequences: *Poecilia reticulata* (XM_008401564.2), *Haplochromis burtoni* (XM_005948835.2), *Amphirion ocellaris* (XM_023267280.1), *Poecilia formosa* (XM_007555367.2), *Lepisosteus oculatus* (XM_015364173.1), *Cynoglossus semilaevis* (XM_008328686.3), *Pundamilia nyererei* (XM_005747175.2), *Kryptolebias marmoratus* (XM_025004618.1), *Takifugu rubripes* (XM_003961712.2), *Oryzias latipes* (NM_001177472.1), *Austrofundulus limnaeus* (XM_014017514.1), *Nothobranchius furzeri* (XM_015966255.1), *Stegastes partitus* (XM_008275532.1), *Astyanax mexicanus* (XM_022680521.1), *Xiphophorus maculatus* (XM_005798133.2), *Poecilia mexicana* (XM_015003126.1), *Oryzias melastigma* (XM_024286964.1). It is evident from the tree that the closest evolutionary relationship for *N. furzeri Col4a1* is shown with the *Perciformes S. partitus;* the *Characiformes A. mexicanus;* the *Cyprinodontiformes X. maculatus, P. Mexicana,* and *A. limnaeus;* the *Beloniformes O. melastigma,* and *O. latipes.*

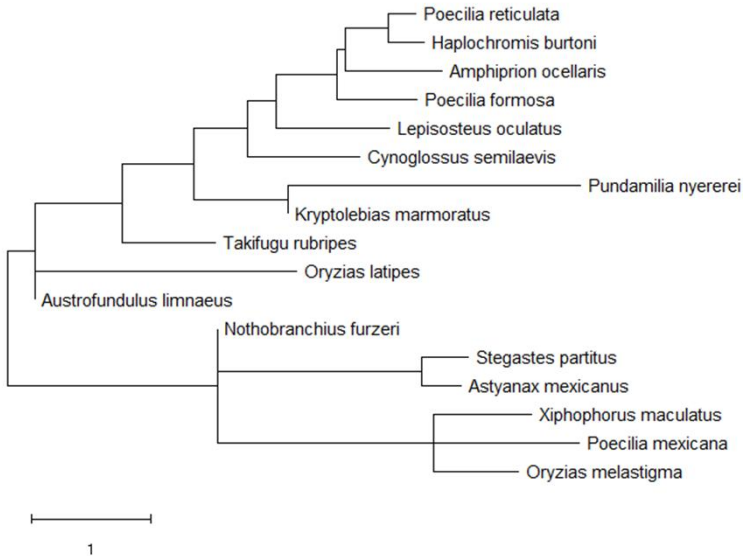

Fig 20 | Col4a1 evolutionary history. The evolutionary history was inferred by using the Maximum Likelihood method and Tamura-Nei model (Tamura et al., 1993). The tree with the highest log likelihood (-146760, 72) is shown. Initial tree(s) for the heuristic search were obtained automatically by applying Neighbor-Join and BioNJ algorithms to a matrix of pairwise distances estimated using the Maximum Composite Likelihood (MCL) approach, and then selecting the topology with superior log likelihood value. The tree is drawn to scale, with branch lengths measured in the number of substitutions per site. This analysis involved 17 nucleotide sequences. Codon positions included were 1st+2nd+3rd+Noncoding. There was a total of 8476 positions in the final dataset. Evolutionary analyses were conducted in MEGA X (Kumar et al., 2018).

5.1.2. Col25a1

A putative *Col25a1* coding sequence was retrieved from the *N. furzeri* transcriptome browser (Petzold et al., 2013). Seven different variants of mRNA sequences are annotated: XM_015946500.1 (X1), XM_015946501.1 (X2), XM_015946502.1 (X3), XM_015946503.1 (X4), XM_015946504.1 (X5), XM_015946505.1 (X6), XM_015946506.1 (X7). Variants X1, X4, X5 have a homology of 100%. Variants X2, X3, X6, and X7 differ only for 1%. Phylogenetic tree was inferred from the aligned

Col25a1 mRNA sequences using Maximum likelihood method and with the Molecular Evolutionary Genetics Analysis (Mega) software [Fig 21]. The tree was constructed on the following sequences: *P. formosa* (XM_016675245.1), *P. reticulata* (XM_008435849.2), *H. burtoni* (XM_005927689.2), *A. ocellaris* (XM_023299956.1), *C. semilaevis* (XM_025062607.1), *K. marmoratus* (XM_017414412.1), *N. furzeri* (XM_015946501.1), *S. partitus* (XM_008294251.1), *X. maculatus* (XM_023346157.1), *O. melastigma* (XM_024288338.1), *O. latipes* (XM_020711604.2). It is evident from the tree that the closest evolutionary relationship for *N. furzeri Col25a1* is shown with the *Perciformes H. burtoni*, and with the *Cyprinodontiformes P. Formosa*, and *X. maculatus*.

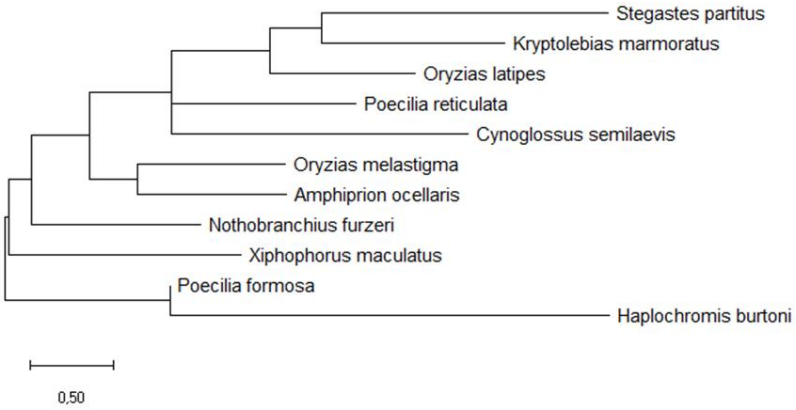

Fig 21 | Col25a1 evolutionary history. The evolutionary history was inferred by using the Maximum Likelihood method and Tamura-Nei model (Tamura et al., 1993). The tree with the highest log likelihood (-79753,38) is shown. Initial tree(s) for the heuristic search were obtained automatically by applying Neighbor-Join and BioNJ algorithms to a matrix of pairwise distances estimated using the Maximum Composite Likelihood (MCL) approach, and then selecting the topology with superior log likelihood value. The tree is drawn to scale, with branch lengths measured in the number of substitutions per site. This analysis involved 11 nucleotide sequences. Codon positions included were 1st+2nd+3rd+Noncoding. There was a total of 6679 positions in the final dataset. Evolutionary analyses were conducted in MEGA X (Kumar et al., 2018).

5.1.3. Id3

A putative *Id3* coding sequence was retrieved from the *N. furzeri* transcriptome browser (Petzold et al., 2013): the sequence is deposited under the GenBank accession number GAIB01124491.1. *N. furzeri Id3* was aligned with the predicted *Id3* sequences available in GeneBank.
Phylogenetic tree was inferred from the aligned Id3 mRNA sequences using Maximum likelihood method and with the Molecular Evolutionary Genetics Analysis (Mega) software [*Fig 22*]. The tree was constructed on the following sequences: *A. limnaeus* (XM_014031932.1), *P. formosa* (XM_007561110.2), *P. reticulata* (XM_008399959.2), *P. mexicana* (XM_015006118.1), *H. burtoni* (XM_005925663.2), *A. ocellaris* (XM_023277440.1), *C. semilaevis* (XM_008309921.3), *K. marmoratus* (XM_017418377.2), *N. furzeri* (XM_015969873.1), *S. partitus* (XM_008306849.1), *X. maculatus* (XM_005812771.3), *O. melastigma* (XM_024268539.1), *O. latipes* (XM_004082237.4). It is evident from the tree that the closest evolutionary relationship for *N. furzeri Id3* is shown with the *Beloniformes O. melastigma, O, latipes,* and the *Perciformes A. ocellaris*.

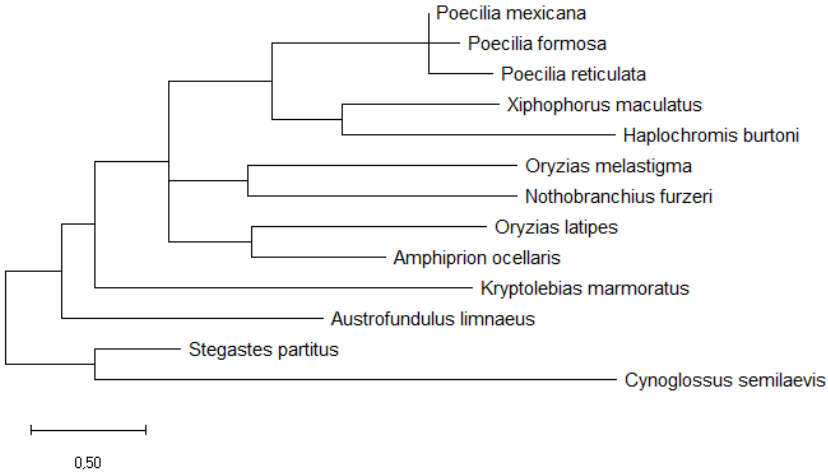

Fig 22 | Id3 evolutionary history. The evolutionary history was inferred by using the Maximum Likelihood method and Tamura-Nei model (Tamura et al., 1993). The tree with the highest log likelihood (-18685,47) is shown. Initial tree(s) for the heuristic search were obtained automatically by applying Neighbor-Join and BioNJ algorithms to a matrix of pairwise distances estimated using the Maximum Composite Likelihood (MCL) approach, and then selecting the topology with superior log likelihood value. The tree is drawn to scale, with branch lengths measured in the number of substitutions per site. This analysis involved 15 nucleotide sequences. Codon positions included were 1st+2nd+3rd+Noncoding. There was a total of 996 positions in the final dataset. Evolutionary analyses were conducted in MEGA X (Kumar et al., 2018).

5.2. Quantitative Real Time PCR

Quantitative Real Time PCR was performed to evaluate Col4a1, and Id3 expression in brain homogenates of young and old each time point, Col4a1, Col25a1 and Id3 mRNAs were housekeeping gene TATA-box binding protein (TBP) and levels were compared using the relative delta curve threshold method. Graphic was built on ΔΔCt values, and $p < 0.01$ is "**", while $p < 0.5$ with "*". The quantitative analysis shows that a moderate augment of Col4a1, Col25a1, and Id3 upon *aging*

significant with: p = 0.0001 for Col4a1*; p = 0.0013 for* Col25a1*; 0.1271 for* Id3 *[*

Fig 23].

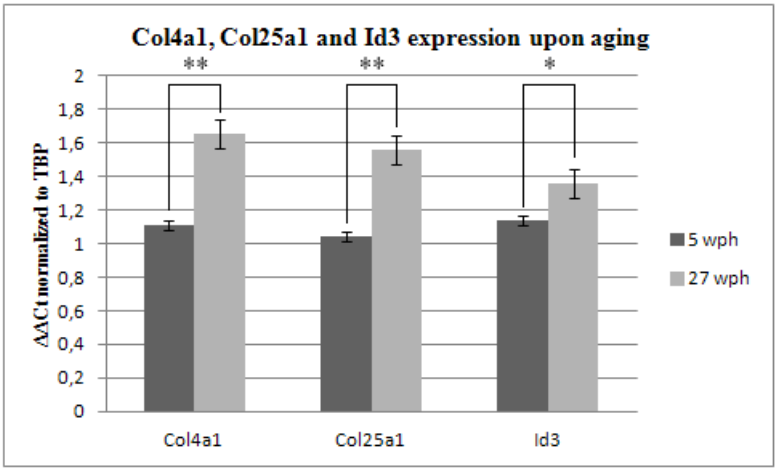

*Fig 23 | Quantitative Real Time PCR for Col4a1, Col25a1 and Id3 upon aging (5 wph versus 27 wph). Graphic was built on ΔΔCt values. p values are: p = 0.0001 for Col4a1; p = 0.0013 for Col25a1; with p = 0.1271 for Id3. "**" indicates p < 0.01, "*" indicates p < 0.5.*

5.3. Fluorescence In Situ Hybridization

In situ experiments with DIG labeled riboprobes for *Col4a1*, *Col25a1* and *Id3* have been conducted on cryostat and paraffin embedded section, and the observed patterns overlap. Signal probe has been observed in young and old brains of *N. furzeri*. Results are summarized in semi-quantitative scheme in Tab 4. Nomenclature follows D'Angelo, 2013. Recognition of labeled neurons and glial cells was based on morphological criteria, and by using specific neuronal and glial markers.

5.3.1. Col4a1 mRNA distribution

In young *N. furzeri* brain, Col4a1 mRNA reveals a slight expression in the optic tectum (OT), specifically in the inner layer of periventricular gray zone (PGZ) and around the longitudinal tori (Tl) [Fig 24].
In old animals, dense positive cells are present in the internal cellular layer (ICL) of olphactory bulbs [Fig 3 a, a"]; few packed cells in the dorso-medial telencephalon (Dm1-2) [Fig 3 a, a', a"] shading along the dorsal zone of dorsal telencephalon (Dd) [Fig 3 a, a'], and numerous cells in the dorso-lateral zone of dorsal telencephalon (Dld) [Fig 3 a]. Weak signal probe is observed in the Dm4, dorsal (Vd), ventral (Vv), posterior (Vp) and supracommissural (Vs) regions of ventral telencephalon [Fig 3 b]. The most evident Col4a1 mRNA signal is located in the habenular (Ha) [Fig 3 c, d], ventro-medial (VM) and anterior (A) thalamic, magnocellular preoptic (PM), anterior preoptic (PPa) and posterior preoptic (PPp) nuclei [Fig 3 d]. In the forebrain, probe signal is mostly concentrated along the ventricles and intense staining is detected also in the optic nerve (ON). In the midbrain, Col4a1 mRNA is differently expressed: few scattered labeled cells are present in the OT [Fig 4 a]; numerous positive cells in the whole PGZ [Fig 4 a, a'] and in the valvula of cerebellum (Va) [Fig 4 a]; dense positive cells are observed near to the lateral longitudinal fascicle (llf) and its nucleus (Nllf) [Fig 4 a, a"], and in the nucleus of lateral valvula (LV) [Fig 4 a]; few dense labeled cells are detected in the dorsal hypothalamus (Hd) [Fig 4 a, a"]; intense signal is observed caudally in the Tl at the margin with PGZ [Fig 4 b]. In the hindbrain, intense Col4a1 mRNA expression is detectable in the granular (gl) [Fig 5 a, c] and molecular (ml) [Fig 5 a] layers of cerebellum, near the central griseum (gc) [Fig 5 a], in the corpus of cerebellum (CCe) and granular eminentiae (EG) [Fig 5 a, b, c]. In addition, few and scattered positive neurons are located more caudally in the cerebellar cristae (CC) [Fig 5 d], near the dorsal district of the medulla oblongata.

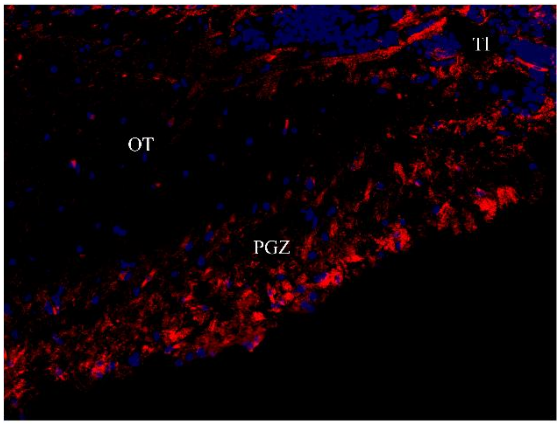

Fig 24| Col4a1 mRNA expression in young N. furzeri brain. Midbrain, transversal cryosections. Abbreviations: OT, optic tectum; PGZ, periventricular gray zone; Tl, longitudinal tori.

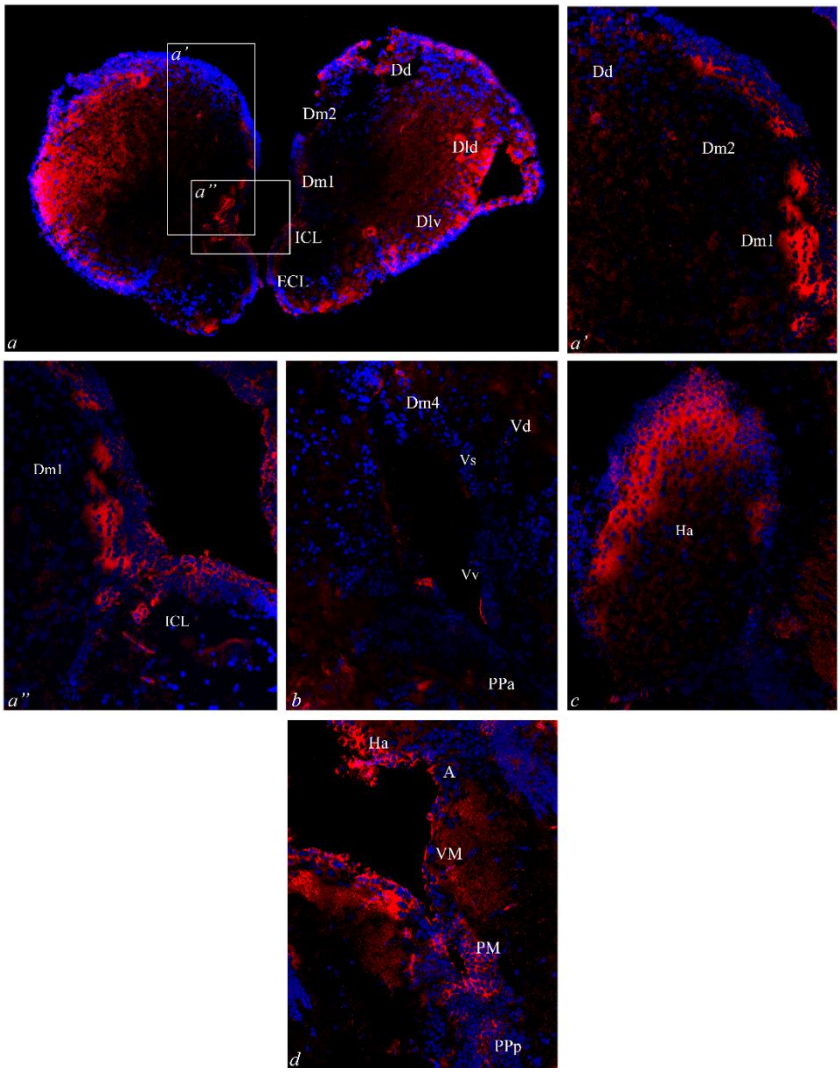

Fig 25| Col4a1 mRNA expression in old N. furzeri brain. Forebrain, transversal cryosections. Abbreviations: A, anterior thalamic nucleus; Dd dorsal zone of dorsal telencephalon; Dld, dorsolateral zone of dorsal telencephalon; Dlv, ventrolateral zone of dorsal telencephalon; Dm, medial zone of dorsal telencephalon; ECL, external cellular layer; Ha, habenular nucleus; Hc, caudal hypothalamus; ICL, internal cellular layer; PM, magnocellular preoptic nucleus; PPp, posterior preoptic nucleus; Vm, medial zone of ventral telencephalon; Vp, posterior zone of ventral telencephalon; Vs, supracommissural zone of ventral telencephalon; Vv, ventral zone of ventral telencephalon.

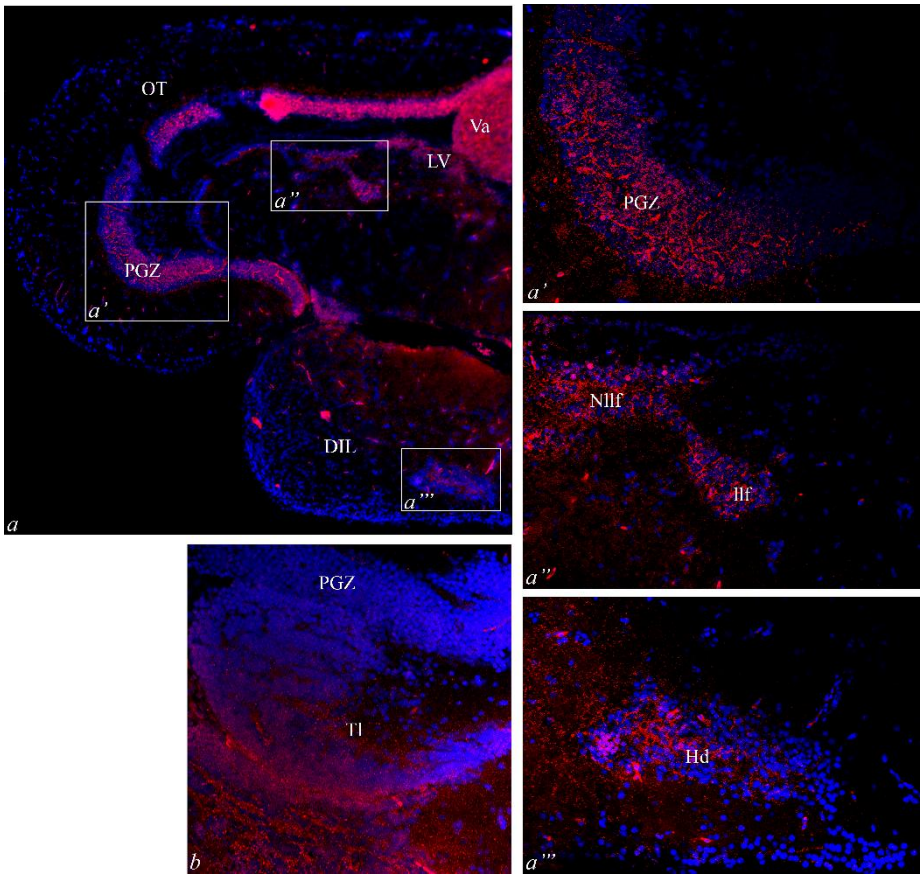

Fig 26| Col4a1 mRNA expression in old N. furzeri brain. Midbrain, transversal cryosections. Abbreviations: DIL, diffuse inferior lobe of hypothalamus; Hd, dorsal hypothalamus; llf, lateral longitudinal fascicle; Nllf, nucleus of lateral longitudinal fascicle; OT, optic tectum; PGZ, periventricular gray zone; Tl, longitudinal tori; Va, valvula of cerebellum.

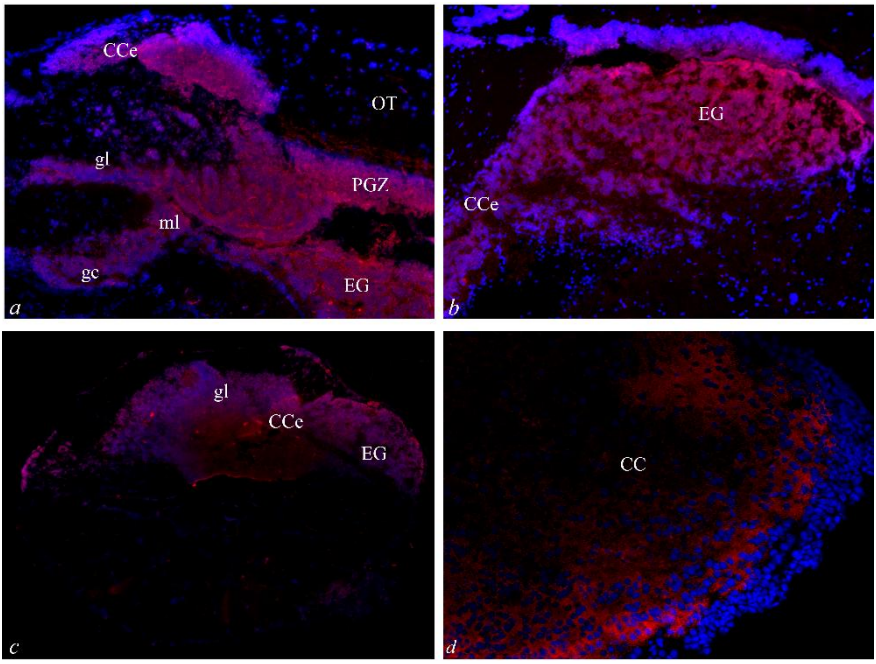

Fig 27| Col4a1 mRNA expression in old N. furzeri brain. Hindbrain. Transversal cryosections. Abbreviations: CC, cerebellar cristae; CCe, corpus of cerebellum; EG, granular eminentiae; gc, central griseum; gl, granular layer of cerebellum; ml, molecular layer of cerebellum; OT, optic tectum; PGZ, periventricular gray zone; Tl, longitudinal tori; Va, valvula of cerebellum.

5.3.2. Col25a1 mRNA distribution

Col25a1 mRNA shows similar distribution pattern to Col4a1.
In young animals, Col25a1 mRNA is expressed only in the midbrain: in the OT, PGZ, glomerular nucleus (NG) [Fig 28 a, b], Hd, posterior recess (NRP) and posterior tuberal (TNp) nuclei [Fig 28 b].
In old *N. furzeri* brain forebrain, labeled cells are detected: in the ICL of olphactory bulbs; Dm1 [Fig 29 a, b], Dm2 [Fig 29 a], Dd [Fig 29 a, c], Dld [Fig 29 a, d], Dlv [Fig 29 a] of dorsal telencephalon; Vp, Vv, and Vs of ventral telencephalon [Fig 29 e]; and, caudally, in the VL [Fig 29 f], dorsal periventricular pretectal nucleus (PPd), PPp, A, VM, PM, and minor commissure (Cmin) [Fig 29 g] of diencephalon; intense probe staining is detected also in the ON. In the midbrain: few cells are concentrated in the layer of OT [Fig 30 a, c, d, f]; numerous cells are located in the PGZ, along its entire rostro-caudal axis [Fig 30 a, c, e, f]; few cells are distributed in the Tl [Fig 30 a – Fig 31 a]; diffuse labeling is detected in NG, NRP and TNp [Fig 30 b]; positive packed cells are localized in semicircular tori (TS), Nllf, llf, and LV [Fig 30 e]; widespread positive cells are present in the diffuse lobe of hypothalamus (DIL) [Fig 30 g, g']. In the hindbrain, Col25a1 mRNA is largely diffused in the EG [Fig 30 f – Fig 31 a, b], in gl and CCe [Fig 31 a], in gc [Fig 31 b].

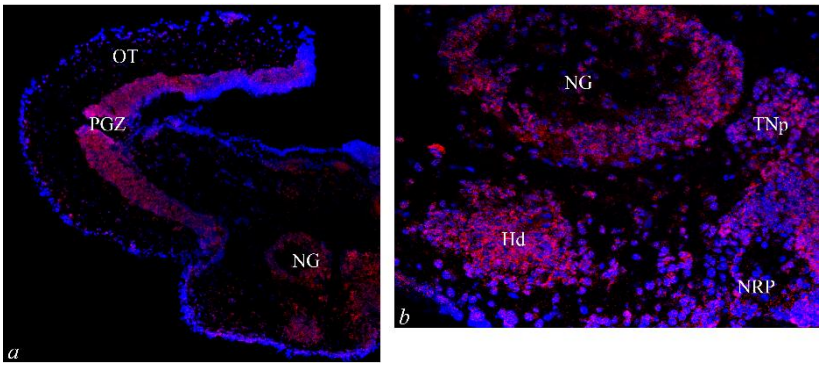

Fig 28| Col25a1 mRNA expression in young N. furzeri brain. Transversal cryosections, midbrain. Abbreviations: Hd, dorsal hypothalamus; NG, glomerular nucleus; NRP, posterior recess nucleus; OT, optic tectum; PGZ, periventricular gray zone; TNp, posterior tuberal nucleus.

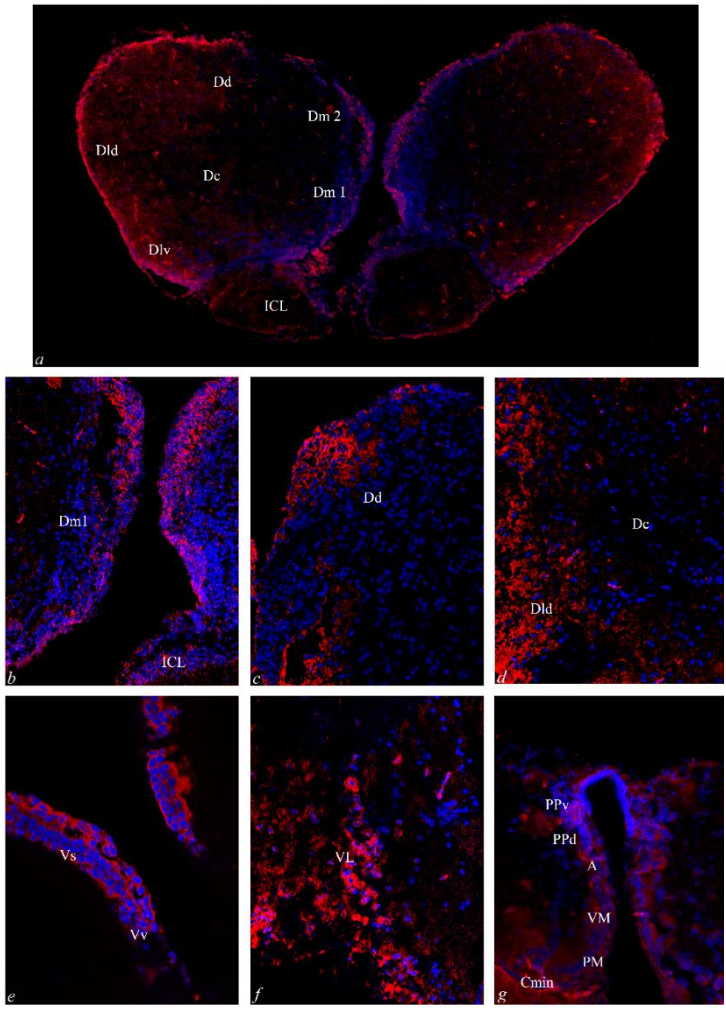

Fig 29| Col25a1 mRNA expression in old N. furzeri brain. Transversal cryosections, forebrain. Abbreviations: A, anterior thalamic nucleus; Cmin, minor commissure; Dc, central zone of dorsal telencephalon; Dd dorsal zone of dorsal telencephalon; Dld, dorsolateral zone of dorsal telencephalon; Dlv, ventrolateral zone of dorsal telencephalon; Dm, medial zone of dorsal telencephalon; ICL, internal cellular layer; PPd, dorsal periventricular pretectal nucleus; PPv, ventral periventricular pretectal nucleus; VL, ventro-lateral thalamic nucleus ; VM, ventro-medial thalamic nucleus; Vs, supracommissural zone of ventral telencephalon; Vv, ventral zone of ventral telencephalon.

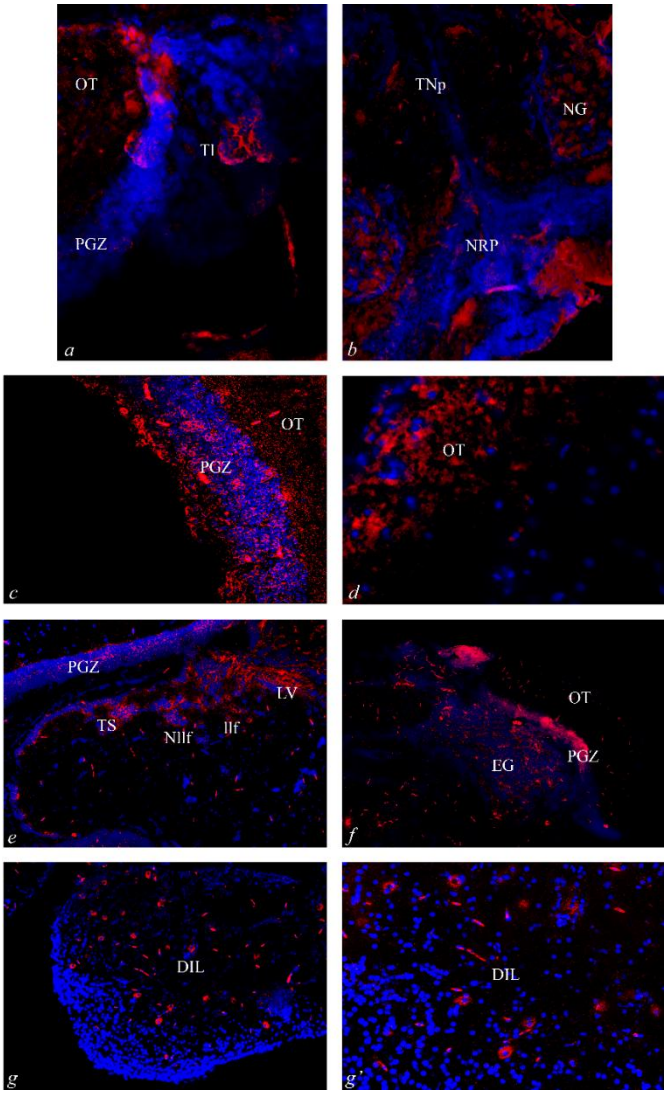

Fig 30 | Col25a1 mRNA expression in old N. furzeri brain. Transversal cryosections, midbrain. Abbreviations: DIL, diffuse inferior lobe of hypothalamus; EG, granular eminentiae; Hd, dorsal hypothalamus; llf, lateral longitudinal fascicle; LV, nucleus of lateral valvula; Nllf, nucleus of lateral longitudinal fascicle; NG, glomerular nucleus; NRP, nucleus of posterior recess; OT, optic tectum; PGZ, periventricular gray zone; TNp, posterior tuberal nucleus; Tl, longitudinal tori; TS, semicircular tori; Va, valvula of cerebellum.

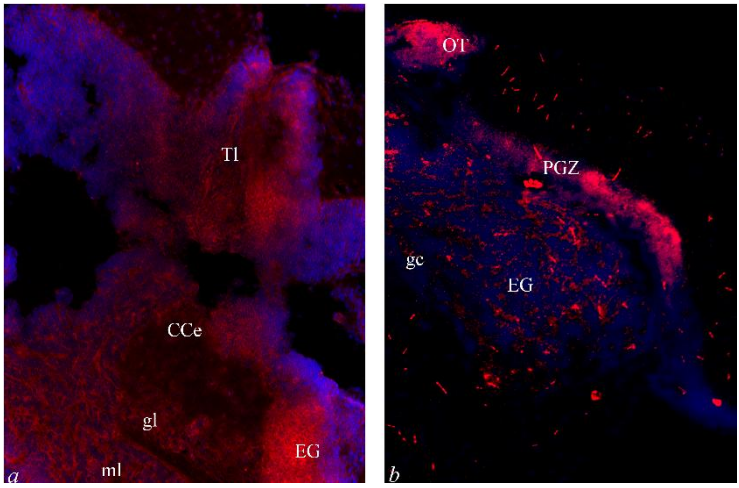

Fig 31| Col25a1 mRNA expression in old N. furzeri brain. Transversal cryosections, hindbrain. Abbreviations: CCe, corpus of cerebellum; EG, granular eminentiae; OT, optic tectum; Tl, longitudinal tori.

5.3.3. Id3 mRNA distribution

In young *N. furzeri* brain, Id3 mRNA is prevalently distributed in midbrain. A slight probe expression is detected in the forebrain, specifically in the Dm [Fig 32 a]; remarkably, diffuse positive cells are located in the hypophysis (Hyp) [Fig 32 b]. In the midbrain, Id3 mRNA is largely diffused: in Tl, PGZ, Hd, lateral hypothalamus (Hl) [Fig 32 c], around the NG and in the central preglomerular nucleus (PGc) [Fig 32 c']. No positive cells are detected in the hindbrain.
In old animals, Id3 mRNA is widely distributed in the forebrain. In the telencephalon: numerous positive cells are present in the ICL of olphactory bulbs [Fig 33 a, b], Dm1-2 [Fig 33 a], Dm3-4 [Fig 33 b]; few scattered positive cells are distributed in the central telencephalic region (Dc) [Fig 33 b, b'], Dld [Fig 33 b']; numerous labeled cells are present in the Dlv [Fig 33 b, b'], in the central zone of ventral telencephalon (Vc) [Fig 33 b'], Vs, and Vv [Fig 33 c]. In the diencephalon: numerous positive cells are located in the preoptic region (PP) [Fig 33 d], Ha [Fig 33 d, e], VL, A, in the intermediate thalamic nucleus (I) [Fig 33 d, d'], in the central pretectal (CPN) and ventral accessory (VAO) nuclei, in the forebrain bundle (fb) [Fig 33 d], in the anterior preglomerular nucleus (PGa) [Fig 33 d]. Strong probe signal is observed in numerous positive cells located in VM, Pm [Fig 33 d, d'], NG, Hl [Fig 33 f], Hd [Fig 33 f, g], central hypothalamus (Hc), periventricular nucleus of posterior tuberculum (TPp), paraventricular organ (PVO) and medial preglomerular nucleus (PGm) [Fig 33 g]; intense probe staining is detected also in the ON. In the midbrain, positive cells are located in the OT, particularly in dorsal [Fig 34 b], and lateral [Fig 34 a, a'] layers of the PGZ, in the Tl [Fig 34 b] and TS [Fig 34 a]. In the hindbrain: numerous Id3 mRNA positive cells are present in the gl, ml, gc of cerebellum [Fig 35 a], and in the EG [Fig 35 a]; few positive cells are present in the CCe [Fig 35 a, b], at the periphery of CC [Fig 35 a, c], and in proximity of the solitary fascicle (sf) [Fig 35 c].

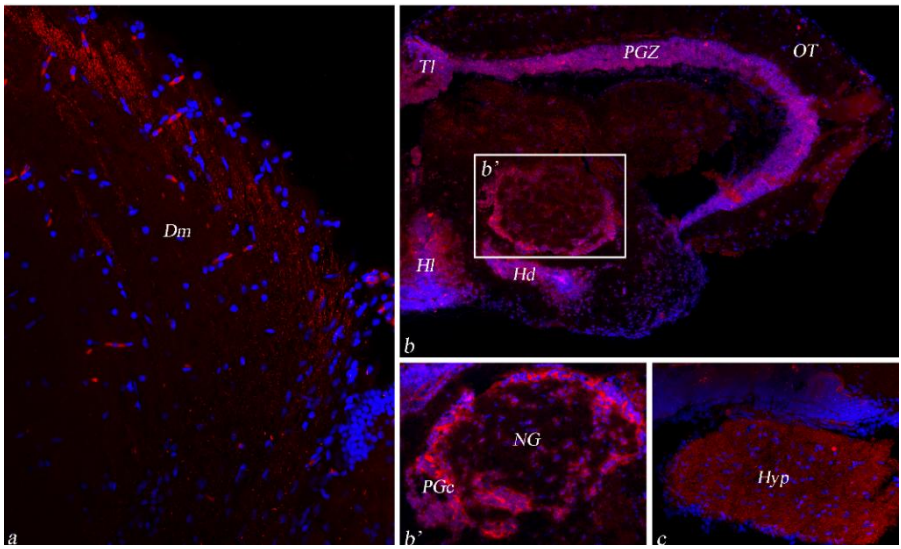

Fig 32| Id3 mRNA expression in young N. furzeri brain. Transversal cryosections, whole brain. Abbreviations: Dm, medial zone of dorsal telencephalon; Hl, lateral hypothalamus; Hyp, hypothalamus; NG, glomerular nucleus; OT, optic tectum; PGc, central preglomerular nucleus; PGZ, periventricular gray zone; Tl, longitudinal tori

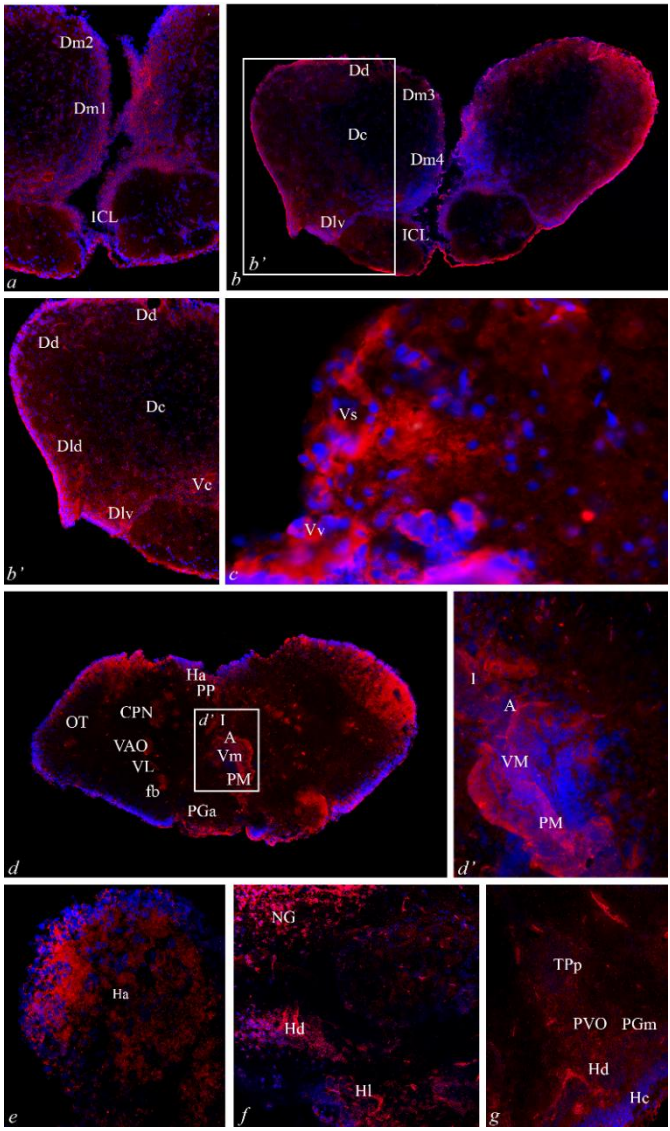

Fig 33| Id3 mRNA expression in old N. furzeri brain. Transversal cryosections, forebrain. Abbreviations: A, anterior thalamic nucleus; CPN, central pretectal nucleus; Dc, central zone of dorsal telencephalon; Dd dorsal zone of dorsal telencephalon; Dld, dorsolateral zone of dorsal telencephalon; Dlv, ventrolateral zone of dorsal telencephalon; Dm, medial zone of dorsal telencephalon; ECL, external cellular layer; fb, forebrain bundle; GL, glomerular layer; Ha, habenular nucleus; Hc, caudal hypothalamus; Hd, dorsal

hypothalamus; Hl, lateral hypothalamus; I, intermediate thalamic nucleus; ICL, internal cellular layer; NG, glomerular nucleus; OT, optic tectum; PGa, anterior preglomerular nucleus; PGm, medial preglomerular nucleus; PGZ, periventricular gray zone; PM, magnocellular preoptic nucleus; PP, preoptic nucleus; PVO, paraventricular organ; Tl, longitudinal tori; TPp, periventricular nucleus of posterior tuberculum; VAO, ventral accessory optic nucleus; Vc, central zone of ventral telencephalon; Vd, dorsal zone of ventral telencephalon; VL, ventro-lateral thalamic nucleus; Vm, medial zone of ventral telencephalon; Vv, ventral zone of ventral telencephalon.

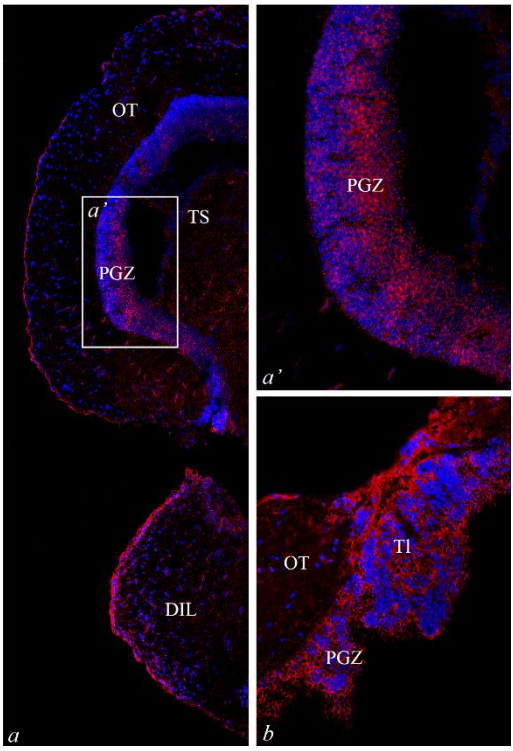

Fig 34| Id3 mRNA expression in old N. furzeri brain. Transversal cryosections, midbrain. Abbreviations: DIL, diffuse inferior lobe of hypothalamus; OT, optic tectum; PGZ, periventricular gray zone; Tl, longitudinal tori; TS, semi-circular tori.

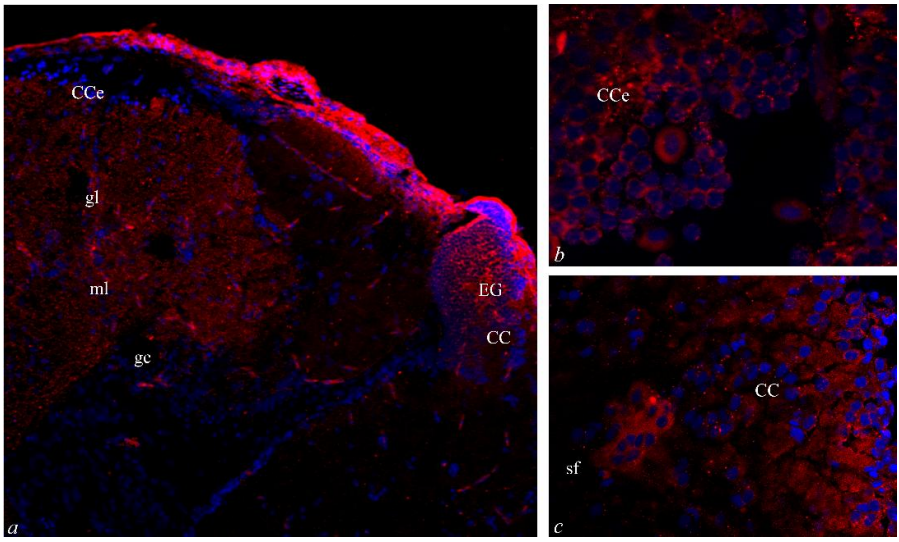

Fig 35| Id3 mRNA expression in old N. furzeri brain. Transversal cryosections, hindbrain. Abbreviations: CC, cerebellar cristae; CCe, corpus of cerebellum; EG, granular eminentiae.

	mRNA					
	Col4a1		Col25a1		Id3	
	young	old	young	old	young	old
Olphactory bulbs						
ECL	-	++	-	+++	-	-
GL	-	++	-	-	-	-
ICL	-	+	-	-	-	+++
Telencephalon						
Dc	-	-	-	-	-	+
Dd	-	++	-	++	-	+
Dlv	-	++	-	+++	-	+++
Dm1-2-3-4	-	++	-	+++	+	+++
Vc	-	-	-	-	-	++
Vm	-	-	-	-	-	+++
Vs	-	+	-	++	-	-
Vv	-	+	-	++	-	-
Diencephalon						
A	-	+++	-	++	-	+++
Cmin					-	-
CPN	-	-	-	-	-	+++
Ha	-	+++	-	-	-	+++
I	-	-	-	-	-	+++
PGa	-	-	-	-	-	++
PM	-	+++	-	++	-	+++
PP	-	++	-	-	-	+++
VAO	-	-	-	-	-	++
VL	-	-	-	+++	-	++
VM	-	+++	-	++	-	+++

Mesencephalon						
DIL	-	-	-	+++	-	+
Hc	-	-	-	-	-	++
Hd	-	+++	+++	-	+++	+++
Hl	-	-	-	-	+++	++
llf	-	+++	-	-	-	-
LV	-	+++	-	+++	-	-
NG	-	-	+++	+++	+++	-
Nllf	-	+++	-	+++	-	-
NRP	-	-	+++	++	-	-
OT	+	+	-	+	-	+
PG	-	-	-	-	+++	-
PGZ	++	+++	+++	+++	+++	+++
PVO	-	-	-	-	-	++
Tl	++	+++	-	+++	+++	+++
TNp	-	-	+++	+	-	-
TPp	-	-	-	-	-	-
TS	-	-	-	+++	-	+
Va	-	+++	-	-	-	-
Rhomboencephalon						
CC	-	++	-	-	-	++
CCe	-	+++	-	+++	-	+++
EG	-	+++	-	+++	-	+++
gl	-	+++	-	+++	-	+++
ml	-	-	-	-	-	+++
sf	-	-	-	+++	-	-

Tab 4| Col4a1, Col25a1, and Id3 distribution in N. furzeri young and old brain.

5.4. Double labeling of fluorescence in situ hybridization and immunofluorescence

To characterize the cytotype of cells expressing Col4a1, Col25a1 and Id3 mRNAs, a double labeling of fluorescence *in situ* hybridization and immunofluorescence was performed by using different markers. Experiments were conducted on old brain sections. Anti-PCNA was employed to detect cells under mitotic division. Then, anti-S100 was used as marker of radial glial cells and neural cells; anti-DCX as marker of new born neurons; anti- HuC/D as marker of cells from early neurogenic stage onwards in post-mitotic cells that have been committed to a neural fate as well as in mature neurons (Grandel et al., 20063). Furthermore, it was also used anti-TH as marker of specific mature neurons (dopaminergic neurons) and neurogenic rate.

5.4.1. Double staining for Col25a1, Col4a1, Id3 mRNAs with PCNA

The overall observed distribution pattern of PCNA in the brain of *N. furzeri* is the same reported by Tozzini et al. (2012). In addition, low distribution of PCNA positive cells in cerebellum and ON has been observed.
In the brain of old *N. furzeri*, Col4a1 mRNA and PCNA colocalize in some areas of forebrain as Vv [Fig 36 a]; of midbrain as OT and its PGZ layer [Fig 36 b, c], and Tl [Fig 36 c].
Col25a1 mRNA and PCNA colocalize in forebrain in supracommissural region of the Vs and Vv and [Fig 36 d]; in midbrain in oculomotor nerve (nerve III), DIL, OT and its PGZ layer, and TS [Fig 36 e] ; in hindbrain in gl and ml of CCe [Fig 36 f].
Id3 mRNA and PCNA colocalize in forebrain in Vv [Fig 36 g]; in midbrain in OT and its PGZ layer, and TS4 [Fig 36 h] ; in hindbrain in gl and ml of CCe, and in the central griseum (gc) [Fig 36 i] . Furthermore, Id3/PCNA colocalization is appreciable in numerous Hyp cells [Fig 36 g].

5.4.2. Double staining for Col25a1, Col4a1, Id3 mRNAs with S100

Col4a1 mRNA and S100 colocalize in numerous neurons of forebrain, caudally in the diencephalon, in PPp [Fig 37 a], Ha, A, VM, and PM [Fig 37 b]; in the hindbrain in gl of the CCe [Fig 37 c]. Furthermore, Col4a1 mRNA and S100 colocalization is detectable in ON [Fig 37 a].
Col25a1 mRNA is expressed in S100 containing cells of forebrain as in the minor commissure (Cmin), VM, A, dorsal periventricular pretectal nucleus (PPd) [Fig 37 d], in Vd, Vv, and ON [Fig 37 e]; of hindbrain in the cerebellar gl and EG [Fig 37 f].
Id3 mRNA and S100 co-localize in the forebrain, specifically in the diencephalic PPp [Fig 37 g], in A, and ON [Fig 37 g, h]; in the midbrain in PGZ and TS [Fig 37 i].

5.4.3. Double staining for Col25a1, Col4a1, Id3 with DCX

Col4a1 mRNA and DCX colocalize only in neurons of forebrain in Dm4, and Vd and Vv [Fig 38 a].
Col25a1 mRNA and DCX positive neurons are only located in the Vs and Vv [Fig 38 b].
Id3 mRNA and DCX colocalized neurons are widely distributed, particularly in the forebrain as in Vs and Vp [Fig 38 c]; in midbrain as in OT and its PGZ layer, and TS [Fig 38 d] of; in hindbrain mainly in the cerebellum ml [Fig 38 e].

5.4.4. Double staining for Col25a1, Col4a1, Id3 mRNAs with HuC/HuD

Col4a1 mRNA and HuC/D colocalization is observed in midbrain only in PGZ [Fig 39 a, b, c] of; gl [Fig 39 b, c], ml, CCe, ventral and dorsal regions of the EG, in the ventral region under the gc [Fig 39 b] of hindbrain.

Col25a1 mRNA and HuC/D colocalization is limited to the most caudal area of forebrain as Vv [Fig 39 d], and in the diencephalic areas comprises between I, A and VM; few co-localized cells are also detectable in the PM [Fig 39 d]; in midbrain as TS [Fig 39 e, f]; in hindbrain in gl and ml of CCe, in gc [Fig 39 e].
Id3 mRNA and HuC/D colocalization is observed in forebrain in Vv, Vs, Dm4 [Fig 39 g]; in midbrain in PGZ and TS [Fig 39 h]. No co-stained positive cells are detected in the hindbrain.

5.4.5. Double staining for Col25a1, Col4a1, Id3 mRNAs with TH

Col4a1 mRNA and TH colocalization is observed in hindbrain, in few neurons in the periventricular area, near gc [Fig.40 a].
Col25a1 mRNA and TH colocalization is widely distributed in the entire brain. *Col25a1*/TH positive cells are located in the caudal forebrain, specifically in ON, in the most ventral area of PPp, and few neurons are present in the thin area lining the ventricle in Ha, A, VM, and PM [Fig 40 b]. In the midbrain *Col25a1*/TH positive are densely colocalized in numerous PGZ neurons [Fig 40 c]. In the hindbrain, few TH containing cells of gl express also *Col25a1* [Fig 40 d].
Id3/TH positive cells are present in the forebrain, more precisely in ON, PPp, PM, and Vp [Fig 40 e]. In the midbrain numerous *Id3*/TH positive cells are well distributed in PGZ and TS [Fig 40 f].

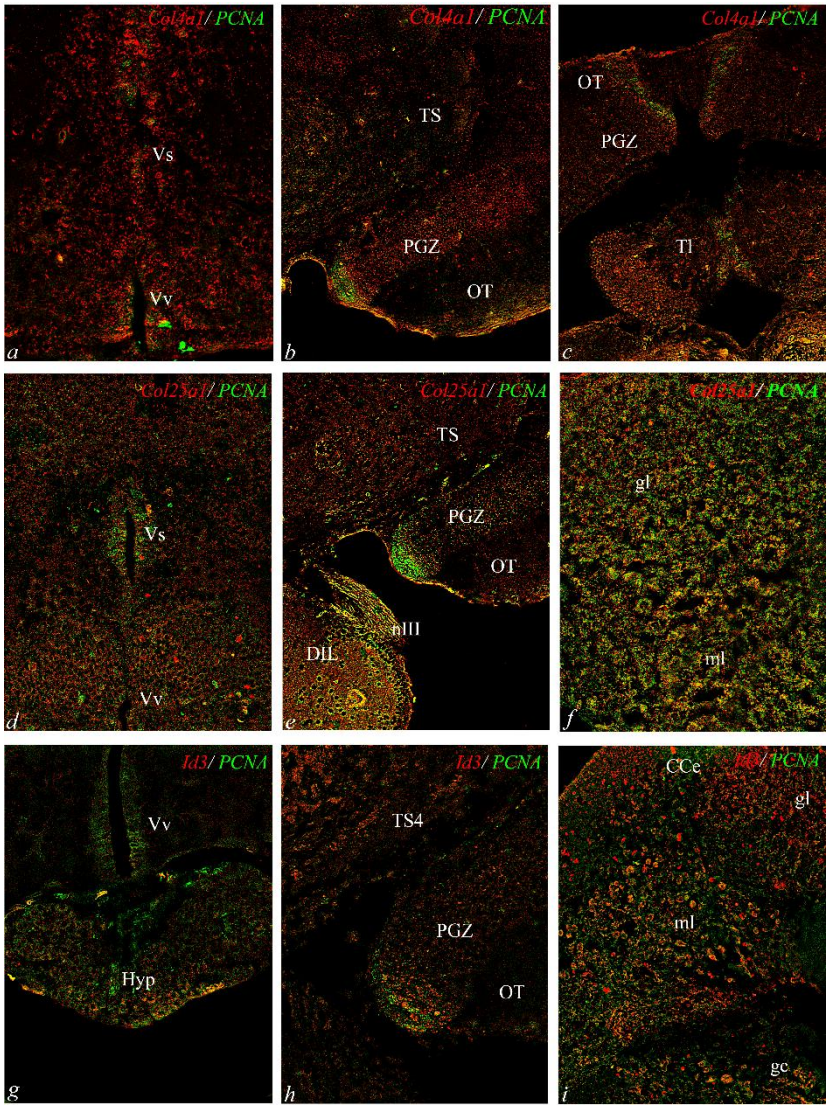

Fig 36| Double labelling of FISH and IF with PCNA, in old N. furzeri brain, transversal sections. Abbreviations: CCe, corpus of cerebellum; DIL, diffuse inferior lobe of hypothalamus; gc, central griseum; gl, granular layer; Hyp, hypophysis; ml, molecular layer; nIII, nerve III; OT, optic tectum; PGZ, periventricular gray zone; PPa, preoptic area; Tl, layer of longitudinal tori; TS, layer of semicircular tori; Vp, posterior zone of ventral telencephalon; Vs, supracommissural zone of ventral telencephalon; Vv, ventral zone of ventral telencephalon.

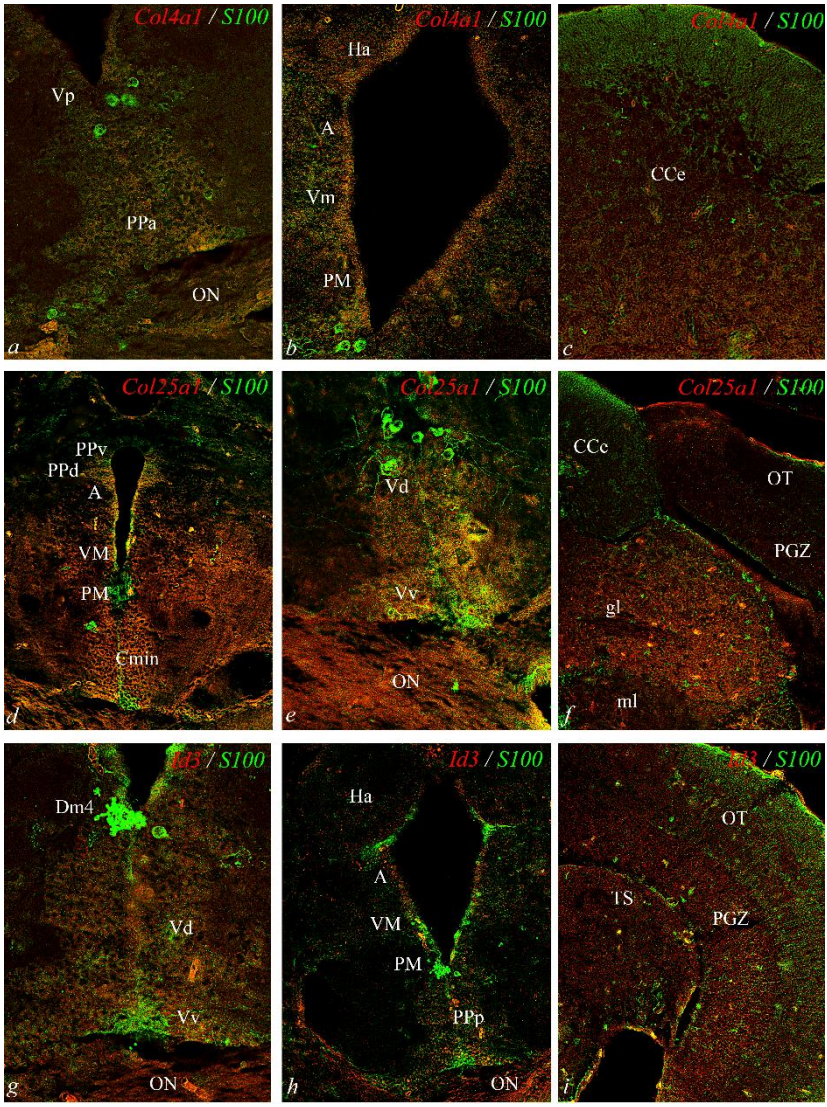

Fig 37| Double labelling of FISH and IF with S100, in old N. furzeri brain, transversal sections. Abbreviations: A, anterior thalamic nucleus; CCe, corpus of cerebellum; Cmin, minor commissure; Ha, habenular nucleus; gl, granular layer; ml, molecular layer; ON, optic nerve; OT, optic tectum; PGZ, periventricular gray zone; PM, magnocellular preoptic nucleus; PPa, preoptic area; PPp, parvocellular portion of preoptic nucleus; SC, suprachiasmatic nucleus; TS, layer of semicircular tori; VM. Ventro-medial thalamic nucleus; Vd, dorsal zone of ventral telencephalon; Vp, posterior zone of ventral telencephalon; Vv, ventral zone of ventral telencephalon.

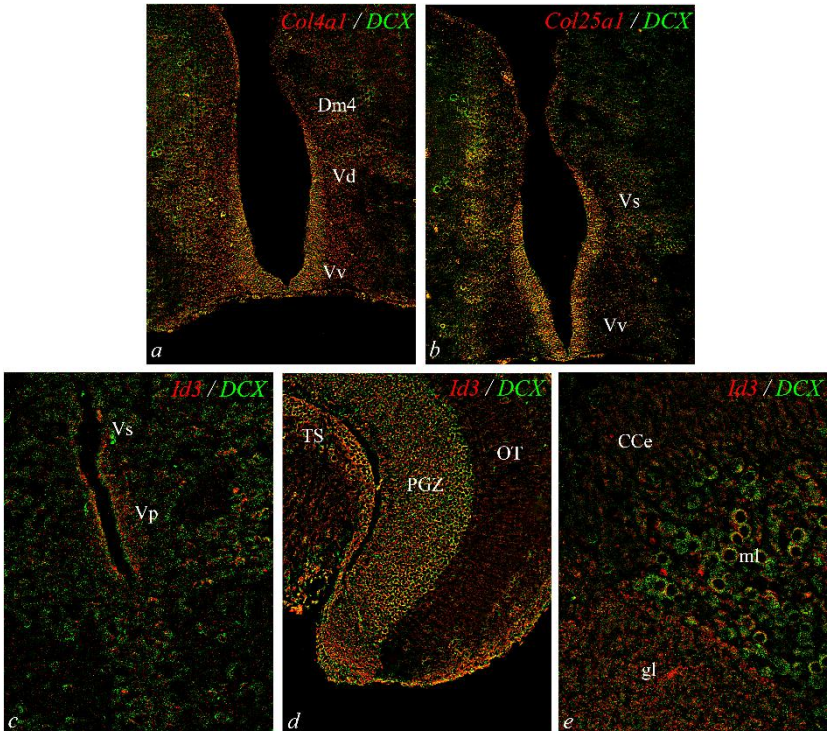

Fig 38| Double labelling of FISH and IF with DCX, in old N. furzeri brain, transversal sections. Abbreviations: CCe, corpus of cerebellum; Dm4, central zone of dorsal telencephalon, layer 4; gl, granular layer; ml, molecular layer; OT, optic tectum; PGZ, periventricular gray zone; PPa, preoptic area; TS, layer of semicircular tori; Vp, posterior zone of ventral telencephalon; Vs, supracommissural zone of ventral telencephalon.

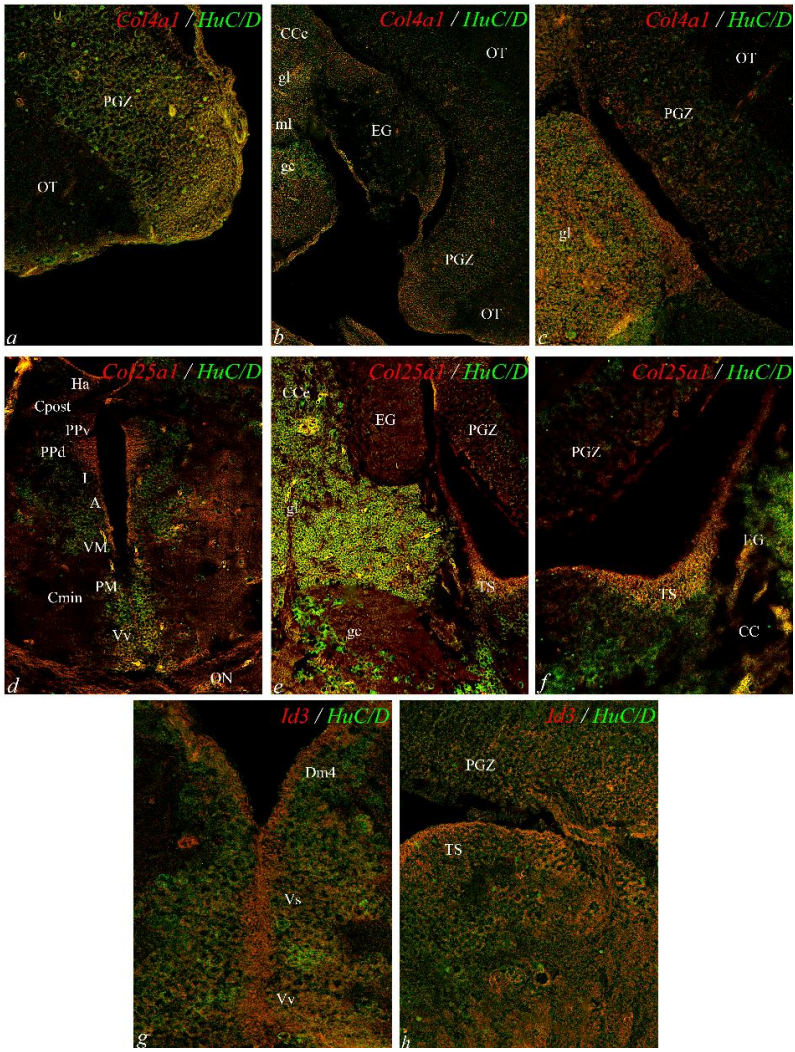

Fig 39| Double labelling of FISH and IF with HuC/D, in old N. furzeri brain, transversal sections. Abbreviations: A, anterior thalamic nucleus; CCe, corpus of cerebellum; Cpost, posterior commissure; Dm4, central zone of dorsal telencephalon, layer 4; EG, granular eminentiae; gc, central griseum; gl, granular layer; Ha, habenular nucleus; I, intermediate thalamic nucleus; ml, molecular layer; ON, optic nerve; OT, optic tectum; PGZ, periventricular gray zone; PM, magnocellular preoptic nucleus; PPd, dorsal periventricular pretectal nucleus; PPv, ventral periventricular pretectal nucleus ; TS, layer of semicircular tori; VM, ventro-medial thalamic nucleus; Vs, supracommissural zone of ventral telencephalon; Vv, ventral zone of ventral telencephalon.

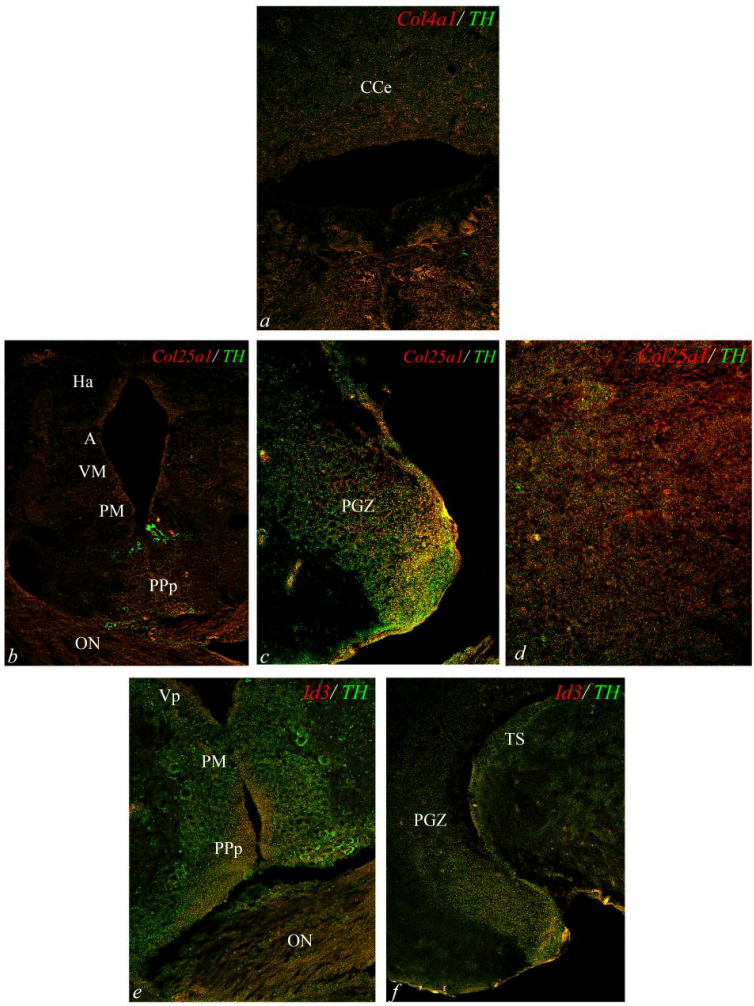

Fig 40 | Double labelling of FISH and IF with TH, in old N. furzeri brain, transversal sections. Abbreviations: A, anterior thalamic nucleus; CCe, corpus of cerebellum; gl, granular layer; Ha, habenular nucleus; ml, molecular layer; ON, optic nerve; PGZ, periventricular gray zone; PM, magnocellular preoptic nucleus; PPp, posterior periventricular pretectal nucleus; TS, layer of semicircular tori; VM, ventro-medial thalamic nucleus; Vp, posterior zone of ventral telencephalon.

5.5. Pearson correlation coefficient

Pearson correlation coefficient (PCC) analysis showed a linear correlation between cells expressing Col4a1, Col25a1, or Id3, and containing neural markers. All correlations are positive, meaning that to a specific mRNA augment corresponds to a specific neural markers augment. In addition, this positive correlation is region-specific.

Proliferating cells (PCNA positive cells) expressing *Col4a1*, were present only in the forebrain and in the midbrain. In the forebrain there was a low ($0 < r_{XY} < 0,3$) correlation between *Col4a1* and PCNA (r = 0.18); while it became moderate ($0,3 < r_{XY} < 0,7$) in the midbrain (r = 0.49). A moderate linear correlation was observed also for Col4a1 mRNA with S100 in the forebrain (r = 0.50) and hindbrain (r = 0.38), DCX in the forebrain (r = 0.51), HuC/D in midbrain (r = 0.70) and hindbrain (r = 0.68) [Tab 5].

PCNA positive cells showed a low correlation with *Col25a1* expressing cells in the forebrain (r = 0.21), moderate in the midbrain (r = 0.58) and in the hindbrain (r = 0.34). A low positive correlation was observed for *Col25a1* with S100 in the midbrain (r = 0.18), while a moderate positive correlation was appreciated with S100 in both forebrain (r = 0.61) and hindbrain (r = 0.40), DCX in the forebrain (r = 0.67), HuC/D in midbrain (r = 0.58) and hindbrain ((r = 0.68). A perfect positive correlation was observed for *Col25a1* and HuC/D in the forebrain (r = 1) [Tab 6].

PCNA positive cells showed a moderate correlation with *Id3* expressing cells in the forebrain (r = 0.31), in the midbrain (r = 0.39), and in the hinbrain (r = 0.46). A moderate positive correlation was detected between *Id3* and S100 in forebrain and midbrain. *Id3* and DCX showed a slight positive correlation in forebrain and hindbrain, while moderate positive in the midbrain. *Id3* and HuC/D showed a moderate positive correlation in forebrain and midbrain [Tab 7].

Furthermore PCC was calculated also among genes' quantitative expression in both young and old *N. furzeri* brain. All genes were positive correlated in both young and old animals. In young animals, a low correlation was observed for *Id3/Col4a1* and *Col4a1/Col25a1*, while a moderate correlation was observed for *Id3/Col25a1*. In old animals, a

strong correlation was observed for *Id3/Col4a1*, moderate for *Id3/Col4a1*, and low for *Id3/Col25a1* [Fig 41].

	Col4a1 PCC to neural markers		
	Forebrain	**Midbrain**	**Hindbrain**
r_{PCNA}	0.19	0.56	-
r_{S100}	0.50	-	0.38
r_{DCX}	0.51	-	-
$r_{HuC/D}$	-	0.70	0.68

Tab 5 | Pearson Correlation Coefficient for Col4a1 mRNA positive cells expressing neural markers. Strong positive correlation is indicated by r > 0,7; moderate for 0,3 < r < 0,7; slight for 0 < r < 0,3.

	Col25a1 PCC to neural markers		
	Forebrain	**Midbrain**	**Hindbrain**
r_{PCNA}	0.21	0.58	0.34
r_{S100}	0.61	0.18	0.40
r_{DCX}	0.67	-	-
$r_{HuC/D}$	1	0.58	0.68

Tab 6 | Pearson Correlation Coefficient for Col25a1 mRNA positive cells expressing neural markers. Strong positive correlation is indicated by r > 0,7; moderate for 0,3 < r < 0,7; slight for 0 < r < 0,3.

	Id3 PCC to neural markers		
	Forebrain	**Midbrain**	**Hindbrain**
r_{PCNA}	0.31	0.39	0.46
r_{S100}	0.35	0.31	-
r_{DCX}	0.13	0.46	0.23
$r_{HuC/D}$	0.35	0.47	-

Tab 7 | Pearson Correlation Coefficient for Id3 mRNA positive cells expressing neural markers. Strong positive correlation is indicated by r > 0,7; moderate for 0,3 < r < 0,7; slight for 0 < r < 0,3.

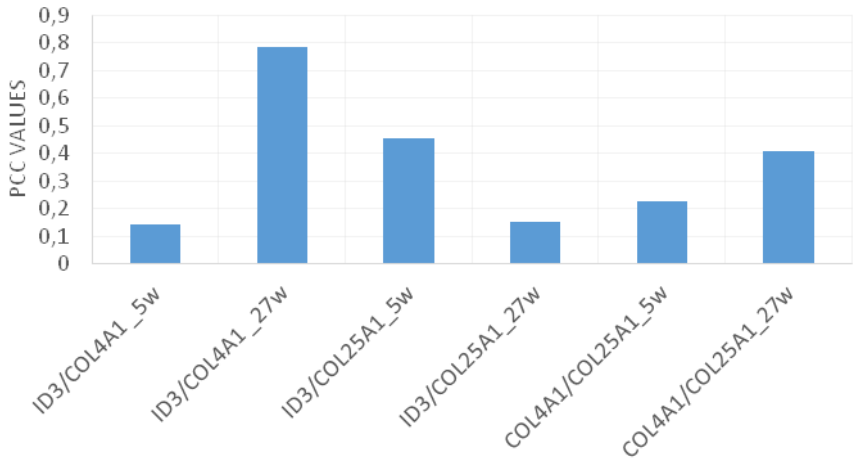

Fig 41| PCC for DEGs quantitaive expression (Col4a1, Col25a1, Id3) in both young and old N. furzeri brain.

D'Angelo, L. (2013) Brain Atlas of an Emerging Teleostean Model: Nothobranchius furzeri. Anatomical Record-Advances in Integrative Anatomy and Evolutionary Biology, 296, 681-691.

Kumar, S., Stecher, G., Li, M., Knyaz, C. and Tamura, K. (2018) MEGA X: Molecular Evolutionary Genetics Analysis across Computing Platforms. Molecular Biology and Evolution, 35, 1547-1549.

Tamura, K. and Nei, M. (1993) ESTIMATION OF THE NUMBER OF NUCLEOTIDE SUBSTITUTIONS IN THE CONTROL REGION OF MITOCHONDRIAL-DNA IN HUMANS AND CHIMPANZEES. Molecular Biology and Evolution, 10, 512-526.

Tozzini, E. T., Baumgart, M., Battistoni, G. and Cellerino, A. (2012) Adult neurogenesis in the short-lived teleost Nothobranchius furzeri: localization of neurogenic niches, molecular characterization and effects of aging. Aging Cell, 11, 241-251.

Chapter 6

Discussions

6. Discussion

The current study investigates the presence of *Col4a1*, *Col25a1* and *Id3* and their potential involvement in adult neurogenesis, by employing an excellent model for aging studies: the teleost *N. furzeri*. These three genes are well conserved during vertebrates' evolution and likely involved in aging process in many species (Bruckner et al., 2000; Vitellaro-Zuccarello et al., 2007; Fox, 2008; Norton et al., 1998; Duncan et al., 1992). Previous studies on *N. furzeri* revealed that *Col4a1*, *Col25a1*, and *Id3* are differentially expressed (brain, skin, and liver) during aging. We therefore questioned if these gene could play a role in the adult neurogenesis of *N. furzeri.*

This survey reports, for the first time, a quantitative and qualitative analysis of *Col4a1*, *Col25a1* and *Id3* in both young and old *N. furzeri* brain, with evident differences in the expression pattern. Quantitative analysis shows an age-related up-regulation of the three genes at the time points (5 wph and 27 wph). Furthermore, Col4a1, Col25a1, and Id3 mRNAs are distributed in neurogenic areas, specifically colocalizing with PCNA marker, reinforcing the hypothesis that they are involved in proliferating events (Tozzini et al., 2012). In addition, the phenotype of cell expressing Col4a1, Col25a1 and Id3 mRNAs has been characterized by means of different neural markers, in the old brain.

6.1. Col4a1, Col25a1 and Id3 are well conserved in course of evolution

Our phylogenetic analysis confirmed that *Col4a1*, *Col25a1*, and *Id3* are very well conserved among *Actinopterygii's*. Furthermore, alignment studies on mRNA sequences have shown a remarkable conservation between *N. furzeri*, the commonly used teleost fish *Danio rerio*, *Mus musculus* and *Homo sapiens*. More specifically: Col4a1 mRNA sequence showed 73% of similarity with *D. rerio*, 45% with *M. musculus*, and 50% with *H. sapiens;* Col25a1 mRNA sequence showed 67,17% of similarity with *D. rerio*, 58,52 % with *M. musculus*, and 55,62% with *H. sapiens;* Id3

mRNA *sequence* showed 65,78 % of similarity with *D. rerio*, 56,29 % with *M. musculus*, and 55,29 % with *H. sapiens*. Therefore, it is evident how these genes are well conserved during evolution. Furthermore, Reichwald and co-workers (2015) showed that Id3 is under positive selection during evolution in *N. furzeri* ($p<0.05$). *Id3* is up-regulated during aging in brain and skin and represents a key component of TGF-β signaling, which regulates inflammation, is involved in aging-related diseases such as tumorigenesis, fibrosis, glaucoma, and osteoarthritis (Krieglstein et al., 2012), and regulates life-history traits in *C. elegans* (Shaw et al., 2007). In *N. furzeri*, the gene shows signs of positive selection, i.e. a radical substitution of a non-polar by a charged aminoacid (aa) followed by a 2-aa deletion (Reichwald et al., 2015). Interestingly, in *N. pienaari*, at 10-aa distance one evolutionarily conserved aa is deleted suggesting convergent evolution (Reichwald et al., 2015).

6.2. Age-related increase of Col4a1, Col25a1 and Id3 in the brain of N. furzeri

qPCR analysis revealed that *Col4a1*, *Col25a1*, and *Id3* are all up-regulated during aging in the brain of *N. furzeri*. Id3 quantitative results agree with data previously published from Reichwald and co-workers (2015) based on RNA-Seq analysis, reporting *Id3* as differentially expressed genes (DEGs), up-regulated during aging in skin and brain. With regards to *Col4a1* and *Col25a1*, in this survey has been demonstrated that they are up-regulated with aging, displaying the highest expression at 27 wph. Remarkably, RNA-Seq data reported *Col4a1* and *Col25a1* as DEGs, and *Col4a1* is down-regulated during aging in brain and skin (Reichwald et al., 2015), whereas no available data on age-related regulation of *Col25a1* are available.

It is worthy to mention that the expression level was lower in RNA-Seq data (8.439 Reads Per Kilobase Million (RPKM)), whereas in the qPCR resulted the ΔCT from *Col4a1* to TBP was 2.82), therefore favouring type II errors (Anders and Huber, 2010).

6.3. Expression of Col4a, Col25a1 and Id3 mRNAs in the brain of young and old N. furzeri, and comparison with other vertebrates

In vertebrate adult NS, collagen genes are expressed in the layers of connective tissue surrounding the central and peripheral nervous system, in basement membranes and in sensory end organs (Hubert et al., 2009). In young *N. furzeri* brain, both collagen genes are expressed only in the midbrain. In contrast, in old brain, they are widely expressed in the periventricular telencephalic areas, in the preoptic and optic areas, and in the cerebellum.

Studies on *Col4a1* are mainly focused on its involvement in disorders that affect many body districts and tissues: ocular dysgenesis, porencephaly, schizencephaly, hydrocephaly, vessels diseases, myopathy, and lung diseases. For this reason, all scientific studies on *Col4a1* conducted so far, are mostly concentrated on gene mutations and cell culture experiments. In vertebrates *Col4a1* presence has been reported in many species: i.e. chicken lung (Loscertales et al., 2016), and mouse lung (Loscertales et al., 2016), brain (Urabe et al., 2002) and fibroblast (Carole et al., 2017). Furthermore, *Col4a1* protein distribution has been described in human kidney (Heidet et al., 2000), murine eye (Saito et al., 2011), ovary (Nakano et al., 2007) and allantois (Mikedis et al., 2009). In teleost brain, *Col4a1* presence has been reported in many species, i.e. catfish (Geng et al., 2017), zebrafish (Takeuchi et al., 2015; Li et al., 2011), and brook trout (Crespo et al., 2013). *Col4a1* mRNA distribution in teleost brain has been not yet studied so far, whilst distribution data are available for adult mouse brain (Allen Brain Atlas, *https://www.brain-map.org/*). *In situ* hybridization data on mouse brain showed that *Col4a1* mRNA is expressed in the isocortex region, olphactory areas, hippocampal formation, cortical subplate, striatum, pallidum, thalamus, hypothalamus, midbrain, pons, medulla, and cerebellum. Bearing in mind the comparison between mammals and teleost brain depicted in Fig 12, murine *Col4a1* distribution pattern is very similar to that observed in old *N. furzeri* brain, mainly concentrated in periventricular areas. Hubert and co-workers (2009) showed that collagen IV and I were distributed in fractone, an extracellular matrix structure present in the lateral wall of the ventricles, one of the main neural stem cell

niches in the adult mammalian brain, reinforcing the idea that collagens are involved in proliferating activity.

Col25a1 is well conserved among vertebrates as human, chimpanzee, Rhesus monkey, dog, cow, mouse chicken and frog, and in other 199 organisms having human orthologues. *Col25a1* is a component of senile plaque amyloid of Alzheimer's disease brains (Castillo et al., 1999; Hashimoto et al., 2002; Verdier et al., 2004; Lansbury et al., 2006; LaFerla et al., 2007). A recent study (Tanaka et al., 2014) has underlined its importance in the formation of proper neuromuscular connection during development. *Col25a1*$^{-/-}$ mice die immediately after birth suggesting that *Col25a1* is necessary for the initial phases of intramuscular motor innervation, required for subsequent target-dependent motoneuron survival and neuromuscular junctions (Tanaka et al., 2014). In teleost, *Col25a1* has been identified in many species, such as zebrafish, medaka, coho and Chinook salmon, rainbow trout, Japanese flounder, red-bellied piranha. However, Col25a1 mRNA distribution in teleost brain has been not yet studied so far, whilst distribution data are available for adult mouse brain (Allen Brain Atlas, *https://www.brain-map.org/*). In mouse brain, Col25a1 mRNA pattern of distribution matches to *Col4a1*: isocortex region, olphactory areas, hippocampal formation, cortical subplate, striatum, pallidum, thalamus, hypothalamus, midbrain, pons, medulla, and cerebellum. Interestingly, in old *N. furzeri* both *Col4a1* and *Col25a1* genes display an overlapping pattern in brain areas homologous to murine brain.

In the young brain of *N. furzeri*, *Id3* displays a wider expression compared to *Col4a1* and *Col25a1*. It is indeed detectable in cells of the telencephalon in the forebrain, and in the optic region of the midbrain. However, its highest expression is appreciable in the old brain.

Id family includes 4 members, all involved in cell differentiation and cell cycle progression by interfering with DNA binding of transcription factors (Lyden et al., 1999). Jen and co-workers (1996) have shown that in mice, all 4 members are expressed during embryonic neurogenesis, exhibiting a distinct spatiotemporal pattern. In adult brain, *Id3* is expressed in isocortex region, olphactory areas, hippocampal formation, cortical sub plate, striatum, pallidum, thalamus, midbrain, pons, medulla, and cerebellum (Allen Brain Atlas, *https://www.brain-map.org/*). The pattern of expression

in old brain of *N. furzeri is* suggestive of an overlapping pattern in brain areas homologous to murine brain.

6.4. Col4a1, Col25a1 and Id3 are all expressed in proliferating brain cells

As already established in literature (Jen et al., 1996; Hubert et al., 2009), *Col4a1*, *Col25a1*, and *Id3* are expressed in proliferating cells, which have been identified by means of PCNA as marker. The observed PCNA distribution pattern in *N. furzeri* brain matches with previous description (Tozzini et al., 2012). The pattern of distribution of mitotic cells in *N. furzeri* is particularly pronounced in the dorsal telencephalon, preoptic area of the diencephalon, Tl, OT and in all cerebellar subdivisions. This distribution pattern confirms also previous studies describing proliferating brain areas in other teleost species. In fact, as already demonstrated in brown ghost (Zupanc and Horschke, 1995), gilt head sea bream (Zikopoulos et al., 2000), goldfish (Meyer, 1978), guppy (Kranz and Richter, 1970), stickleback (Ekström and Ohlin, 1995), and zebrafish (Zupanc et al., 2005; Grandel et al., 2006), PCNA positive cells are distributed exactly in the same brain regions as *N. furzeri*.
Remarkably, in addition to the previous description (Tozzini et al, 2012), in this survey the proliferating activity has been observed also in the ON, hypophysis and cerebellum.
In *N. furzeri*, not all *Col4a1*, *Col25a1*, and *Id3* mRNAs expressing cells were positive to PCNA. Among the three mRNAs, the highest co-distribution pattern is seen between *Col25a1* and PCNA. However, co-labeling with PCNA and *Col4a1*, *Col25a1*, and *Id3* mRNAs is shown in the well-established neurogenic areas: periventricular zone of ventral telencephalon, in the PGZ and TS. This observation corroborates the initial hypothesis that also in this model species *Col4a1*, *Col25a1*, and *Id3* are possibly involved in neurogenic proliferating activities.

6.5. Col4a1, Col25a1 and Id3 neurogenic pattern in aged brain

To determine whether *Col4a1*, *Col25a1* and *Id3* expressing cells are involved in neurogenic process, it was employed different neural markers for different neural progenitors: anti-S100, anti-DCX, anti-HuC/D, and anti-TH.

S100 distribution pattern in *N. furzeri* confirm previous studies of D'Angelo et al. (2012): OB, and in different areas of the telencephalic hemispheres, in the ON, habenular nuclei, cortical thalamic nucleus, DIL, along the diencephalic ventricle, in the dorsal optic tract, Tl, PGZ, along the mesencephalic ventricle, Va, CCe.

In mammals' adult brain, DCX expression is retained within areas of continuous neurogenesis, i.e. the hippocampus and the SVZ / OB axis (Brown et al., 2003), and rarely expressed outside these regions (Nacher et al., 2001). During adult neurogenesis, expression of DCX starts as neuroblasts are generated, peaks during the second week, and is downregulated concomitantly with the appearance of mature neuronal marker. No data are available for this marker distribution in zebrafish, since a DCX orthologue is present neither in the assembled zebrafish genome nor in the collections of zebrafish expressed sequence tags. In contrast, *N. furzeri* genome contains a DCX gene (Tozzini et al., 2012). Again, also for DCX distribution pattern, data collected in this survey confirm the previous studies of Tozzini and co-workers (2012), in which DCX is mostly related to the telencephalic region.

HuC/D proteins are expressed from an early neurogenic stage onwards in postmitotic cells that have been committed to a neural fate as well as in mature neurons (Barami et al, 1995). In teleost fish, proliferation zones of all brain subdivisions are surrounded by HuC/D-positive neuronal nuclei. As for the zebrafish, positive HuC/D staining has been observed in the ventral telencephalic regions, in the preoptic and thalamic areas, in the tectal zone and in the Tl, in the cerebellar zone (Grandel et al., 2006).

TH is the enzyme which converts the L-tyrosine in L-3, 4-dihydroxyphenylalaline, which, in turn, is the precursor for dopamine. Since during aging it is known that there is an evident decrease in the synthesis of dopaminergic neurons, it is used not only as marker for TH

positive cells, but also as marker for neurogenic rate. In fact, aging decline features comprise changes in the realative quantity of TH containing neurons. For example age-related declines in the activity of TH are the main cause of motor deficits in Parkinson's desease.

6.5.1. Forebrain

In the forebrain region, *Col4a1, Col25a1* and *Id3* are widely expressed. Furthermore, they show a specific cytotype pattern, in relationship to each brain area.
Only few S100 containing cells express also *Col4a1, Col25a1* and *Id3,* more precisely in the preoptic diencephalic area and in the ON. Grandel and co-workers have already shown a few S100 distribution pattern in zebrafish, similarly to that of other teleost fish, suggesting that most of the proliferating cells of the forebrain are neurogenic and only few are gliogenic. Furthermore, the antibody employed in this study has a strong reactivity for S100β, but also weakly for S100α1 (predominantly expressed in neuronal cells, endothelium, neuropil, gl and ml) and S100α6 (expressed by neurons of restricted brain areas such as amygdala and entorhinal cortex, and in some astrocytes), suggesting that *Col4a1, Col25a1* and *Id3* could regulate neuronal differentiation more than glial one.
All three genes are co-expressed in DCX containing cells in the telencephalic region. *Col4a1* and *Col25a1* are both express in DCX containing cells of ventral telencephalic hemispheres and the signal is still present dorsally in the Dm4. *Id3/DCX* cells are less expressed in the forebrain: only few cells caudally in the telencephalon, between Vs and Vp. This distribution pattern suggests that *Col4a1, Col25a1* and *Id3,* in the telencephalic region, are expressed specifically in migrating neuronal precursors of the developing CNS (des Portes et al., 1998; Gleeson et al., 1998). This peculiarity is well conserved among vertebrates from mammals to birds and adult reptiles, to adult teleost and sharks (Quintana-Urzainqui et al., 2014), confirming *N. furzeri* as an excellent model for adult neurogenic studies.
A conspicuous part of HuC/D cell population of the forebrain expresses also *Col25a1* and *Id3.* These co-expressing cells are localized in the

diencephalic areas, mainly in preoptic area. This expression pattern has also been observed for S100, suggesting that maybe *Col25a1* and *Id3* could lead to the differentiation of few radial glial cells into neurons.
Few TH containing cells of forebrain also express *Col25a1*, more in details in the preoptic diencephalic region: Ha, A, VM, PM, and PPp. Since the same pattern has been observed for HuC/D, it is possible that these cells later differentiate into dopaminergic neurons. In addition, *Id3* positive cells express TH in the preoptic diencephalic region: Vp, PM, PPp, and ON. Also in this latter case, it is possible to suppose that *Id3* positive cells later differentiate into dopaminergic neurons since they are expressed in the same region also in DCX and HuC/D containing cells.

6.5.2. Midbrain

Midbrain neurogenic areas mainly interest the PGZ and Tl, and cytotype express are radial glial cells, neurons, new-born neurons, and oligodendrocytes.
Among the three genes, the most expressed in the optic tectum is *Id3*, and it is the only one being co-expressed both in S100 and DCX containing cells of PGZ and TS. *Id3*/S100 cells are present in few scattered cells in the thin line of the PGZ lining the ventricle. This evidence leads to the possibility that *Id3/S100* expressing cells are positive to S100α1. However, only the ventral edge of the PGZ specifically expresses S100β (Ito et al., 2010), so a few of *Id3* neurogenic activity could interest glial proliferation.
A more intense labeling has been observed instead for *Id3*/DCX cells, which are numerous and located in the TS lining the ventricle, but the higher signal is detectable in all the three layers of the PGZ and in the superficial deep white and gray zone of the OT. Proliferating cells in the mitotic region of the PGZ does not have glial properties but NE characteristics (Ito et al., 2010). This observation sustains the hypothesis that *Id3* in the optic region is much more involved in neural proliferation than in glial differentiation.
In the midbrain is also detectable a specific HuC/D pattern, overlapping for all the three genes: dense neurons in the PGZ, more numerous in the ventricular surface and shading going towards the dorsal tectal area. As

already described, this region has NE characteristic, sustaining once again the hypothesis that *Col4a1*, *Col25a1* and *Id3* are involved in neural proliferation and differentiation.
In the midbrain TH containing cells express only *Col25a1* and *Id3*. Both mRNAs are expressed in TH positive cells of PGZ; furthermore, *Id3*/TH cells are detectable in TS. *Col25a1*/TH cells of PGZ likely resemble PCNA pattern but are not located in the same area where DCX and HuC/D have been detected. On the other hand, *Id3*/TH pattern perfectly matches that of both DCX and HuC/D, suggesting that maybe in these regions the renew of dopaminergic neurons still persists during aging.

6.5.3. Hindbrain

Hindbrain proliferation activity is very high and localized in each cerebellar division, Cytotype expressed in these area comprises: NE progenitors in the thin proliferative dorsal midline, together with proliferating neurons and Bergmann-like glia progenitors; along the dorsal cerebellar lateral walls are located proliferating neuroblasts, Bergmann-like glial cells, and Purkinje neurons; in the most central region, in the gl and ml layers are located neurons and new born neurons.
Col4a1, *Col25a1* and *Id3* are expressed in S100 containing cells of the hindbrain. The fact that cerebellar cells are S100β negative, suggest once again that *Col4a1*, *Col25a1* and *Id3* regulates neural proliferation and differentiation. In fact, in these regions, cells are immunoreactive mostly to S100α1.
Some DCX containing cells of the hindbrain co-express only *Id3*, specifically in the layer of Purkinje. In vertebrates, DCX is a marker of migration-ready postmitotic neurons (Zimatkin et al., 2016). According to this, *Id3* could regulate the proliferation of new born neurons until they migrate into the destination site.
Col4a1 and *Col25a1* are expressed in some HuC/D positive cells respectively of the CCe and EG, and of the CC and EG. These regions lack of glial progenitors, whilst are characterized by NE-like polarized cells, new-born neurons and mature neurons. Particularly, in the CCe the co-expression is concentrated in the gl, which hosts new-born cells in a cap-

protrusion in its midline during their migration toward the ml. This helps to confirm the involvement of *Col4a1* and *Col25a1* in neurons differentiation and possibly migration.
Only few *Col25a1* positive cells also contain TH, specifically in CCe. Since numerous *Col25a1/HuC-D* neurons have been observed in gl, it could be possible that these cells differentiate into dopaminergic neurons during they migration in the rostral cerebellar region.

Aberg, M. A. I., Aberg, N. D., Hedbacker, H., Oscarsson, J. and Eriksson, P. S. (2000) Peripheral infusion of IGF-I selectively induces neurogenesis in the adult rat hippocampus. Journal of Neuroscience, 20, 2896-2903.

Anders, S. and Huber, W. (2010) Differential expression analysis for sequence count data. Genome Biology, 11.

Barami, K., Iversen, K., Furneaux, H. and Goldman, S. A. (1995) HU PROTEIN AS AN EARLY MARKER OF NEURONAL PHENOTYPIC DIFFERENTIATION BY SUBEPENDYMAL ZONE CELLS OF THE ADULT SONGBIRD FOREBRAIN. Journal of Neurobiology, 28, 82-101.

Brown, J. P., Couillard-Despres, S., Cooper-Kuhn, C. M., Winkler, J., Aigner, L. and Kuhn, H. G. (2003) Transient expression of doublecortin during adult neurogenesis. Journal of Comparative Neurology, 467, 1-10.

Bruckner, G., Grosche, J., Schmidt, S., Hartig, W., Margolis, R. U., Delpech, B., Seidenbecher, C. I., Czaniera, R. and Schachner, M. (2000) Postnatal development of perineuronal nets in wild-type mice and in a mutant deficient in tenascin-R. Journal of Comparative Neurology, 428, 616-629.

Castillo, G. M., Lukito, W., Wight, T. N. and Snow, A. D. (1999) The sulfate moieties of glycosaminoglycans are critical for the enhancement of beta-amyloid protein fibril formation. Journal of Neurochemistry, 72, 1681-1687.

Crespo, D., Pramanick, K., Goetz, F. W. and Planas, J. V. (2013) Luteinizing hormone stimulation of in vitro ovulation in brook trout (Salvelinus fontinalis) involves follicle contraction and activation of proteolytic genes. General and Comparative Endocrinology, 188, 175-182.

D'Angelo, L., de Girolamo, P., Cellerino, A., Tozzini, E. T., Varricchio, E., Castaldo, L. and Lucini, C. (2012) Immunolocalization of S100-Like Protein in the Brain of an Emerging Model Organism: Nothobranchius Furzeri. Microscopy Research and Technique, 75, 441-447.

des Portes, V., Pinard, J. M., Billuart, P., Vinet, M. C., Koulakoff, A., Carrie, A., Gelot, A., Dupuis, E., Motte, J., Berwald-Netter, Y., Catala, M., Kahn, A., Beldjord, C. and Chelly, J. (1998) A novel

CNS gene required for neuronal migration and involved in X-linked subcortical laminar heterotopia and lissencephaly syndrome. Cell, 92, 51-61.

Duncan, M., Diciccobloom, E. M., Xiang, X., Benezra, R. and Chada, K. (1992) THE GENE FOR THE HELIX LOOP HELIX PROTEIN, ID, IS SPECIFICALLY EXPRESSED IN NEURAL PRECURSORS. Developmental Biology, 154, 1-10.

Ekstrom, P. and Ohlin, L. M. (1995) Ontogeny of GABA-immunoreactive neurons in the central nervous system in a teleost, Gasterosteus aculeatus L. Journal of Chemical Neuroanatomy, 9, 271-288.

Fox, M. A. (2008) Novel roles for collagens in wiring the vertebrate nervous system. Current Opinion in Cell Biology, 20, 508-513.

Galligan, C. L. and Fish, E. N. (2017) Interleukin-34 Promotes Fibrocyte Proliferation. Journal of Interferon and Cytokine Research, 37, 440-448.

Geng, X., Liu, S. K., Yuan, Z. H., Jiang, Y. L., Zhi, D. G. and Liu, Z. J. (2017) A Genome-Wide Association Study Reveals That Genes with Functions for Bone Development Are Associated with Body Conformation in Catfish. Marine Biotechnology, 19, 570-578.

Gleeson, J. G., Allen, K. M., Fox, J. W., Lamperti, E. D., Berkovic, S., Scheffer, I., Cooper, E. C., Dobyns, W. B., Minnerath, S. R., Ross, M. E. and Walsh, C. A. (1998) doublecortin, a brain-specific gene mutated in human X-linked lissencephaly and double cortex syndrome, encodes a putative signaling protein. Cell, 92, 63-72.

Grandel, H., Kaslin, J., Ganz, J., Wenzel, I. and Brand, M. (2006) Neural stem cells and neurogenesis in the adult zebrafish brain: Origin, proliferation dynamics, migration and cell fate. Developmental Biology, 295, 263-277.

Hashimoto, T., Wakabayashi, T., Watanabe, A., Kowa, H., Hosoda, R., Nakamura, A., Kanazawa, I., Arai, T., Takio, K., Mann, D. M. A. and Iwatsubo, T. (2002) CLAC: a novel Alzheimer amyloid plaque component derived from a transmembrane precursor, CLAC-P/collagen type XXV. Embo Journal, 21, 1524-1534.

Heidet, L., Cai, Y., Guicharnaud, L., Antignac, C. and Gubler, M. C. (2000) Glomerular expression of type IV collagen chains in normal and X-linked Alport syndrome kidneys. American Journal of Pathology, 156, 1901-1910.

Hubert, T., Grimal, S., Carroll, P. and Fichard-Carroll, A. (2009) Collagens in the developing and diseased nervous system. Cellular and Molecular Life Sciences, 66, 1223-1238.

Ito, Y., Tanaka, H., Okamoto, H. and Ohshima, T. (2010) Characterization of neural stem cells and their progeny in the adult zebrafish optic tectum. Developmental Biology, 342, 26-38.

Jen, A. C., Wake, M. C. and Mikos, A. G. (1996) Review: Hydrogels for cell immobilization. Biotechnology and Bioengineering, 50, 357-364.

Kranz, D. Richter, W. (1970) Autoradiographic studies on the localization of the matrix zones of the diencephalon of young and adult Lebistes reticulatus (Teleostae). Z. Mikrosk. Anat. Forsch., 82, pp. 42-66

Krieglstein, K., Miyazono, K., ten Dijke, P. and Unsicker, K. (2012) TGF-beta in aging and disease. Cell and Tissue Research, 347, 5-9.

LaFerla, F. M., Green, K. N. and Oddo, S. (2007) Intracellular amyloid-beta in Alzheimer's disease. Nature Reviews Neuroscience, 8, 499-509.

Lansbury, P. T. and Lashuel, H. A. (2006) A century-old debate on protein aggregation and neurodegeneration enters the clinic. Nature, 443, 774-779.

Li, Q. L., Frank, M., Thisse, C. I., Thisse, B. V. and Uitto, J. (2011) Zebrafish: A Model System to Study Heritable Skin Diseases. Journal of Investigative Dermatology, 131, 565-571.

Loscertales, M., Nicolaou, F., Jeanne, M., Longoni, M., Gould, D. B., Sun, Y. W., Maalouf, F. I., Nagy, N. and Donahoe, P. K. (2016) Type IV collagen drives alveolar epithelial-endothelial association and the morphogenetic movements of septation (vol 14, 59, 2016). Bmc Biology, 14.

Lyden, D., Young, A. Z., Zagzag, D., Yan, W., Gerald, W., O'Reilly, R., Bader, B. L., Hynes, R. O., Zhuang, Y., Manova, K. and Benezra, R. (1999) Id1 and Id3 are required for neurogenesis, angiogenesis and vascularization of tumour xenografts. Nature, 401, 670-677.

Mikedis, M. M. and Downs, K. M. (2009) Collagen Type IV and Perlecan Exhibit Dynamic Localization in the Allantoic Core Domain, a Putative Stem Cell Niche in the Murine Allantois. Developmental Dynamics, 238, 3193-3204.

Meyer, R. L. (1978) Evidence from thymidine labeling for continuing growth of retina and tectum in juvenile goldfish. Experimental neurology.

Nacher, J., Crespo, C. and McEwen, B. S. (2001) Doublecortin expression in the adult rat telencephalon. European Journal of Neuroscience, 14, 629-644.

Nakano, K., Naito, I., Momota, R., Sado, Y., Hasegawa, H., Ninomiya, Y. and Ohtsuka, A. (2007) The distribution of type IV collagen alpha chains in the mouse ovary and its correlation with follicular development. Archives of Histology and Cytology, 70, 243-253.

Norton, J. D., Deed, R. W., Craggs, G. and Sablitzky, F. (1998) Id helix-loop-helix proteins in cell growth and differentiation. Trends in Cell Biology, 8, 58-65.

Quintana-Urzainqui, I., Anadon, R. and Rodriguez-Moldes, E. C. I. (2014) Development of the Terminal Nerve System in the Shark Scyliorhinus canicula. Brain Behavior and Evolution, 84, 277-287.

Reichwald, K., Petzold, A., Koch, P., Downie, B. R., Hartmann, N., Pietsch, S., Baumgart, M., Chalopin, D., Felder, M., Bens, M., Sahm, A., Szafranski, K., Taudien, S., Groth, M., Arisi, I., Weise, A., Bhatt, S. S., Sharma, V., Kraus, J. M., Schmid, F., Priebe, S., Liehr, T., Gorlach, M., Than, M. E., Hiller, M., Kestler, H. A., Volff, J. N., Schartl, M., Cellerino, A., Englert, C. and Platzer, M. (2015) Insights into Sex Chromosome Evolution and Aging from the Genome of a Short-Lived Fish. Cell, 163, 1527-1538.

Saito, K., Yonezawa, T., Minaguchi, J., Kurosaki, M., Suetsugu, S., Nakajima, A., Nomoto, H., Morizane, Y., Sado, Y., Sugimoto, M., Kusachi, S. and Ninomiya, Y. (2011) Distribution of alpha(IV) collagen chains in the ocular anterior segments of adult mice. Connective Tissue Research, 52, 147-156.

Shaw, W. M., Luo, S., Landis, J., Ashraf, J. and Murphy, C. T. (2007) The C-elegans TGF-beta dauer pathway regulates longevity via insulin signaling. Current Biology, 17, 1635-1645.

Takeuchi, M., Yamaguchi, S., Yonemura, S., Kakiguchi, K., Sato, Y., Higashiyama, T., Shimizu, T. and Hibi, M. (2015) Type IV Collagen Controls the Axogenesis of Cerebellar Granule Cells by Regulating Basement Membrane Integrity in Zebrafish. Plos Genetics, 11.

Tanaka, T., Wakabayashi, T., Oizumi, H., Nishio, S., Sato, T., Harada, A., Fujii, D., Matsuo, Y., Hashimoto, T. and Iwatsubo, T. (2014) CLAC-P/Collagen Type XXV Is Required for the Intramuscular Innervation of Motoneurons during Neuromuscular Development. Journal of Neuroscience, 34, 1370-1379.

Tozzini, E. T., Baumgart, M., Battistoni, G. and Cellerino, A. (2012) Adult neurogenesis in the short-lived teleost Nothobranchius furzeri: localization of neurogenic niches, molecular characterization and effects of aging. Aging Cell, 11, 241-251.

Urabe, N., Naito, I., Saito, K., Yonezawa, T., Sado, Y., Yoshioka, H., Kusachi, S., Tsuji, T., Ohtsuka, A., Taguchi, T., Murakami, T. and Ninomiya, Y. (2002) Basement membrane type IV collagen molecules in the choroid plexus, pia mater and capillaries in the mouse brain. Archives of Histology and Cytology, 65, 133-143.

Verdier, Y., Zarandi, M. and Penke, B. (2004) Amyloid beta-peptide interactions with neuronal and glial cell plasma membrane: Binding sites and implications for Alzheimer's disease. Journal of Peptide Science, 10, 229-248.

Vitellaro-Zuccarello, L., Bosisio, P., Mazzetti, S., Monti, C. and De Biasi, S. (2007) Differential expression of several molecules of the extracellular matrix in functionally and developmentally distinct regions of rat spinal cord. Cell and Tissue Research, 327, 433-447.

Zikopoulos, B., Kentouri, M. and Dermon, C. R. (2000) Proliferation zones in the adult brain of a sequential hermaphrodite teleost species (Sparus aurata). Brain Behavior and Evolution, 56, 310-322.

Zimatkin, S.M. Karniushko, O.A. (2016) Expression of doublecortin and neun in the developing cerebellar neurons in rat. Morfologiia, 149 (1), 38-42

Zupanc, G. K. H. and Horschke, I. (1995) PROLIFERATION ZONES IN THE BRAIN OF ADULT GYMNOTIFORM FISH - A QUANTITATIVE MAPPING STUDY. Journal of Comparative Neurology, 353, 213-233.

Chapter 7

Conclusions

7. Conclusions

In this survey it is reported for the first time the localization of Col4a1, Col25a1, and Id3 mRNAs in the brain of both young and old *N. furzeri* brains. Furthermore, it has been demonstrated that all the three genes are up-regulated during aging in both young and old animals' brains.
Double labeling of FISH/IF with PCNA was then employed to demonstrate *Col4a1*, *Col25a1*, and *Id3* presence in proliferating cells, since they are all expressed in neurogenic areas. Data confirmed that they are co-expressed in many PCNA containing cells. Furthermore, cytotype of neural cells expressing *Col4a1*, *Col25a1*, and *Id3* was characterized by means of FISH/IF experiments with neural markers S100, DCX, HuC/D, and TH, demonstrating that they are all expressed mainly in proliferating/mature neurons. This relation was also confirmed by Pearson Statistical analyses, which demonstrated that all genes are positively correlated to all neural markers, showing a low correlation coefficient with glial cells and a moderate/high one with neural cells. Pearson Correlation Coefficient was also calculated on genes' quantitative expression in both young and old *N. furzeri* brain, showing that all genes are positive correlated with different PCC values: in young animals, a low correlation is observed for *Id3/Col4a1* and *Col4a1/Col25a1*, while a moderate correlation is observed for *Id3/Col25a1*; in old animals, a strong correlation is observed for *Id3/Col4a1*, moderate for *Id3/Col4a1*, and low for *Id3/Col25a1*.
In summary these data: demonstrate that *Col4a1*, *Col25a1*, and *Id3* are all expressed in neurogenic areas of *N. furzeri* young and old brain, and that they are all up-regulated during aging; confirm their involvement in neural proliferation and differentiation, as it was widely demonstrated in other vertebrate species; demonstrate that they are all expressed in neural cells at different developmental stages rather that in radial glia. In this sense, this study represents a solid basis to further investigation on the specific pathways involving *Col4a1*, *Col25a1*, and *Id3* in the aging brain.